The Dissertation Committee for Moses An Kai Certifies that this is the approved version of the following dissertation:

Implementation and Lessons Learned from the Texas Synchrophasor Network

Committee:

W. Mack Grady, Supervisor

Aristotle Arapostathis

Mircea D. Driga

Glenn Masada

Surya Santoso

Implementation and Lessons Learned from the Texas Synchrophasor Network

by

Moses An Kai, B.S.E.E.;M.S.E.

Dissertation

Presented to the Faculty of the Graduate School of

The University of Texas at Austin

in Partial Fulfillment

of the Requirements

for the Degree of

Doctor of Philosophy

The University of Texas at Austin

December, 2012

Dedication

I would like to thank my parents, Ying and Grace, for their love and encouragement throughout my academic pursuit. I would also like to thank my brothers, Samuel and Joshua, for their support and encouragement throughout. I am very grateful for the love and support from Amanda Woosley. Finally, I would like to thank my supervisor, W. Mack Grady for the wonderful topic and guidance throughout my graduate and undergraduate studies.

Acknowledgements

The author would like to acknowledge Schweitzer Engineering Laboratories for their ongoing equipment support, Electrical Power Research Institute for their financial support, and the support of Scott Bayer of Austin Energy and Andrew Mattei of Brazos Electric Power Cooperative who provide and maintain PMU stations.

Implementation and Lessons Learned from the Texas Synchrophasor Network

Moses An Kai, Ph.D

The University of Texas at Austin, 2012

Supervisor: W. Mack Grady

In 2008, the University of Texas at Austin established the Texas Synchrophasor Network. This dissertation examines the equipment, programs, and analysis done by the network. The network monitors voltages in the ERCOT grid plus several other points outside Texas. The monitoring points are mainly 120V wall outlets. Main observations include wind generation up to 20% of total does not affect grid inertia or damping. Methods to utilize synchrophasor to estimate West Texas thevenin equivalent impedance and direction of generator unit trips are also discussed.

Table of Contents

List of Tables

List of Figures

Chapter 1: Definition of Synchrophasors and Their Importance to Electric Power Grids

Synchronized phasors (synchrophasors) are a fairly new technology. It was not until the Global Positioning System (GPS) was developed in the 1980s, that a good way to synchronize the phasor measurements became available. However, high costs prevented phasor measurement units (PMU) from wide-spread use. Recently, commonly used distance relays have been equipped with synchronized measurement capabilities. Additionally, certain relays and Digital Fault Recorders (DFRs) only require a firmware upgrade to become PMU-capable. This has allowed synchrophasor technology to become a reality in daily use. [1]-[3]

1.1: SYNCHROPHASOR BASICS

In order to understand synchrophasors, one must first recall that a sinusoidal waveform function y(t) is represented in the time domain by (1-1).

$$y(t) = A\cos(\omega t + \phi) \tag{1-1}$$

where:

$y(t)$ = system voltage

A = amplitude

ω = angular frequency, in radians per second

t = time, in seconds

ϕ = angle shift from the peak of the voltage waveform to time zero (or the reference)

Fig. 1.1 shows the sinusoid and its corresponding phasor representation. Angle ϕ is used to specify the value that y(t) has at the reference time, t = 0. The larger the angle

ϕ, the farther the sinusoid moves to the left of the t = 0 reference. In the phasor plane, a larger ϕ means that the phasor is rotated farther in the counterclockwise direction from the real axis.

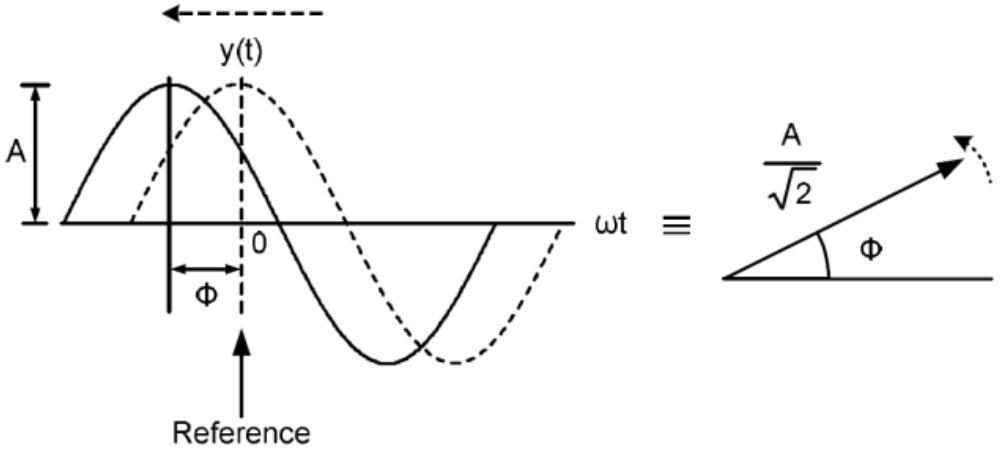

Figure 1.1: Sinusoidal function represented in the time domain and translated to phasor representation.

The angle of a phasor by itself has little significance without a reference. It is common for individual relays to use VA at 0 degrees as a reference for all current and voltage phasors within the device. This is a somewhat arbitrary design decision. However, comparing the angle difference of VA voltage between two separate devices does not give accurate results unless both the waveforms are sampled at exactly the same moment in time.

Synchrophasors allow for precise measurement of voltage, current, phase angle, frequency, and other power system data from different PMUs with exact time stamps. This is possible when a universal time source, a satellite-synchronized clock, serves every PMU. Each PMU uses the universal time source to create a phasor representation of a constant sinusoidal reference signal. The IEEE Standard 1344-1995 defines the start of the second as the time reference for establishing the phasor's phase angle value. The

peak of the reference sinusoid is at the top of each second. This reference signal is the same across all PMUs in the network. A reporting instant, identified by a time tag, defines the absolute relationship between any measured signal and the reference in every device on the power system [2,4].

1.2: SYNCHROPHASOR IMPORTANCE

Global renewable energy investments continue to increase [5] and though it can be predicted, it cannot be directly controlled. Therefore, there is a need for a grid health monitor to observe the margin of grid stability. This dissertation shows the effectiveness of using synchronized phasor measurements as a grid health monitor. Other works for synchrophasor-related Smart Grid Investment Grant (SGIG) can be found in [6]-[8].

In order to show this effectiveness, real data is needed for analysis. Even though most utility companies have PMUs and have data to work with, they are reluctant to share the data with researchers. To protect real-time phasor data and enable data access to researchers, the North American SynchroPhasor Initiative (NASPI) developed the Phasor Data-Sharing Agreement on February 22, 2010 [9]. The Texas Synchrophasor Network was established so that researchers at the University of Texas at Austin are able to have access to real-time phasor data. Chapter 2 will discuss the Texas Synchrophasor Network in more detail.

Conventional wide area monitoring systems such as SCADA (supervisory control and data acquisition), only monitor the grid at a frequency of one sample every 1-4 seconds [3]. However, PMUs are required by the IEEE Standard for Synchrophasor Measurements for Power Systems C37.118 to sample at a rate of at least 10 samples per second for a 60Hz system [10]. In addition, synchrophasor data has applications in wide-

area monitoring, real-time operations, power system planning, forensic analysis, and smart grid [11]. This dissertation will also show that synchrophaors give high resolution for events. For the simple transmission system shown in Figure 1.2, the power flow between points 1 and 2 is shown in (1-2).

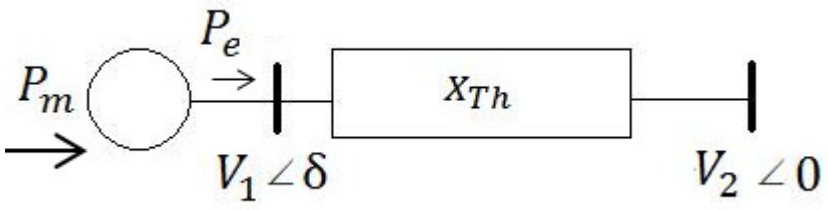

Figure 1.2: Simple Transmission System Model

$$P = \frac{V_1 \cdot V_2}{X_{TH}} \sin \delta \tag{1-2}$$

As the voltages of the two buses and the thevenin impedance between them does not vary significantly during short time periods; the changes in power flow directly affects the angle, δ. Finally, modal analysis on the voltage phase angle gives information on system damping. With the streaming phasor data, a continual monitoring of system damping will show whether grid stability is deteriorating over a period of minutes or hours.

Chapter 2: The Texas Synchrophasor Network

The Texas Synchrophasor Network was started in 2008 thanks to the funding of Electric Power Research Institute (EPRI), Center for the Commercialization of Electrical Technologies (CCET), and equipment donation by Schweitzer Engineering Laboratories (SEL). The network was installed for multiple reasons. Besides giving researchers at UT Austin access to real time data, it was established to prove that comprehensive analysis of data gathered from a few strategically-placed PMUs can be immensely valuable. Initial goals of analysis included studying how high penetration levels of wind generation in Texas affect overall grid operations and stability. Invaluable lessons have also been learned regarding the validity of wall outlet voltage measurements, daily grid operations and grid response to disturbances, how to simply and economically install synchrophasor systems, and how to collect, automatically sift, and analyze large amounts of data.

2.1: EQUIPMENT AND COMMUNICATION

Figure 2.1 depicts an equipment connection for a synchrophasor network. The local PMU station at UT Austin is used as the base station for the Texas Synchrophasor Network. Figure 2.2 shows the physical setup at UT Austin. The equipment for the base station includes:

1. SEL-3378 Synchrophasor Vector Procesor (SVP)
2. SEL-421 Phasor Measurement Unit
3. SEL-2401 Satellite-Synchronized Clock
4. SEL-5076 SynchroWAVe Archiver (optional)
5. SEL-5077 SynchroWAVe Server (optional)
6. SEL-5078 SynchroWAVe Console (optional)

7. SEL-3401 Satellite-Synchronized Clock Display (optional)

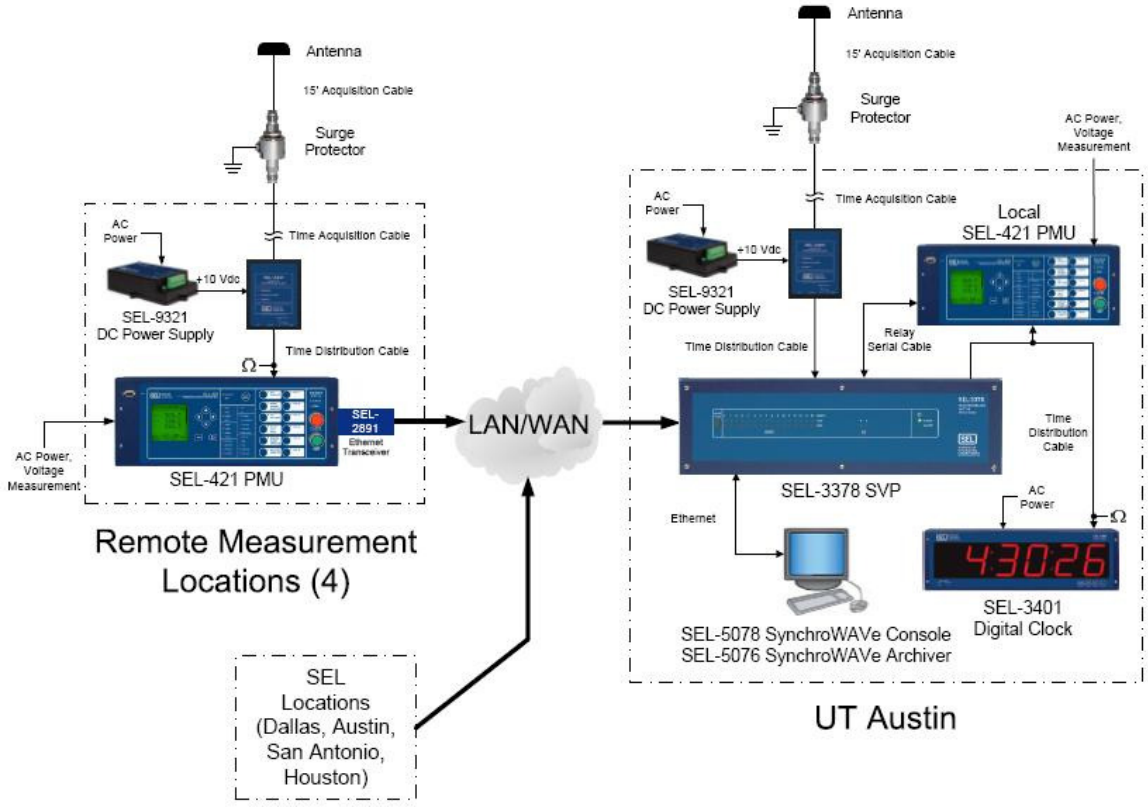

Figure 2.1: Overview of Equipment Connection for a Synchrophasor Network

Figure 2.2: Synchrophasor Setup at UT Austin

The purpose of the synchrophasor vector processor is to time-align the phasor data received from the phasor measurement unit. It also has the capability of analyzing the data in real-time. In the Texas Synchrophasor Network, this function is used for modal analysis. There are many alternative devices that may be used. The Schweitzer alternatives include the SEL-3373 Station Phasor Data Concentrator (PDC), SEL-3530 Real-Time Automation Controller, and SEL-5073 SynchroWAVe PDC software.

The Schweitzer relay SEL-421 is capable of single and three-pole tripping schemes. It is also able to protect both compensated and uncompensated lines by using "five zones of phase and ground-distance elements in communications-assisted schemes, with directional overcurrent backup protection. Optional high-speed elements can be used to achieve subcycle operating time for most fault types and source impedance ratios." [12] The 421 is also capable of phasor measurements and is used as PMUs in the Texas Synchrophasor Network. There are many other options for PMUs. We note that the 421 is serially connected to the SVP.

The SEL-2401 satellite-synchronized clock is a compact, precision-time device. An antenna is connected to the SEL-2401 in order for it to obtain signal from the satellites in orbit. As a precaution, a surge protector was installed between the antenna and the SEL-2401. A +12VDC wall wart is used to power the satellite clock, however any DC power source ranging from 9-30 VDC would be sufficient to power the device. There are also multiple devices that would serve this purpose. The 2401 is essential as the 421 uses this high quality time signal to create a 60 Hz signal. This reference signal is compared to the measured voltage waveform to obtain a voltage phase angle and magnitude. A compensation angle can be added to remove any known net transformer phase shifts. The frequency is measured according to the rate of change of the voltage

phase angle. Since the SEL-421 is compliant with IEEE C37.118 standards, the total vector error is ≤ 1% [10],[12].

The equipment for a remote station is similar to a base unit. Figure 2.3 shows the equipment used at the Cloudcroft remote station. However, a SEL-2890/2891 ethernet transceiver is needed for the remote 421s to send data to the SVP. The ethernet transceiver is setup to connect to one of the RS-232 ports on the 421 and send the 421 data via internet. Most remote stations use a static IP with a specified port for this connection. However, some remote stations have their transceiver Dynamic Host Configuration Protocol (DHCP) enabled. This allows more flexibility when establishing network communications at remote stations. A comprehensive step-by-step setup procedure can be found in Appendix A.

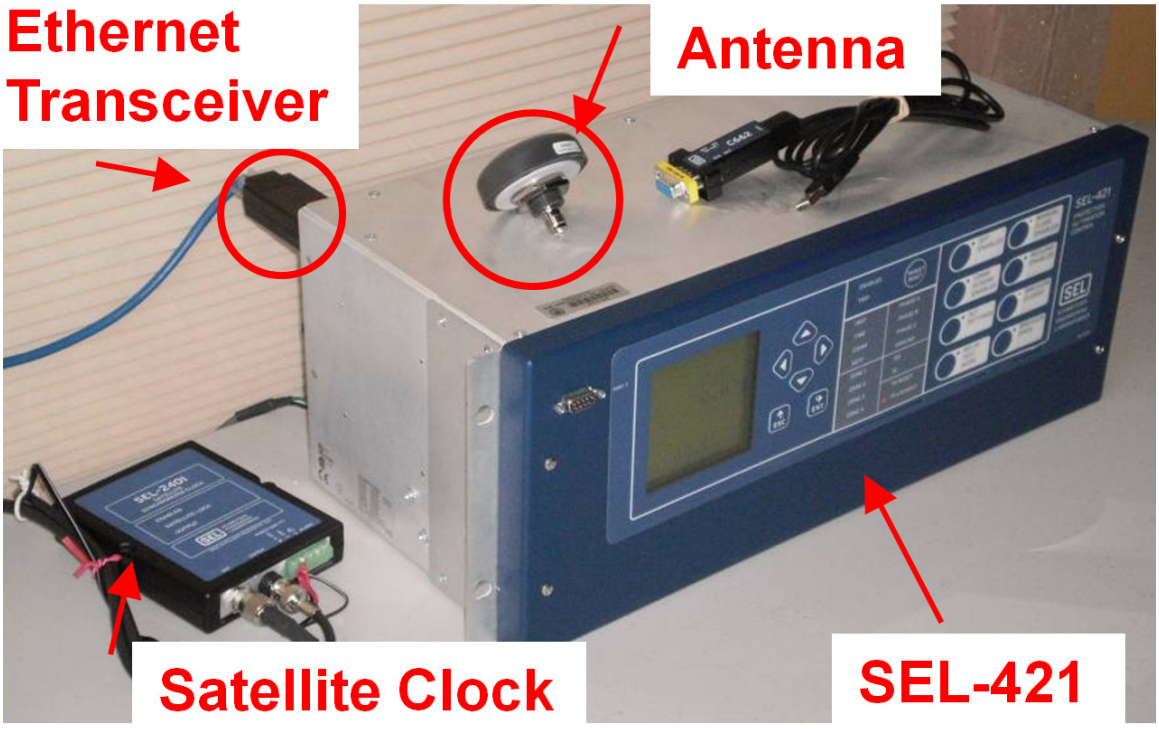

Figure 2.3: Cloudcroft Remote PMU Station Equipment

2.2: GRIDS AND STATIONS

The Texas Synchrophasor Network consists of a local PMU station located at the Engineering-Science Building (ENS) 212 of the University of Texas at Austin. As of June, 2013, remote PMU stations in the ERCOT grid are located at the McDonald Observatory, the University of Texas-Pan American, the Harris 69kv Substation, and Brazos Electric in Waco. For a better understanding of the distance and placement of the stations, a map of Texas with active PMUs in the Texas Synchrophasor Network is shown in Figure 2.4. Aside from these, we currently have remote PMU stations in the Western and Eastern Interconnection at Maryland, California, and Nebraska. At other points in time, remote stations were located at the SEL offices of Houston, Fair Oaks Ranch/Boerne, Pullman WA, Charlotte NC, Guadalajara and Mexico City Mexico, and Brazil. Aside from SEL offices, we had remote stations at Knoxville TN and Cloudcroft NM.

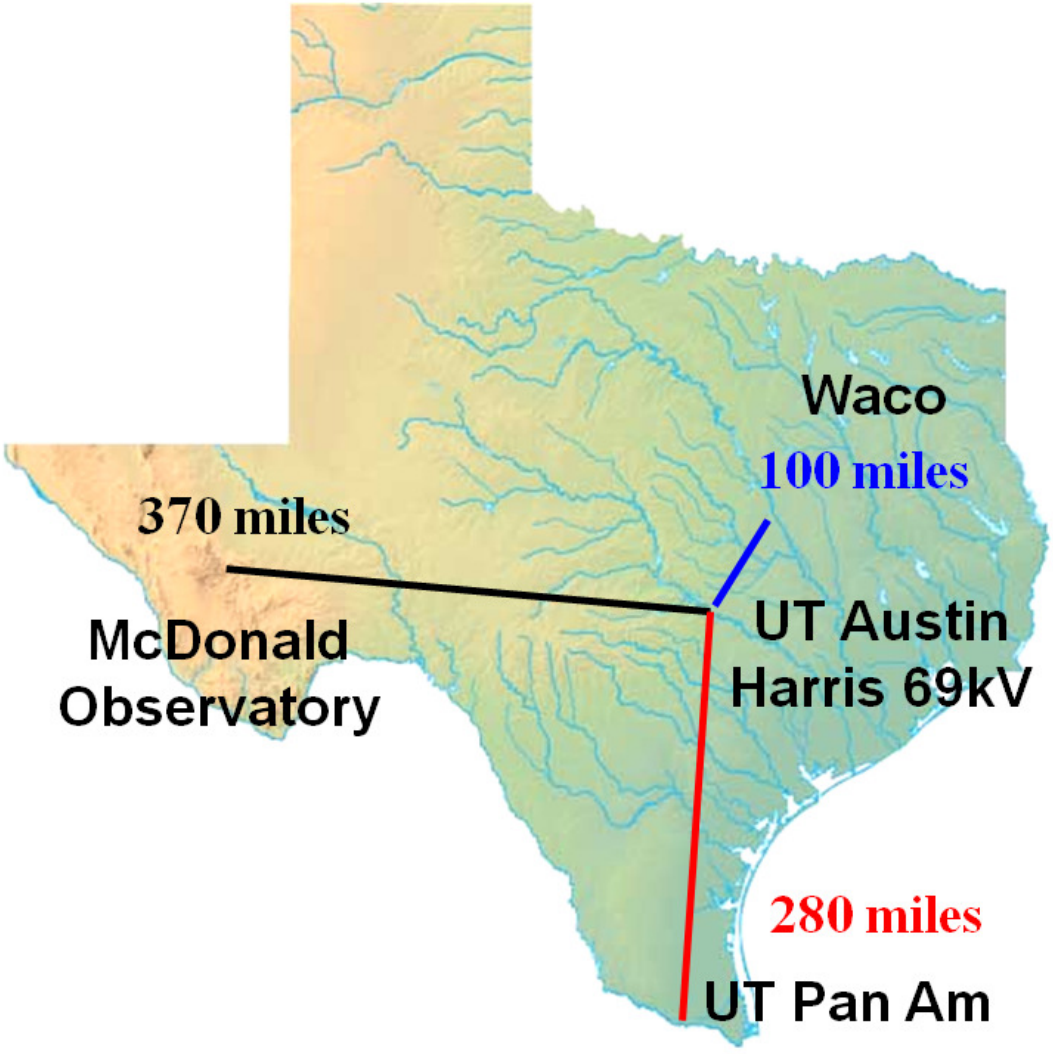

Figure 2.4: The Texas Synchrophasor Network in ERCOT

Chapter 3: Synchrophasor Programs

Multiple synchrophasor programs are used in this research. The programs used for communication with PMUs, view streaming data, and archive them are SEL programs. These include the SVP Configurator, SEL-5077 SynchroWAVe Server, SEL-5078 SyncrhoWAVe Console, and SEL-5076 SynchroWAVe Archiver. The programs used to validate, screen, and analyze the data are developed at UT Austin. These include the PMU Daily Screener, the PMU Waveform Analyzer, and the PMU Modal Analysis.

The SEL SynchroWAVe programs are focused more on real-time while the programs developed at UT Austin are focused on post-event analysis. There is currently no real-time program that is considered as a "commercially sustainable, production-grade reliability tool", but available programs include [3],[13]-[16]:

- Synchronized Measurement and Analysis in Real Time (SMART) by Southern California Edison (SCE)
- Phasor Real Time Dynamics Monitoring System (RTDMS) by Consortium for Electric Reliability Technology Solutions (CERTS)
- e-terravision by Alstom's AREVA T&D
- PowerWorld Retriever by PowerWorld Corporation

3.1: SEL PROGRAMS

3.1.1: SVP Configurator

The SVP Configurator is the program that performs internal analytical calculations and controls the settings of the SEL-3378 SVP. The program is split so priorities can be set for different tasks. Tasks include receiving data and inputting it into the local space internal to the SEL-3378 for desired analysis. Other tasks include calculating angle differences to be fed in as an input to the modal analysis. The SVP is able to compute up to 15 modes for each input signal. The current input signals are the angle difference between McDonald Observatory and UT Austin and UT Pan Am and UT Austin. The SVP configurator controls the input and output of the SVP. It is here that you set the IP address and PMU ID for each connected device. Without the correct IP and ID of each device, there will be no established communication. To ensure everything is working properly and to help debug problems, the SVP Configurator contains error messages defined by the programmer in each task. It is also important to note that once the program is uploaded to the SEL-3378, even if the computer is turned off, the SVP will still be running the program and will continue to communicate with clients. This allows users to work on adding new tasks while not having to stop the SVP from functioning. Figure 3.1 shows the SVP Configurator with a check on input 1. We note that input 1 is connected and there are no errors, therefore we see “True” beside the appropriate statuses.

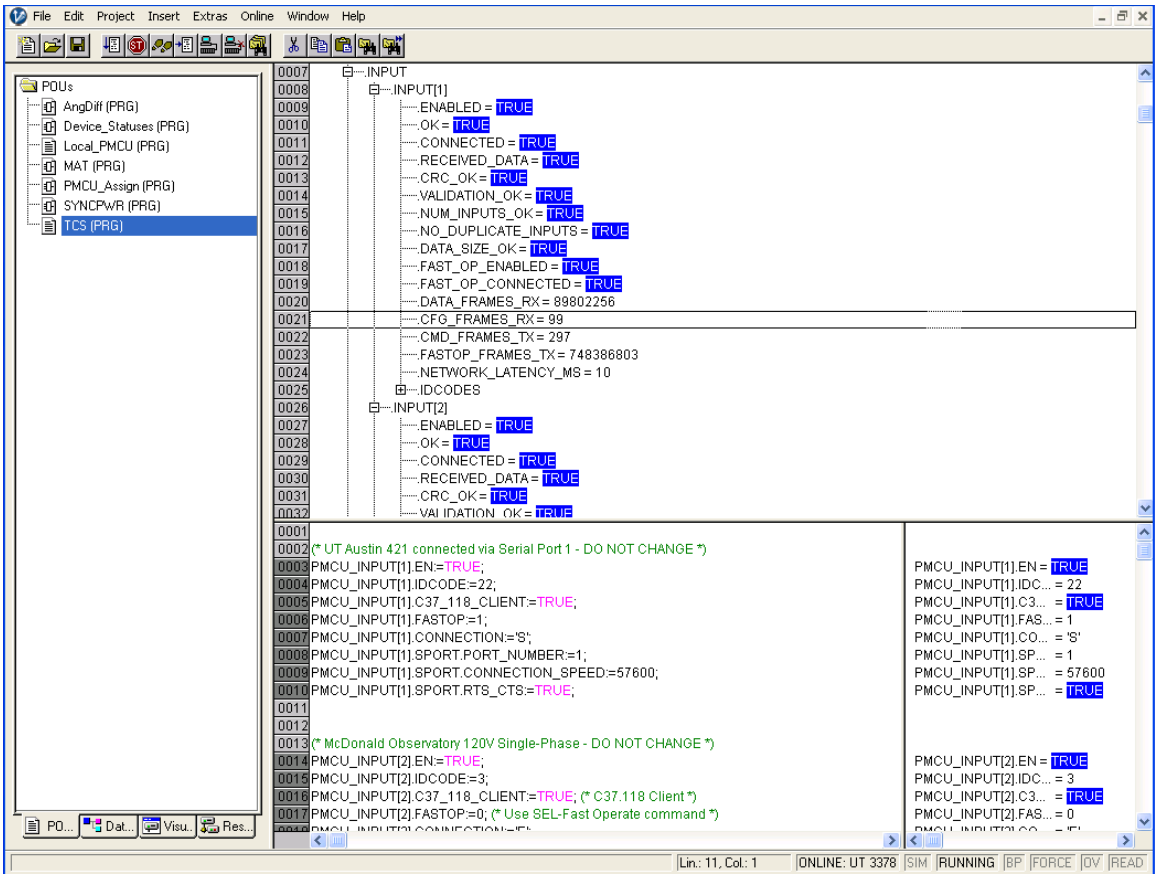

Figure 3.1: SVP Configurator

3.1.2: SEL-5077 SynchroWAVe Server

The SynchroWAVe Server, shown in Figure 3.2, is an intermediate communication program that is used to rebroadcast synchrophasor data. This program was required in our setup simply because the SVP has two outputs: one from time aligning all the input data and another from performing the modal analysis.

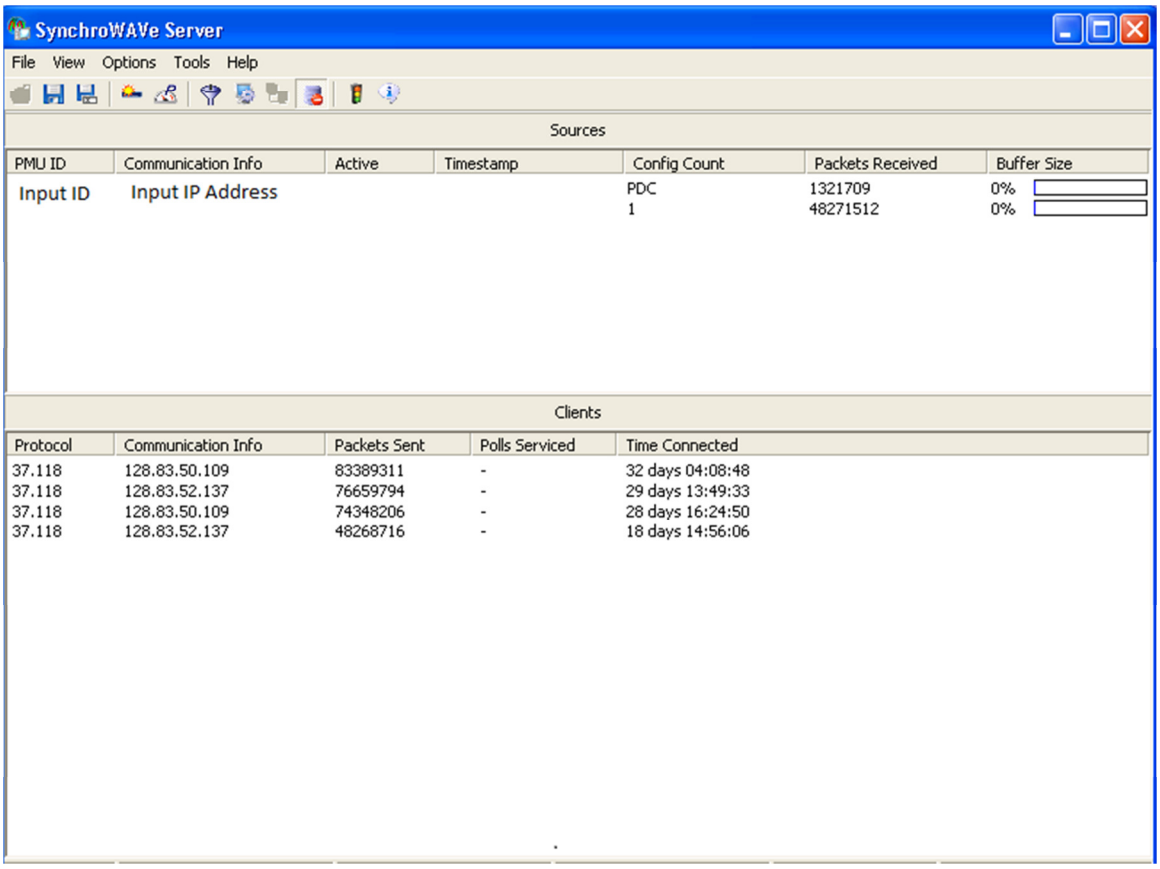

Figure 3.2: SynchroWAVe Server

3.1.3: SEL-5078 SynchroWAVe Console

The SynchroWAVe Console is used to view the real time data being sent to the SVP. The program can display frequency data and phasor data such as shown in Figure 3.3. We note the figure shows UT Austin as the reference for the phasor display. It is important to note here that the communication can be setup by either programming the SEL-3378 to have the Console as a client or to connect to the SynchroWAVe Server. Without the correct PMU ID, IP address, data port, and command port numbers, the Console will be unable to receive information to display.

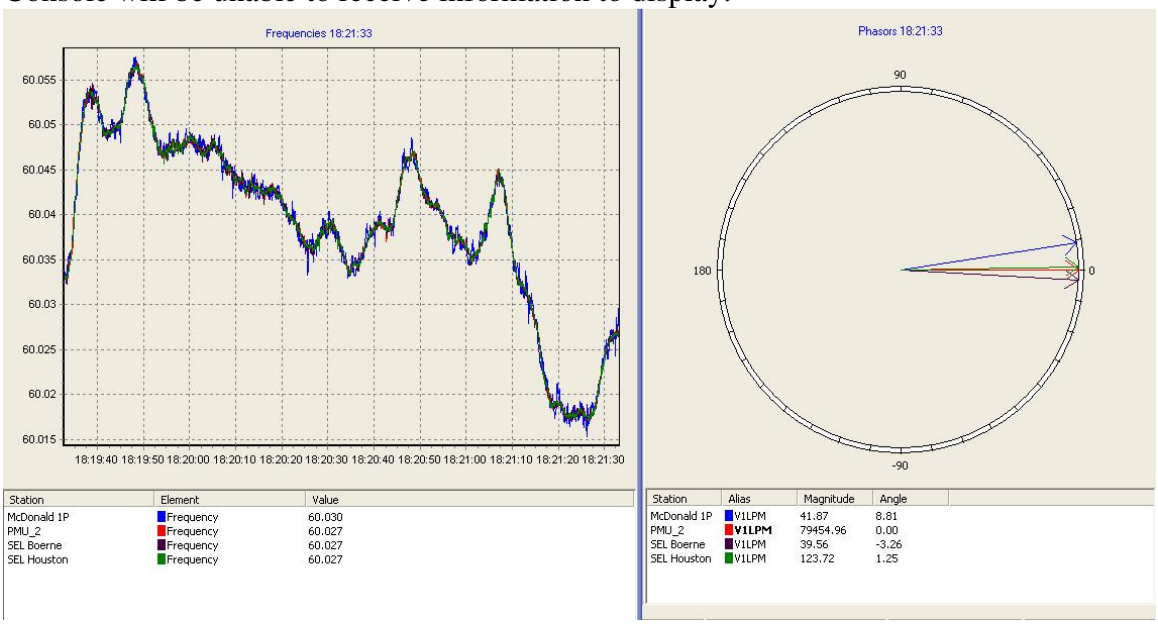

Figure 3.3: SynchroWAVe Console displaying Frequency and Phasor

3.1.4: SEL-5076 SynchroWAVe Archiver

The SynchroWAVe Archiver is a program that archives desired data chosen from the data sent to the SVP. Currently, the Archiver is recording daily phasors of all the stations as well as the modal analysis being done by the SVP Configurator. The rate at which the data is being sent is 30 messages per second. The Archiver is setup to archive the data in hourly csv files in the form of year, month, day, time, UT, Austin, 3378, Phasor. For example, "120312,08000000,UT,Austin,3378,Phasor" is the phasor data for March 12th, 2012 at 8am GMT. Similar to the SynchroWAVe Console, the Archiver will only receive information if the SVP is preprogrammed to send information to the Archiver or programmed to connect to a SynchroWAVe Server. It is important to note that the Archiver will not automatically choose which parameters to archive. Therefore a "New Recorder" must be created under "Tools"→ "Archives" for desired settings. Figure 3.4 shows the Archive screen with the phasor settings. The green arrows are the parameters chosen to be archived. We note here the PMU names that show up are a result of the PMU settings.

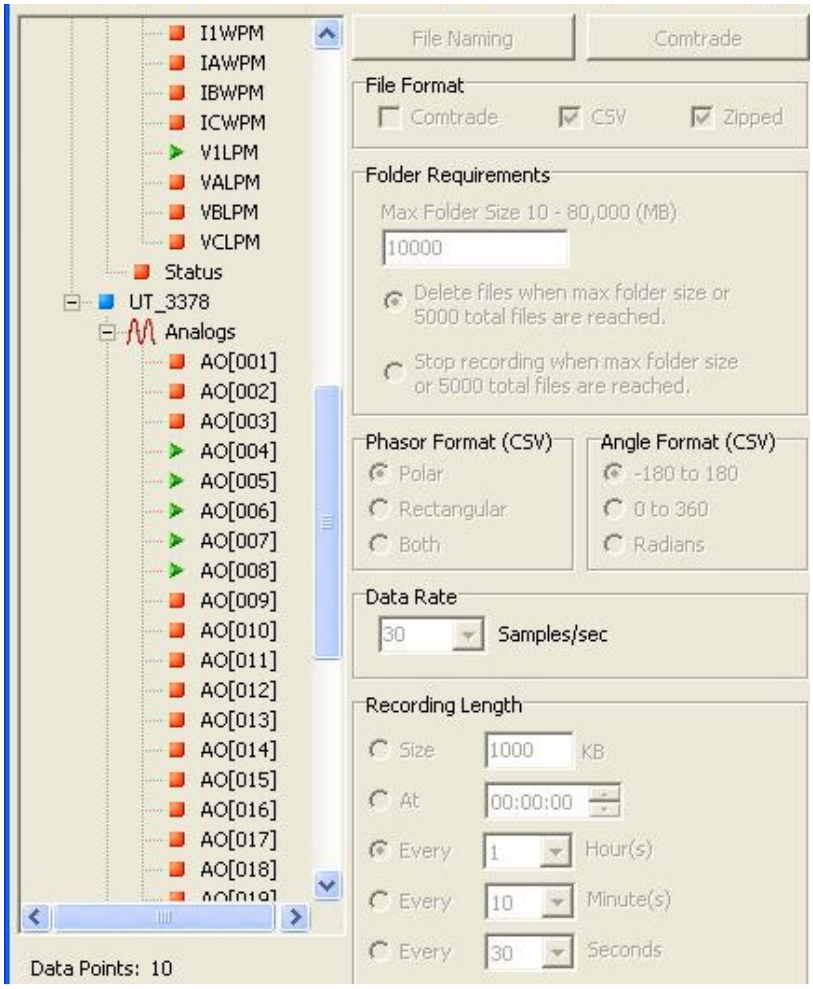

Figure 3.4: SynchroWAVe Archiver

3.2: DATA INTEGRITY BY DAILY SCREENER

The Daily Screener program is a user friendly Visual Basic program that allows the user to efficiently scan through a day's phasor data to find errors in the file, events that may have occurred, and amount of dropouts. An option to scan the entire day or multiple days is also present. A quick method to view which units are online is to scan only the first minute. Once the first minute is scanned, the user can choose to keep

certain PMUs offline and also select which PMU to set as the reference. This function is to allow PMUs from different grids to be archived in the same file, but still be analyzed. A dropout list box will continue to build as more hours are screened. This allows an easy view of hourly drop outs. This program also writes the results into a date-tagged file which allows for an ease of reading, logging of possible events, and plotting of angle averages. This program is currently the most efficient method for us to plot weekly averages which give insight to slow events as described in section 5.1. Figure 3.5 shows the Daily Screener and Figure 3.6 shows the results in the date-tagged file.

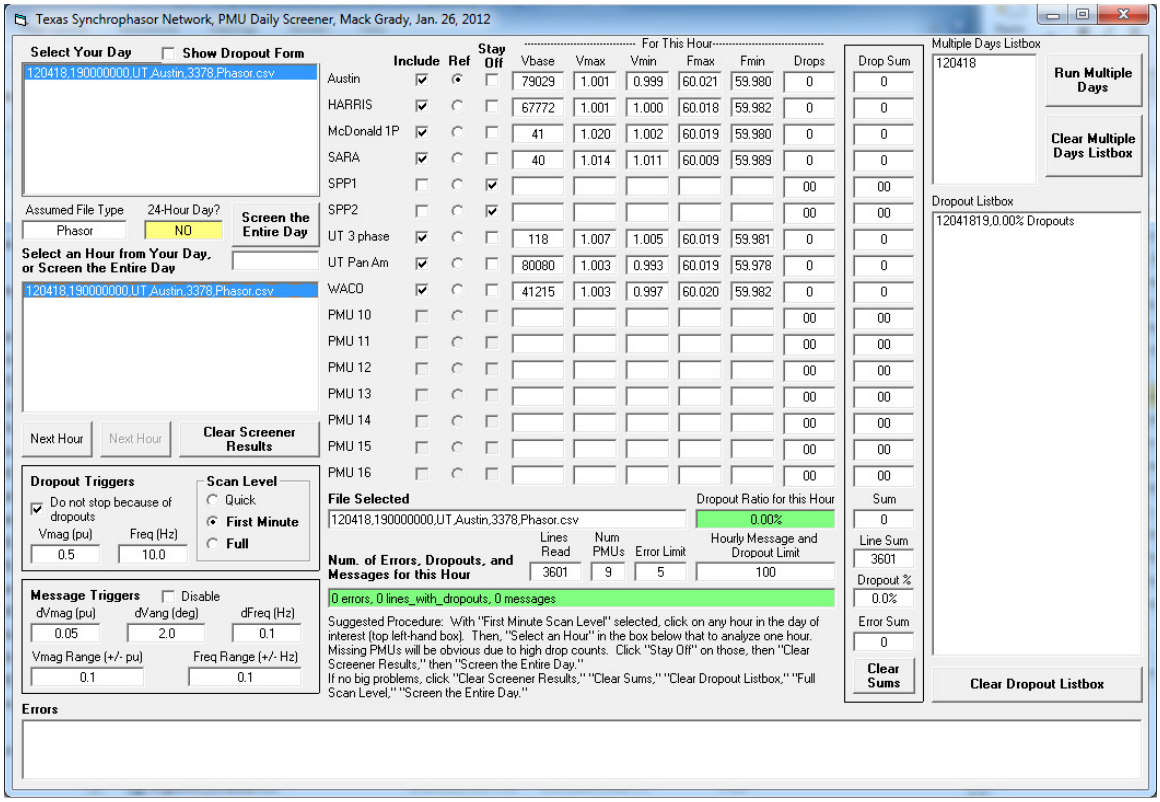

Figure 3.5: Daily Screener

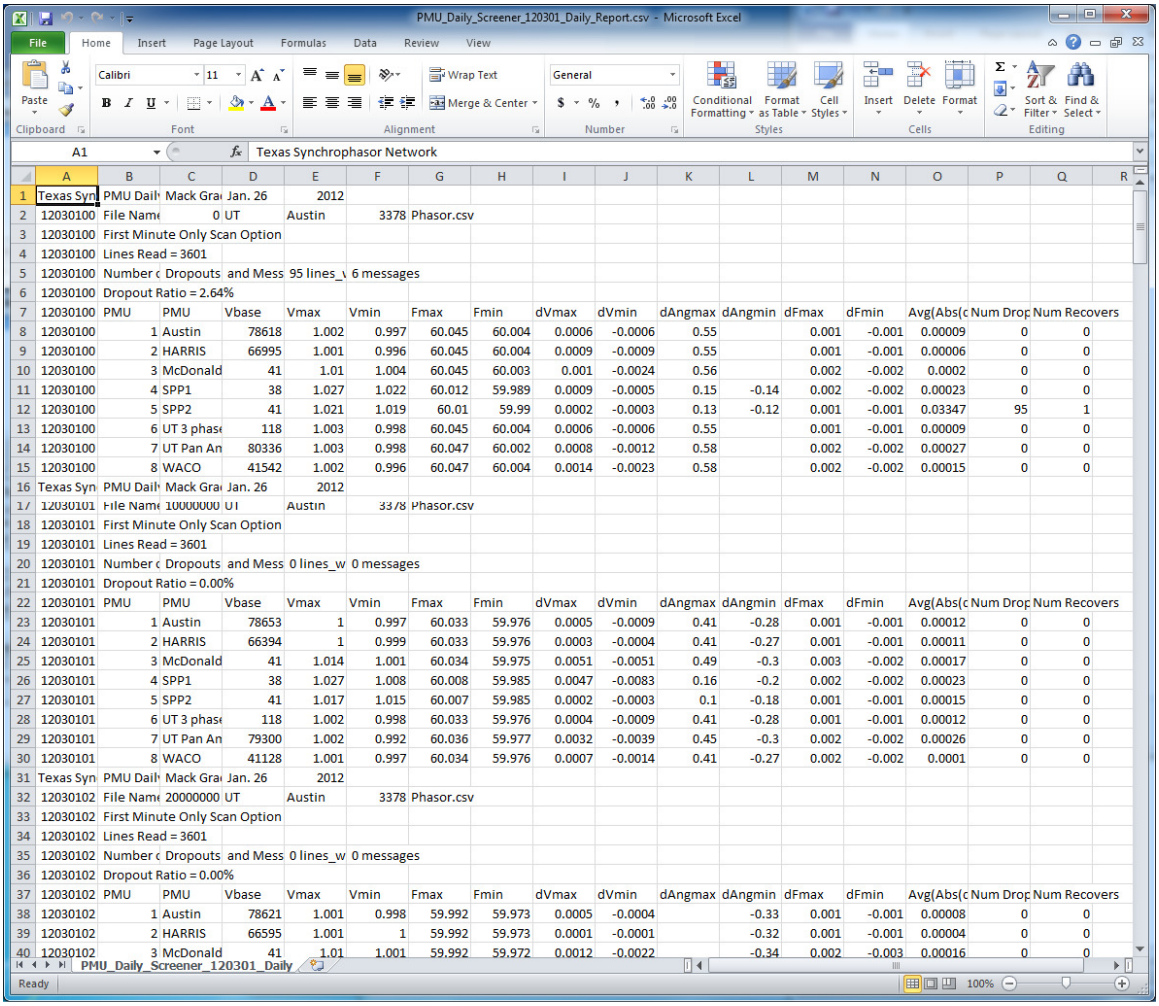

Figure 3.6: Daily Screener Results

3.3: WAVEFORM ANALYZER

The Waveform Analyzer, shown in Figure 3.7, is used to analyze the phasor data once the data has been validated by the Daily Screener. When the program first starts, a list of available phasor data in the folder will appear for the user to choose from. Once an hour is chosen, the program automatically defaults to the minute containing the largest change in frequency of that hour and plots the angles. The program defaults with plotting

only the McDonald Observatory and UT Pan Am with respect to Austin 1-phase. This program allows the user to select the number of PMUs to plot and the PMU to be used as reference. This is an essential function as not all PMUs are in the same grid. Even though all grids operate at 60 Hz, different grids operate at slightly different frequencies. The user may also choose to plot voltage magnitude, frequency, or voltage phase angle. Since not all PMUs have their net 30 degrees removed, an angle correction may be added. A choice of x-axis and y-axis boundaries can also be chosen, but generally the max/min option will display the plots the best.

Additional analysis functions are the Fast Fourier Transform (FFT) plot and the ringdown detection. The FFT give insight to the frequency of oscillation and aids the ringdown detection algorithm. The user is able to choose to screen the hour or day for unusual events. The ringdown detection algorithm may be changed, but is defaulted to values that have given the best results through experience. Another method to analyze the data is to use the different windows at the left side of the program. The first window lists the minutes chronologically. The second window lists the minutes with increasing frequency change. The last window lists the minutes with increasing angle change. To aid in recording the minute(s) of interest, a text file is saved for each plot viewed. The name of the text file is located directly beneath the main plot.

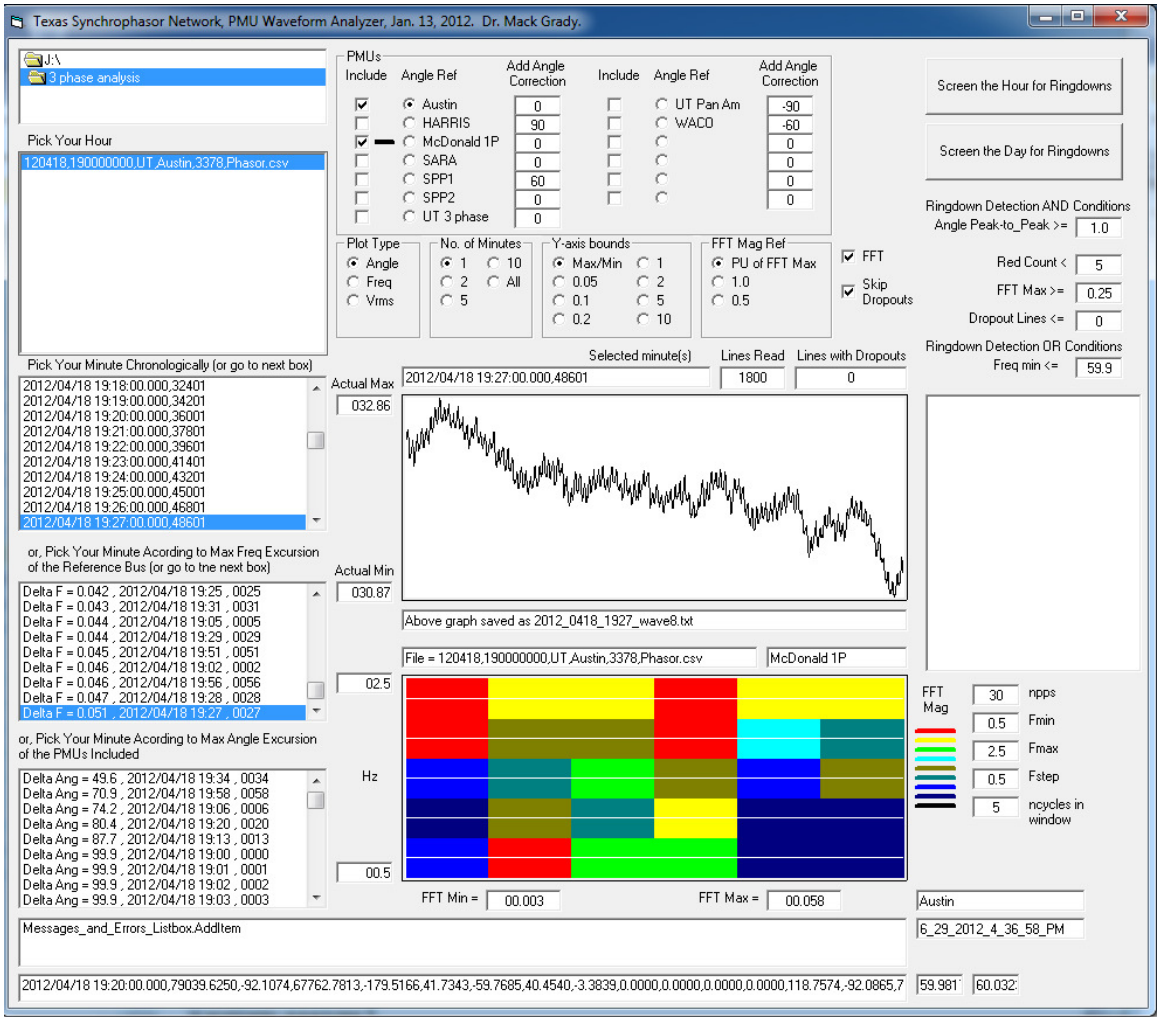

Figure 3.7: Waveform Analyzer

3.4: MODAL ANALYSIS

The Modal Analysis program takes the archived modal data and plots three graphs: Frequency vs. Damping Ratio with Magnitude in color, Frequency vs. Time with Damping Ratio in color, and Frequency vs. Time with Magnitude in color. Figure 3.8 shows the main screen of the program and example plots of the results are shown in Figures 3.8 – 3.11. As can be seen in Figure 3.8, the top left box displays a list of files

you can display. Once a file is selected, the user can choose the input signal to get the voltage phase angle of McDonald Observatory with respect to UT Austin or UT Pan Am with respect to UT Austin. In order to quickly observe certain points, there are three boxes that show the magnitude, frequency, and damping ratio. Clicking on any of the numbers in those boxes will automatically take you to the line containing that data. It is also important to note the screening feature this program presents. At the bottom of the main screen, the user is allowed to choose the range of magnitude, frequency, and damping ratio desired and click on the "Screen Points" button. A list of points falling into the screening parameters will be displayed. If desired, the user can plot those points simply by clicking on them. Please note that the user should clear the screen before doing this.

In Figure 3.9, the scatter plot is frequency vs. damping ratio with magnitude shown in color. The box shows the main mode of the plot and the values are given below the scatter plot. In the example shown, the main mode has frequency = 0.67 Hz, average magnitude = 0.24, and damping ratio = 0.27. Figures 3.10-11 show the scatter plot of frequency vs. time with magnitude and damping ratio in color respectively. This allows for easy identification of trends that appear.

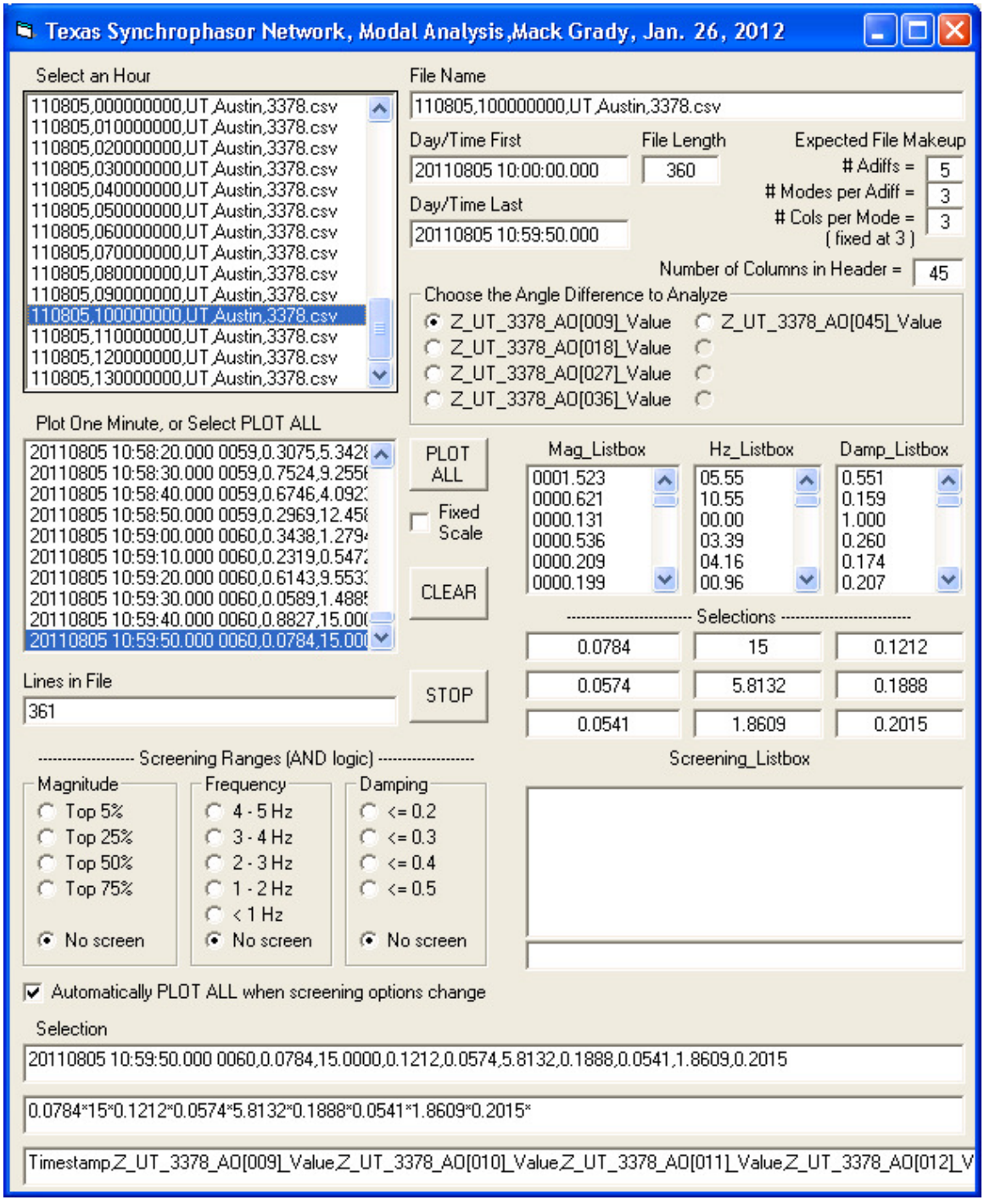

Figure 3.8: Modal Analysis main screen

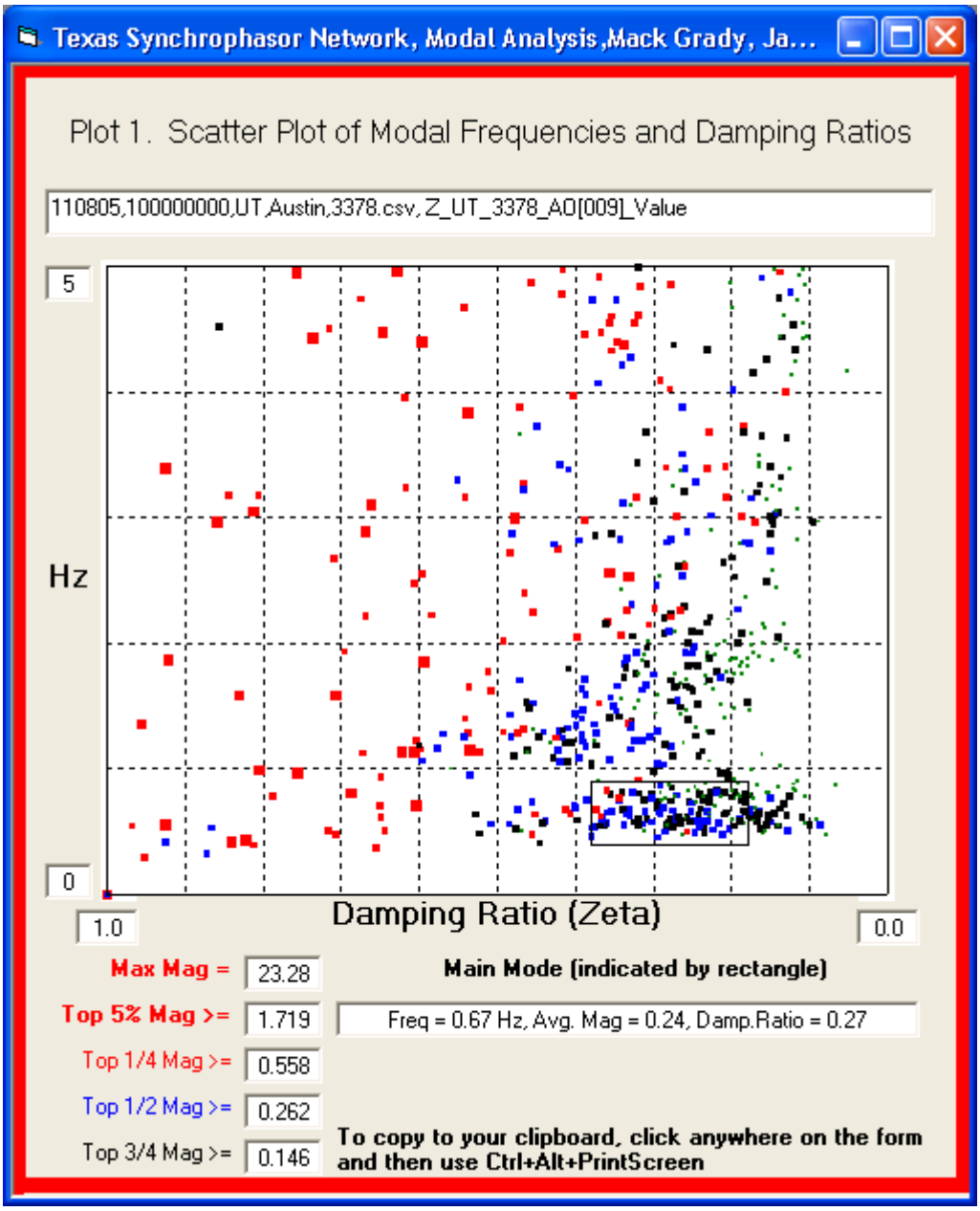

Figure 3.9: Modal Analysis Frequency vs. Damping Ratio with Magnitude

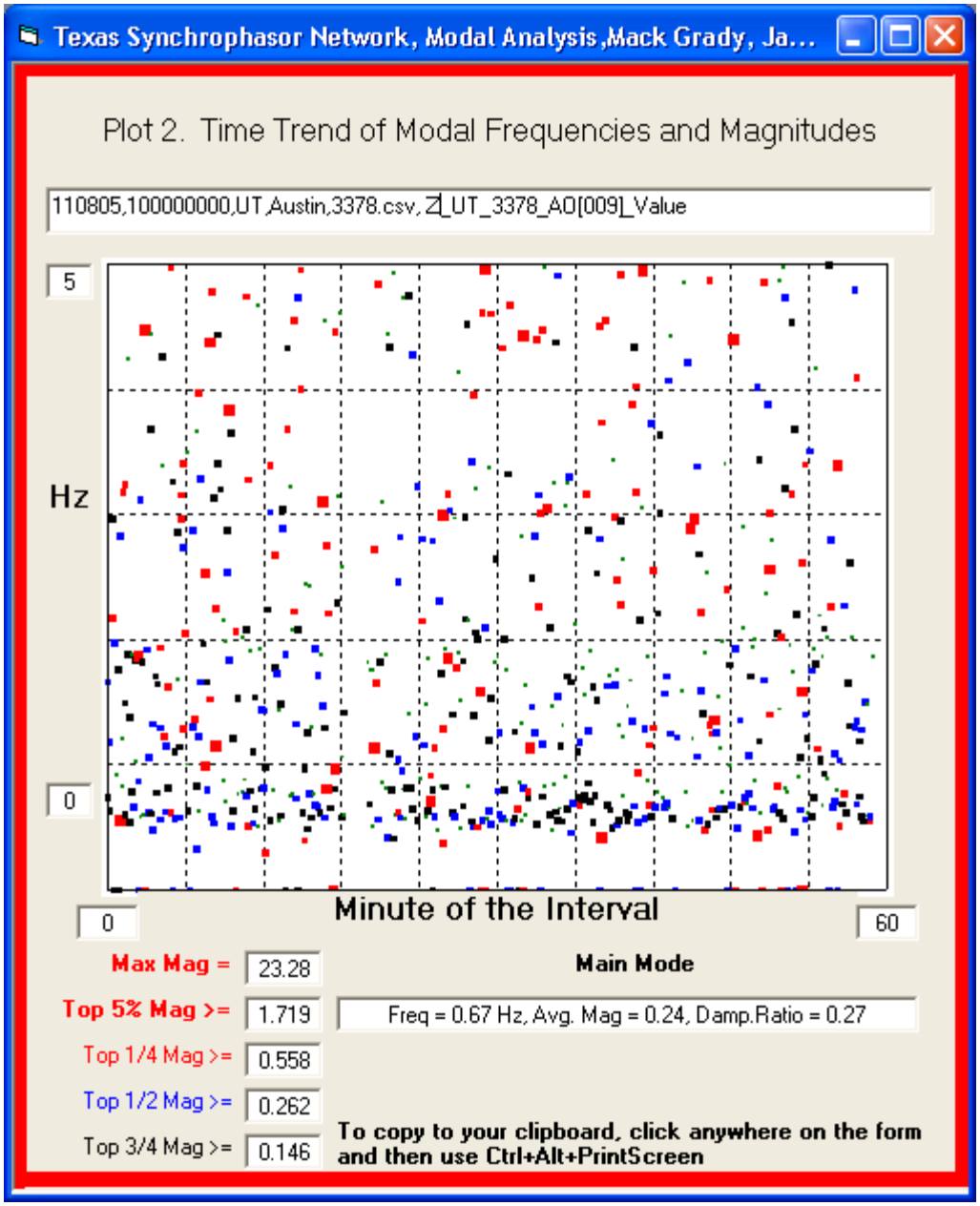

Figure 3.10: Modal Analysis Frequency vs. Time with Magnitude

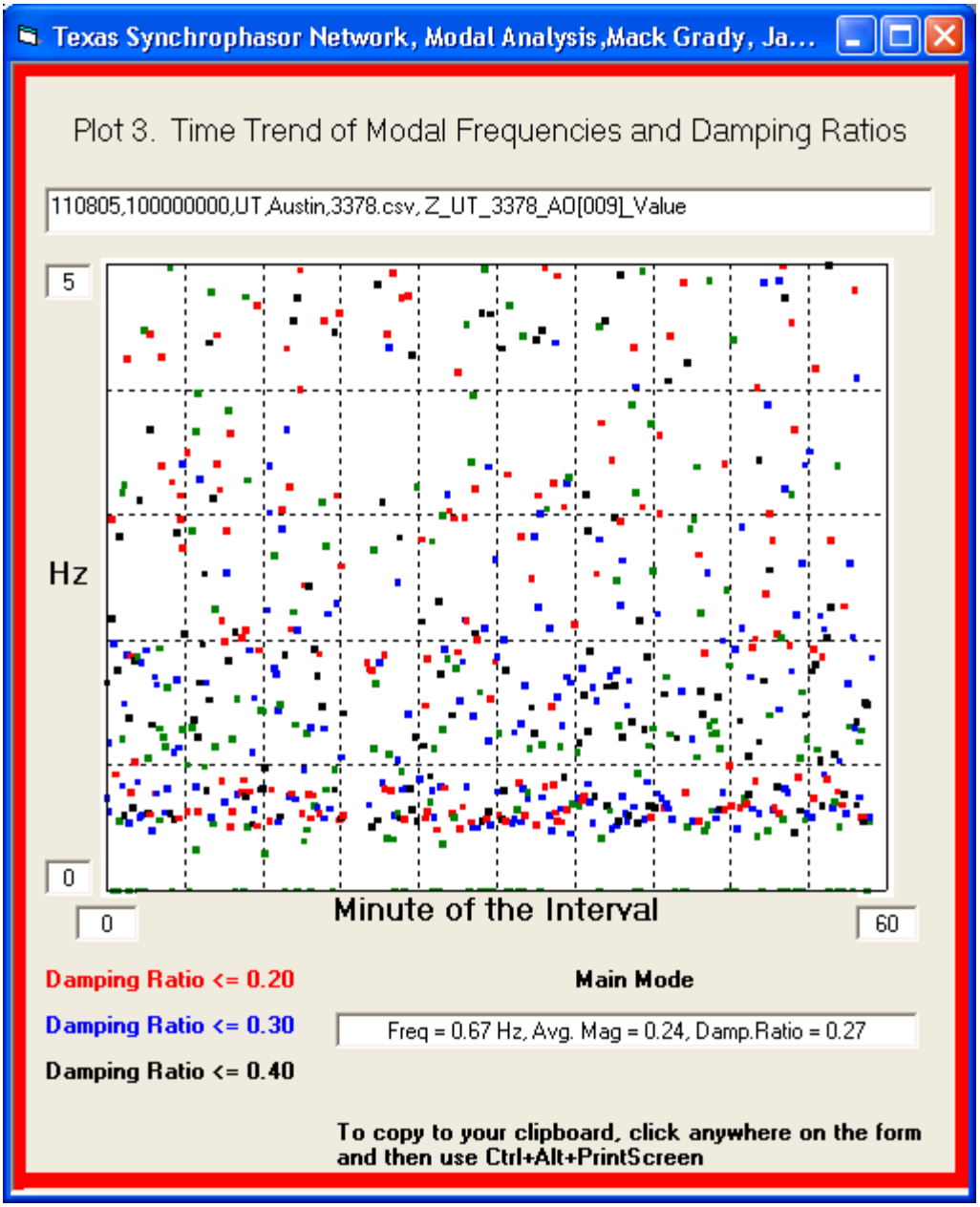

Figure 3.11: Modal Analysis Frequency vs. Time with Damping Ratio

Chapter 4: Key Lessons Learned

This chapter documents the key lessons we have learned from the Texas Synchrophasor Network. These lessons include verification that 120V wall outlets are suitable for synchrophasor analysis, the impact of connecting units in 3-phase instead of 1-phase, impact of wind generation on grid damping ratio and inertia, and estimating West Texas thevenin impedance.

4.1: LESSON #1: PMU CONNECTION ANALYSIS

The Texas Synchrophasor Network is an independent network; therefore access to high voltage is not readily available. As such, it was of interest to determine the effects of using 120V wall outlets as the input to our PMUs. A secondary interest was to determine whether a significant impact occurs when the unit is connected in 3-phase instead of 1-phase.

Aside from physical connections, there are concerns regarding bandwidth for PMU data. As of June, 2012, a total of 11 PMUs are streaming data in and are archived hourly. Each archived file includes the magnitude, phase angle, and frequency of the unit. The current zipped hourly file is less than 9 Megabytes (MB). The current uncompressed hourly file is 30 MB with each addition PMU adding 2.5 MB. This translates to each additional PMU adding approximately 700 bytes per second.

4.1.1: 120V Wall Outlets are Suitable for Synchrophasor Analysis

Most of our PMUs are connected to 120V wall outlets or building supply voltages. SEL-421 relays/PMUs accept either “single phase input” or “three phase positive sequence input.” At McDonald Observatory, UT Austin, and Boerne (San

Antonio), we use 120V single phase as our input signal. At Houston, we use 120V three-phase positive sequence. Therefore it is of interest to determine the effects of using 120V wall outlets.

Obviously, 120V wall outlets are not as high in quality as what you would expect from PMUs connected directly to a transmission grid. Distribution feeders and buildings contain noise, but this noise tends to be well above the 0.5 – 5 Hz range-of-interest for synchrophasors and can be filtered out of the analysis. Besides that, SEL-421s are well filtered and designed to perform flawlessly in electrically noisy environments, such as transmission or distribution faults.

There is some load-related phase angle shift through substation transformers and along feeders, beyond that due to Y-Δ transformers. My own experience with harmonic studies on distribution feeders is that this additional phase shift is less than 3º or 4º over the entire load range, i.e. "no load" to "full load." Over periods of minutes or even hours, this extra shift is rather constant and thus has little or no impact on observed system oscillation modes and damping rates. A good fixed estimate is 2º [17]. A partial answer to the 120V question can be made by comparing the angles of Austin, Boerne, and Houston to McDonald.

Consider the two-minute interval shown in Figure 4.1, which occurred shortly before midnight on April 9. The three graphs are the relative angles of McDonald Observatory with respect to Boerne (top), Austin (middle), and Houston (bottom). Wind generation is about 17% of total generation. The phase angles are relatively constant across the two-minute interval. It is clear that the three graphs are essentially the same except for their average values

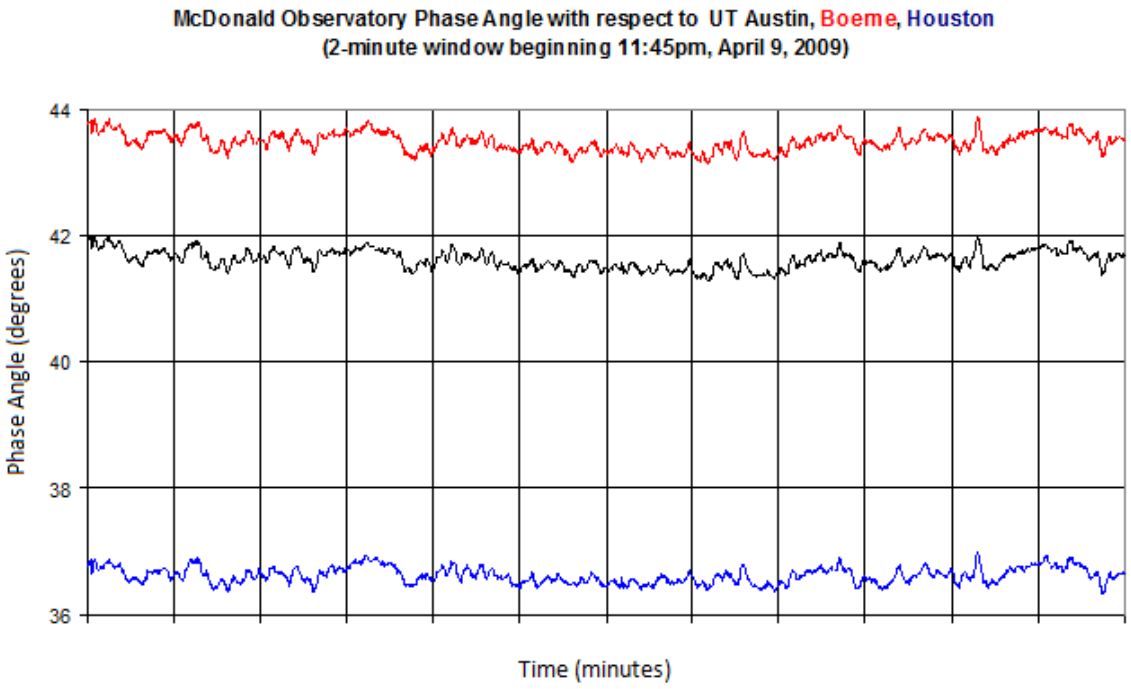

Figure 4.1: McDonald Observatory voltage phase angle with respect to Boerne, UT Austin, and Houston beginning 11:45pm CDT, April 9, 2009

Using the correlation function (4-1), the correlation between all three pairs of two curves are given in Table 4.1.

$$Correl(X,Y) = \frac{\Sigma(x-\bar{x})(y-\bar{y})}{\sqrt{\Sigma(x-\bar{x})^2\,\Sigma(y-\bar{y})^2}} \qquad (4\text{-}1)$$

Table 4.1: Correlation Values

Vector X	Vector Y	Linear Correlation
McDonald – UT Austin	McDonald – Boerne	0.98
McDonald – Boerne	McDonald – Houston	0.91
McDonald – Houston	McDonald – UT Austin	0.92

The correlations are very strong, which means that from the McDonald Observatory vantage point, the waveshapes of the UT Austin, Boerne, and Houston angle variations are essentially identical except for their average value and possible scale factor.

Now, examine the scatter plots shown in Figure 4.2 to 4.4. Each X and Y axes spans 1º. Diagonal lines are drawn at 45º to assist in interpreting the plots. Figure 4.2 appears to have a 45º slope. This indicates that from the McDonald viewpoint, UT Austin and Boerne angles are varying with almost exactly the same magnitude. This is logical because UT Austin and Boerne are only 80 miles apart, yet very far from McDonald. Figure 4.3 appears to have a slope slightly less than 45º. This means that when viewed at McDonald, Houston varies slightly less than Boerne. This is reasonable because Houston is 150 miles further and has a huge inertia. Figure 4.4 is consistent with Figure 4.3, i.e. its slope is slightly greater than 45º, indicating that Austin varies more than Houston.

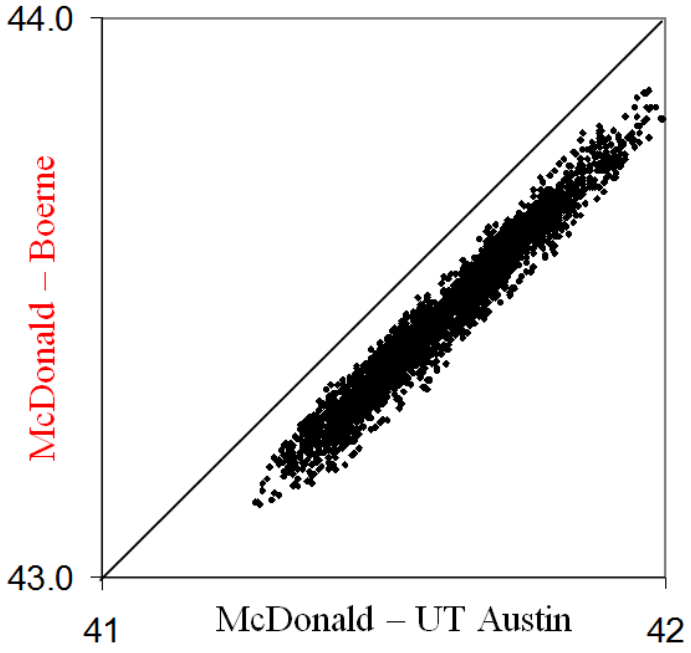

Figure 4.2: Scatter plot of McDonald Observatory with respect to Boerne vs McDonald Observatory with respect to UT Austin

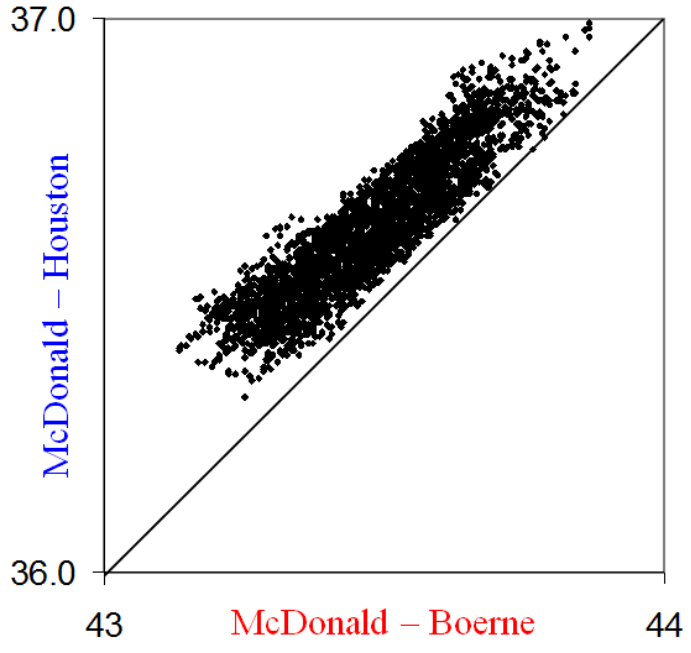

Figure 4.3: Scatter plot of McDonald Observatory with respect to Houston vs McDonald Observatory with respect to Boerne

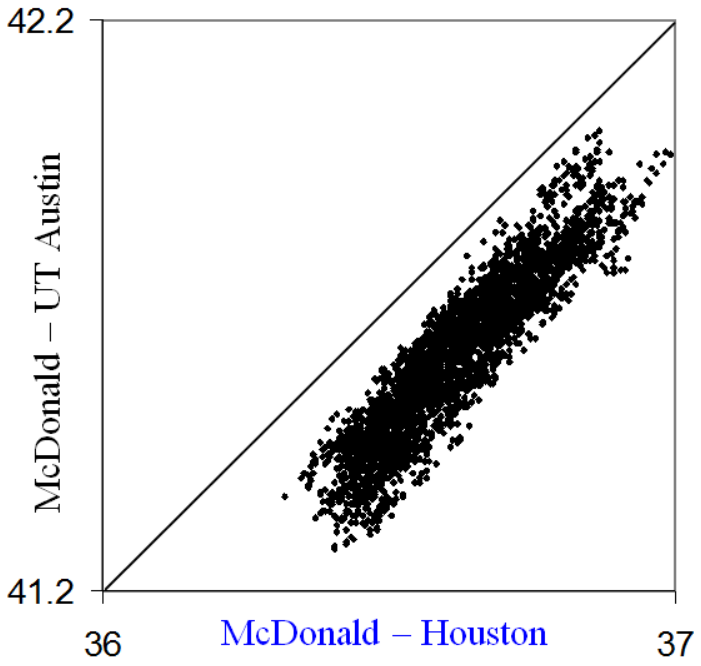

Figure 4.4: Scatter plot of McDonald Observatory with respect to UT Austin vs McDonald Observatory with respect to Houston

After our Harris 69kV substation PMU was installed, we were able to compare our 120V PMUs with a high voltage PMU. Fig. 4.5 shows the voltage ringdown at McDonald Observatory with respect to UT Austin 120V wall outlet and nearby Harris 69kV substation. The fixed net 30 degree phase shift between UT Austin 120V and Harris 69kV has been removed. The variable but steady power flow phase shift through the substation transformer has also been removed. The waveform shows that a 120V outlet PMU gives a resolution that is nearly identical to the 69kV. The difference is insignificant for any of the phasor applications we have come across.

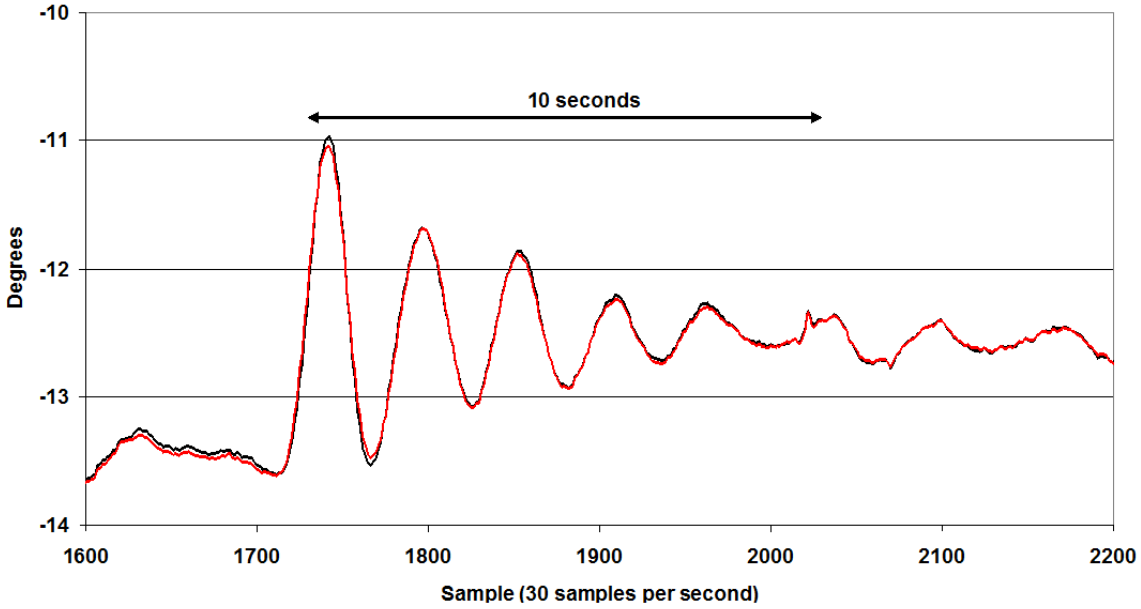

Figure 4.5: Voltage ringdown at McDonald with respect to 120V UT Austin (black) and 69kV Harris (red)

4.1.2: 3-PHASE VS 1-PHASE

In order to observe the effect of connecting our PMUs as 3-phase instead of 1-phase, a 3-phase PMU was installed next to the UT Austin 1-phase unit. The 3-phases were brought in from different outlets and were first tested by viewing them on an oscilloscope to determine they were 3 different phases. To statistically analyze the data, we must first recall that the SEL-421 measures positive sequence phase angle based off available voltage or current information. That is, if only phase A was being recorded, the positive sequence being reported is only calculated based off phase A. However, if all 3 phases are being recorded, then only when all 3 phases are balanced will the positive sequence produce the same angle as phase A. Also recall that the frequency is measured according to the positive sequence. Therefore, since 1) it is difficult to compare the

voltage phase angle for the 1-phase reading and 3-phase reading and 2) measured frequency is based off 3 positive sequence voltage which is calculated according to all 3 phases being received, we can conclude that a statistical analysis on the recorded frequency will give a good indication whether a 3-phase connection for each PMU is required. We note that the initial assumption is that the 3-phase connection will be more accurate.

Since the Harris 69kV substation is not connected to a wall outlet, the frequency measurements from this unit can be taken as the frequency to be compared with. In Figure 4.6, for the hour of 2011, November 22, 1800 GMT, we plotted the Harris frequency on the y-axis and both UT 1-phase and UT 3-phase on the x-axis. A linear regression line for both clusters was calculated and the results are:

UT 1-phase: $y = 0.004304 + 0.999928x$

UT 3-phase: $y = 0.004223 + 0.999930x$

A correlation coefficient was also calculated and the results are:

UT 1-phase: $r = 0.999945$

UT 3-phase: $r = 0.999946$

From this, it is already apparent that there are very minimal differences between a one phase and three phase connection. Furthermore, an f-test was performed in order to see what the squared sum of error for the hour is.

UT 1-phase: $SSE = 0.002257$

UT 3-phase: $SSE = 0.002234$

The squared sum of error is the error between the regression line and the observation points. This result means that the 3-phase connection shows a closer linear relationship to the Harris unit when compared to the 1- phase unit. When the same analysis was done on multiple hours, they all showed similar results. Table 4.1 shows

compiled results of differences for an entire day. It should be noted that even though there is a difference, it is insignificant as it takes 5 significant digits to notice a difference. Most frequency events are only significant to the 2nd or 3rd significant digit.

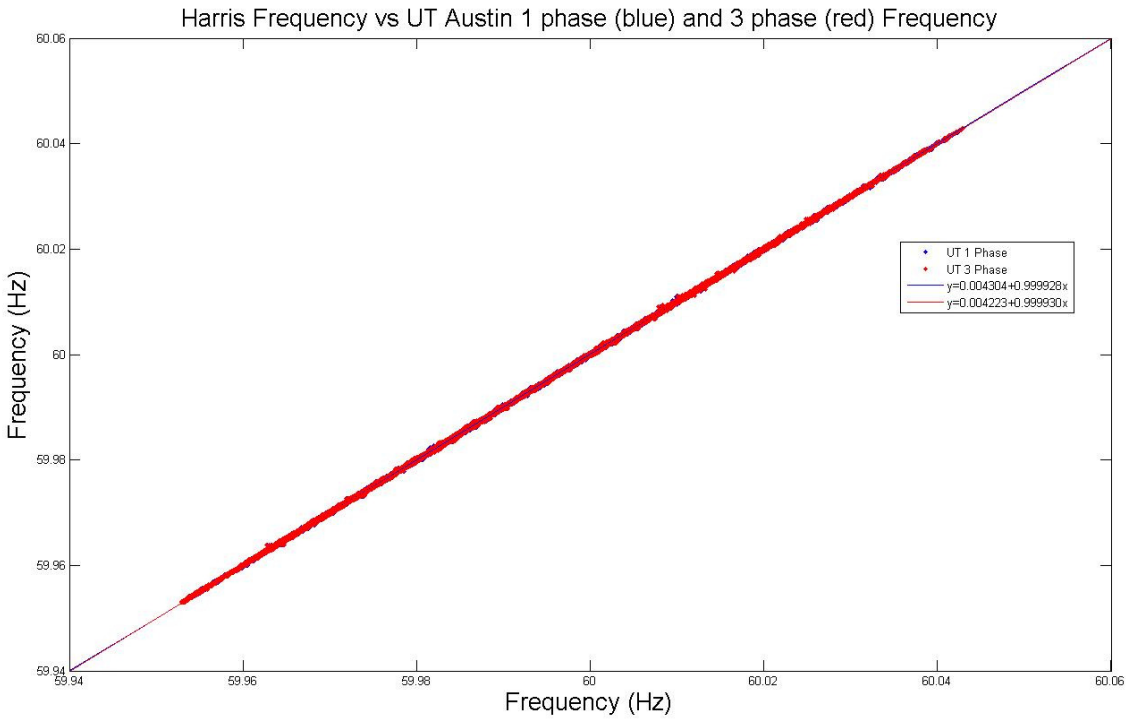

Figure 4.6: Linear Correlation of UT 1-phase and 3-phase vs Harris 69kV

Table 4.2: 1-phase and 3-phase Correlation

Hour	R diff	Beta1 diff	SSE diff
0	-0.0000005	0.0000313	-0.0000141
1	0.0000069	0.0000489	0.0000841
2	0.0000022	0.0000045	0.0000986
3	0.0000007	-0.0000127	0.0000367
4	0.0000001	-0.0000091	0.0000077
5	0.0000028	0.0000082	0.0001020
6	0.0000013	0.0000166	0.0000482
7	0.0000005	0.0000059	0.0000259
8	0.0000032	0.0000183	0.0001593
9	0.0000015	0.0000158	0.0001167
10	0.0000015	-0.0000096	0.0000920
11	0.0000019	0.0000194	0.0001398
12	0.0000019	0.0000118	0.0001107
13	-0.0000002	0.0000174	-0.0000057
14	0.0000030	-0.0000174	0.0000930
15	0.0000023	0.0000299	0.0000674
16	0.0000029	-0.0000054	0.0000985
17	-0.0000003	0.0000209	-0.0000149
18	0.0000039	0.0000373	0.0001074
19	0.0000022	0.0000010	0.0000752
20	0.0000025	-0.0000086	0.0000771
21	0.0000054	0.0000160	0.0001442
22	0.0000062	0.0000073	0.0001486
23	0.0000020	-0.0000267	0.0000713

An interesting observation was made in the frequency on April 18, 2012 at 1900 GMT as seen in Figure 4.7. Our Harris 69kV substation PMU measured frequency with no oscillations, while the UT Austin 1-phase and 3-phase PMUs showed constant un-damped oscillations. The 1-phase connected PMU shows the larger peak-to-peak oscillation. This indicates that the connection does make a difference, but the magnitude of the difference is so small that it is still insignificant. This can be seen in Figure 4.8.

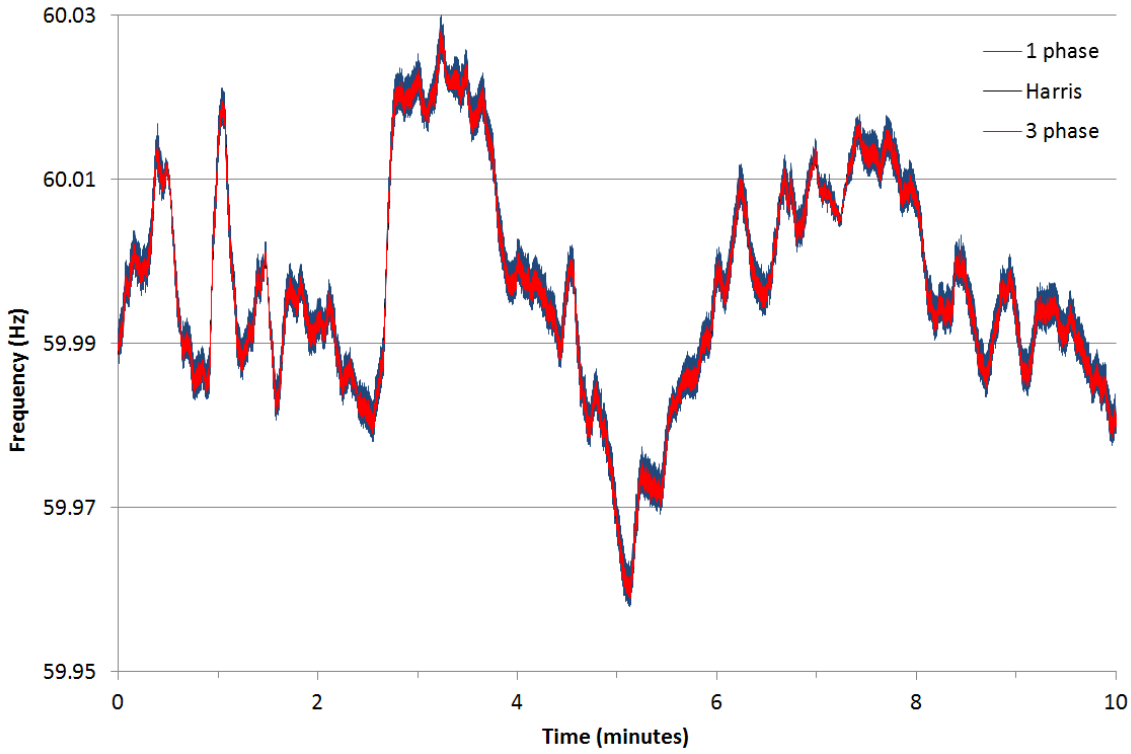

Figure 4.7: Frequency Oscillation at UT Austin on April 18, 2012, 19:00GMT

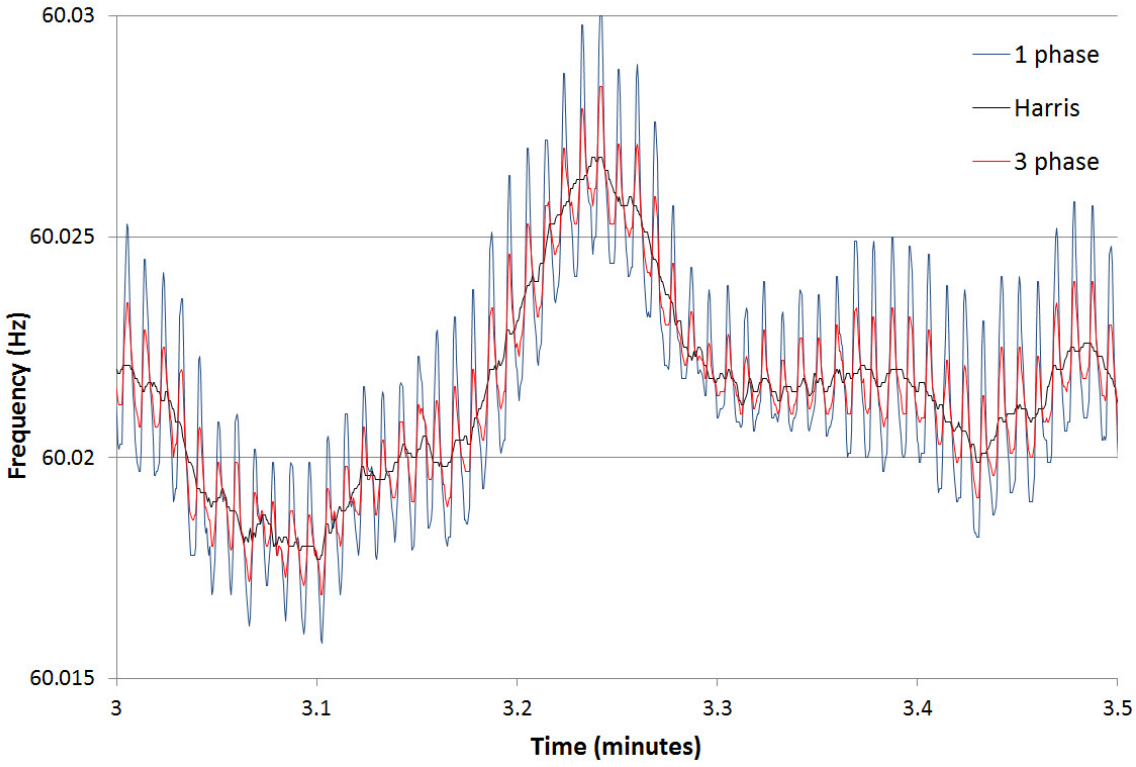

Figure 4.8: 30-second zoom-in of Frequency Oscillation on April 18, 2012, 19:00GMT

To further analyze the event, we use prony analysis. The result, shown in Figure 4.9, shows that a small magnitude and un-damped mode near 2.0 Hz is present. This leads us to believe that the 2.0 Hz is caused by the local generator at UT Austin. However, further investigation at the UT power plant yielded no results.

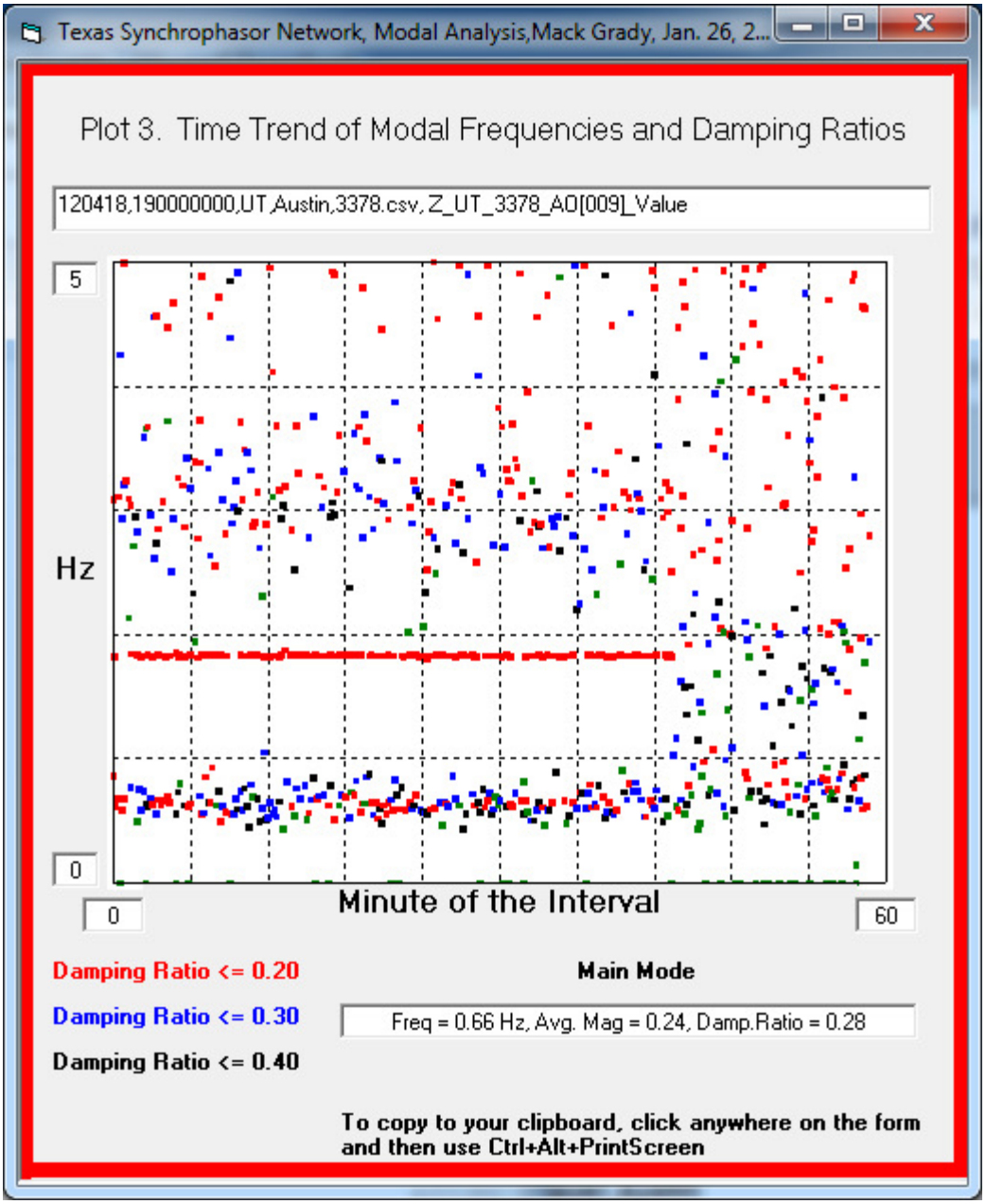

Figure 4.9: Modal analysis for frequency oscillation on April 18, 2012, 19:00GMT

We note a very similar 2Hz mode is established by wind generation as shown in Figure 4.10-11 [18]. This specific mode has been observed to appear with periods of wind ramping.

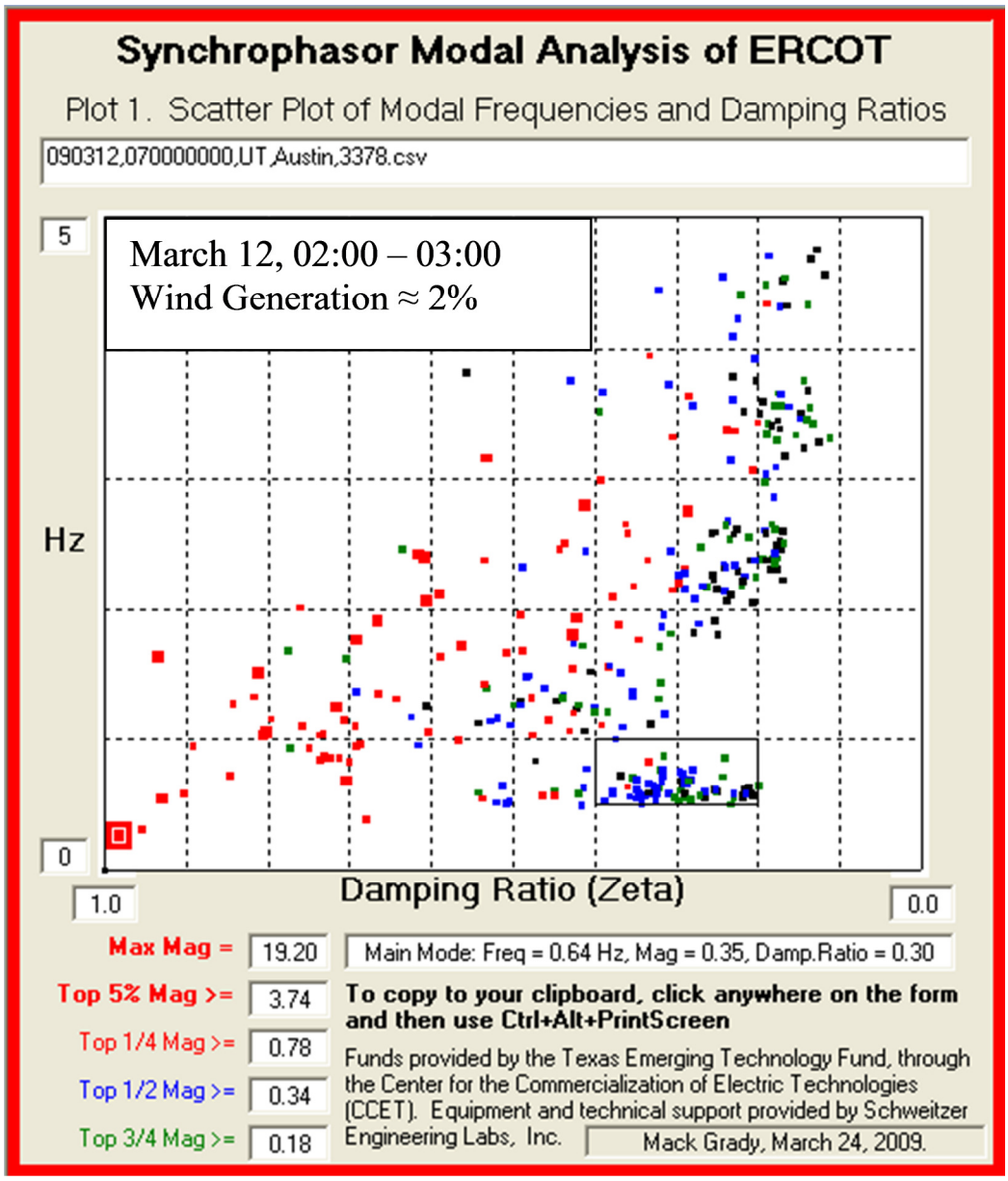

Figure 4.10: Modal analysis plot for low wind generation

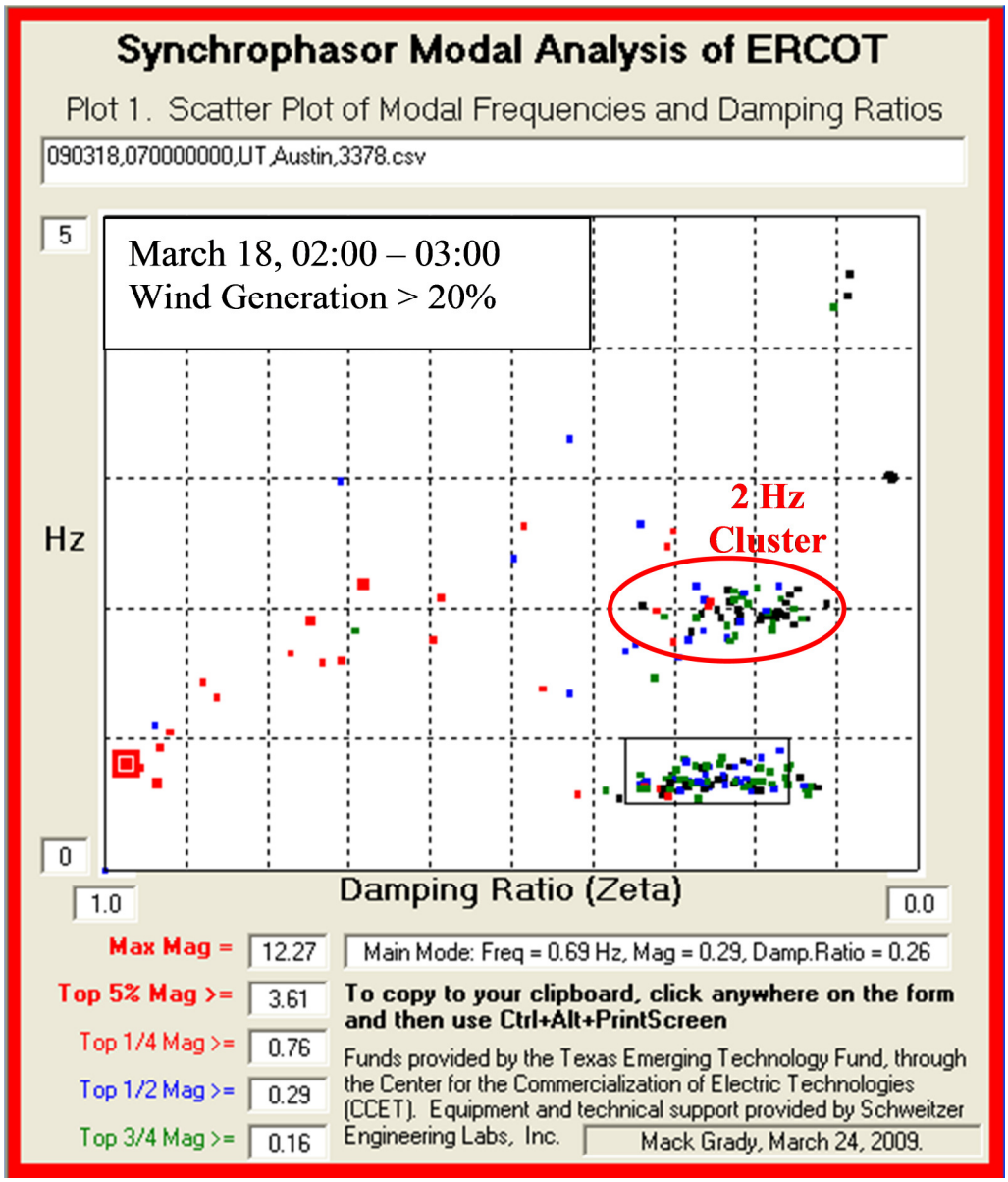

Figure 4.11: .Modal analysis plot for high wind generation

4.2: LESSON # 2: WIND GENERATION DOES NOT AFFECT GRID DAMPING

As global renewable energy continues to grow, wind generation is the most prominent. This is mainly because wind generation prices are the closest out of all renewables to conventional generation. However, many think increased wind generation brings about grid instability. With wind generation sometimes exceeding 25% in ERCOT, it is important to understand the impact of high penetration wind. This was achieved with the Texas Synchrophasor Network by utilizing the SVP to calculate and record modal data.

The modal data is calculated with the prony analysis method [19]-[22]. Even though the analysis is done in real-time and recorded hourly, it can also be reconstructed using a MATLAB program created at UT Austin. This program is also used as a secondary screening process. Prony analysis uses linear combinations of exponential terms to a signal x(t) with the form:

$$x(t) = \sum_{i=1}^{n} A_i e^{\alpha_i t} cos(2\pi f_i t + \theta_i) \quad (4\text{-}2)$$

where:

A_i = magnitude

α_i = damping constant

f_i = frequency

θ_i = phase angle

Grid damping is a good measure of grid stability. With little damping, oscillations can easily grow and cause instability. Too much damping would cause a disturbance to reach the new stability point slower. In [23], a ringdown analysis for more than 200 unit trips was done to study the 2nd order underdamped response. Fig. 4.12 shows the result of the normalized damping ratio as a function of % wind generation. There does not appear to be any correlation between grid damping and wind generation

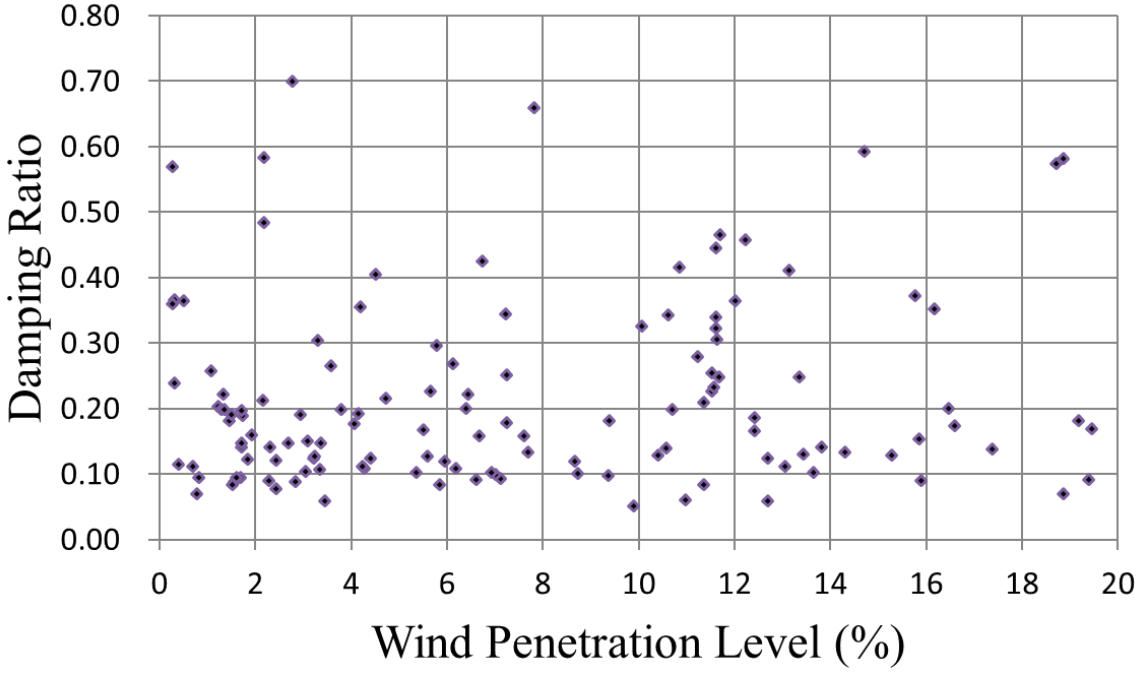

Figure 4.12: Damping ratio versus wind generation (% of Total), Sep 2009 through Feb 2010

4.3: LESSON # 3: WIND GENERATION DOES NOT AFFECT GRID INERTIA

Forty-two generation trips and one DC tie trip have been analyzed over the months of June through November 2010. Each event was significant enough to be reported on ERCOT's Daily Grid Report. Grid inertia is obtained from the initial slope of the frequency droop curves. The first few seconds of the droop are due entirely to inertia, before governors have time to react. To understand how estimated inertia is calculated from a generator unit trip, the expression for inertia and frequency droop is derived as follows:

$$W_{ke} = \frac{1}{2} J \omega_s^2 \tag{4-3}$$

Taking the derivative:

$$\frac{dW_{ke}}{dt} = J\omega_s \frac{d\omega_s}{dt} \tag{4-4}$$

The rate of change of stored energy is net input mechanical power minus net electrical output power:

$$\frac{dW_{ke}}{dt} = P_m - P_e \tag{4-5}$$

There is power balance before a unit trip:

$$P_m^{pre} = P_e \tag{4-6}$$

When one of the many generators trips (i.e., loss of ΔP_m), P_e temporarily remains unchanged because voltage regulators maintain load voltage and load power. Frequency has not changed enough to affect load power. Thus generators begin to give up some of their stored kinetic energy (commonly called the inertial droop).

$$\frac{dW_{ke}}{dt} = J\omega_s \frac{d\omega_s}{dt} = P_m^{pre} - P_e - \Delta P_m = -\Delta P_m \tag{4-7}$$

$$J\omega_s = \frac{-\Delta P_m}{d\omega_s/_{dt}} \tag{4-8}$$

The H constant is defined as:

$$H \equiv \frac{\frac{1}{2}J\omega_s^2}{P_{rated}} = \frac{1}{2}\frac{(J\omega_s)\cdot\omega_s}{P_{rated}} = \frac{1}{2}\left[\frac{-\Delta P_m}{d\omega_s/_{dt}}\right]\frac{\omega_s}{P_{rated}} \tag{4-9}$$

Rewriting:

$$H = \frac{1}{2}\left[\frac{-\Delta P_m}{P_{rated}}\right]\frac{\omega_s}{d\omega_s/_{dt}} = \frac{-\Delta P_m}{2P_{rated}}\frac{2\pi f_s}{2\pi\left(df_s/_{dt}\right)} = \frac{-\Delta P_m f_s}{2P_{rated}\left(df_s/_{dt}\right)} \tag{4-10}$$

H has the units of seconds. The correct interpretation is that the kinetic energy in the equivalent system machine corresponds to H seconds of rated power. Thus, the machine could provide rated power for H seconds, at which time it would have spun down to zero RPM.

The multiplier f_s term in the numerator can be considered constant. P_{rated} is post-event and should not contain the tripped generator. Post-event spinning reserve (excluding that of the tripped generator) should be included in P_{rated}.

Summarizing (4-10), ΔP_m is the MW tripped, f_s is 60 Hz, P_{rated} is total post-trip generation MW plus post-trip spinning reserve, and $\frac{df_s}{dt}$ is the inertial slope of the frequency droop immediately after the trip occurs.

An example of estimated grid inertia, H, is illustrated as follows. Consider the event shown in Figure 4.13. Total generation is 59,874 MW, spinning reserve is 6,237 MW, and the tripped MW is 824. The ERCOT Daily Grid Report states: "Deployed 688 MW Responsive Reserve Service from actual adjusted Responsive Reserve of 4200 MW with an obligation of 2300 MW when frequency dropped to 59.84 Hz due to XXXX tripped with 824 MW. ERCOT load 60503 MW."[24] The sources of the data and important notes concerning their use are

1. MW trip values are from ERCOT Daily Grid Reports (formerly posted on the ERCOT web site but discontinued after Dec. 1, 2010).
2. Total Generation MW, Spinning Reserve MW, and Wind Generation MW are 1-minute averages (formerly streamed on the ERCOT web site but discontinued after Dec. 1, 2010).
3. Frequency measurements are taken by the Texas Synchrophasor Network, with stations in Austin (two locations, U.T. Austin campus and at nearby Harris substation), McDonald Observatory, and U.T. Pan American, with 30 points per second. Some unit trips are not reported here due to internet problems.
4. Frequency measurements at all reporting stations are shown. A few graphs have only one reporting station. Most have all four.
5. The spinning reserve of a tripped unit is estimated from total spinning reserve using its fraction of total MW generation.

The first step in determining H is to draw the dashed line used to estimate inertia slope $\frac{df_s}{dt}$. Measuring the slope of the dashed line yields $\frac{df_s}{dt}$ = 0.0425 Hz per second (falling). Next, the prorated share of spinning reserve of the tripped generation is estimated to be:

$$6237 \cdot \frac{824}{59874} = 85.8\ MW \tag{4-11}$$

Substituting into (7) yields:

$$H = \frac{-\Delta P_m f_s}{2P_{rated}\left(\frac{df_s}{dt}\right)} = \frac{-824 \cdot 60}{2 \cdot [(59874-824)+(6237-85.8)] \cdot (-0.0425)} \tag{4-12}$$

H = 8.91 sec.

The process was used for all forty-two events found in June through November 2010. The H estimates are displayed in several ways to help identify correlation with wind generation. The most revealing plots are shown in Figures 4.14 and 4.15

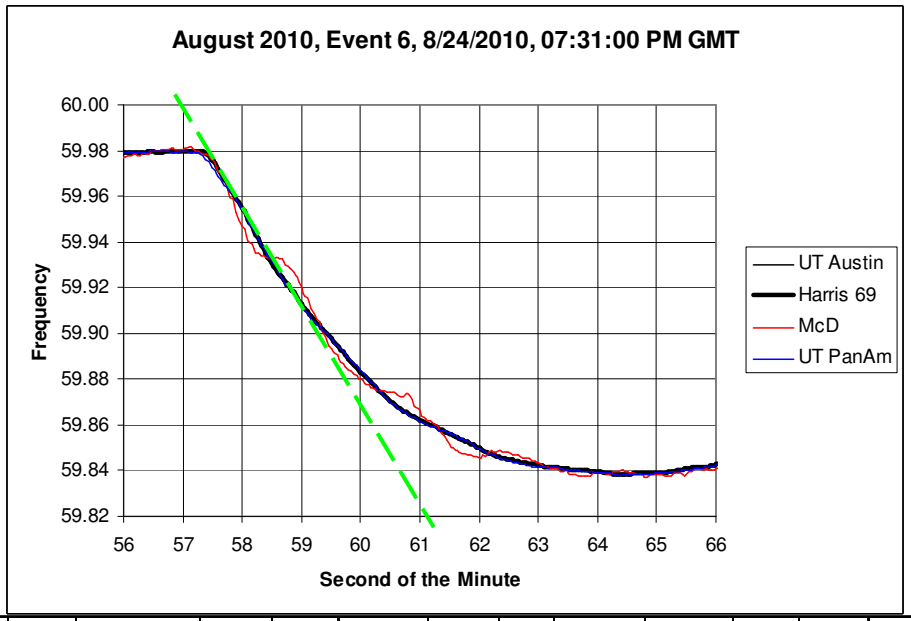

Month of 2010	Day	Event for Month	GMT	Day of Year	Tot Gen MW	Spinning Reserve MW	Wind Gen % of Total	MW Trip	Est. Lost Spinning Reserve MW	Inertia Slope (Hz/sec)	H (sec)	Fdrop to Nadir (Hz)	Nadir Slope (Hz/sec)	Inertia Slope / Nadir Slope
Aug.	24	6	19:31 GMT	236	59874	6237	7.11	824	85.8	0.0425	8.91	0.141	0.0193	2.20

Figure 4.13: Frequency plot for August 24, 2010, 7:31 PM GMT

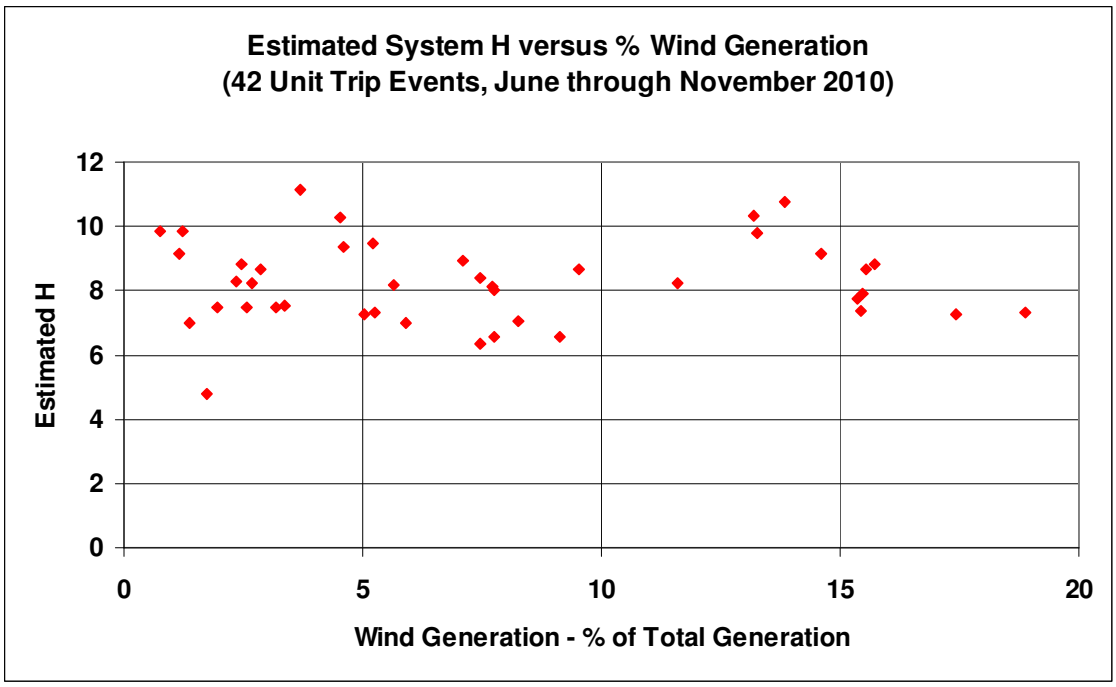

Figure 4.14: Scatter Plot of H Estimates versus Wind Generation (% of Total)

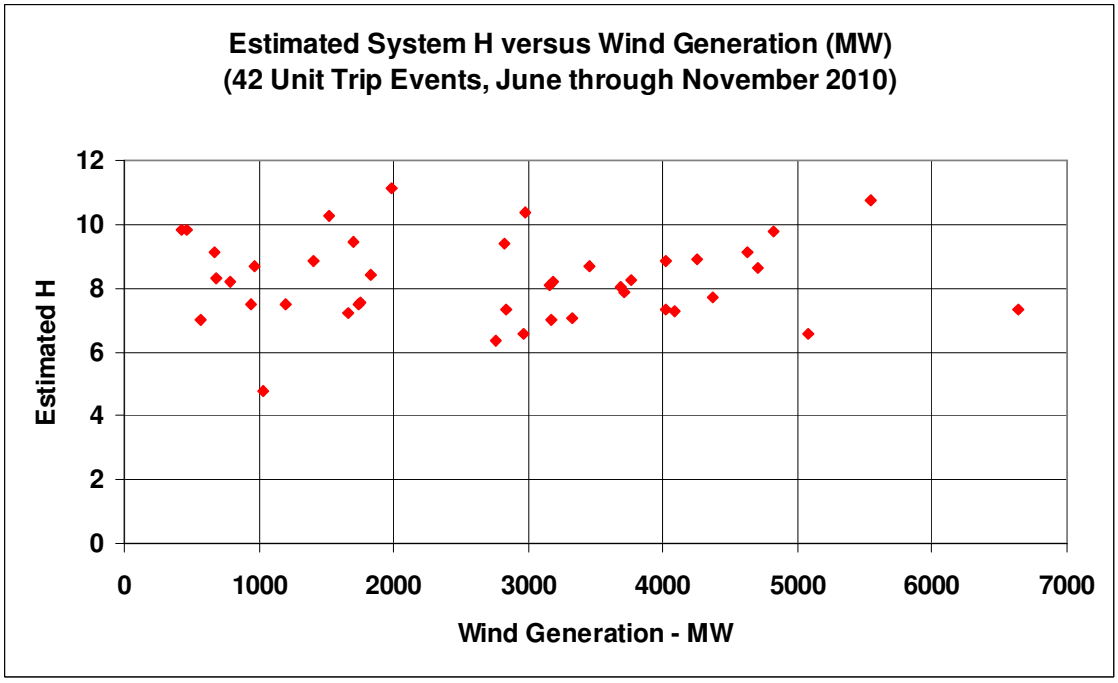

Figure 4.15: Scatter Plot of H Estimates versus Wind Generation (MW)

Scatter plots of H versus MW tripped and total MW are shown in Figures 4.16 and 4.17. Neither shows any significant correlation.

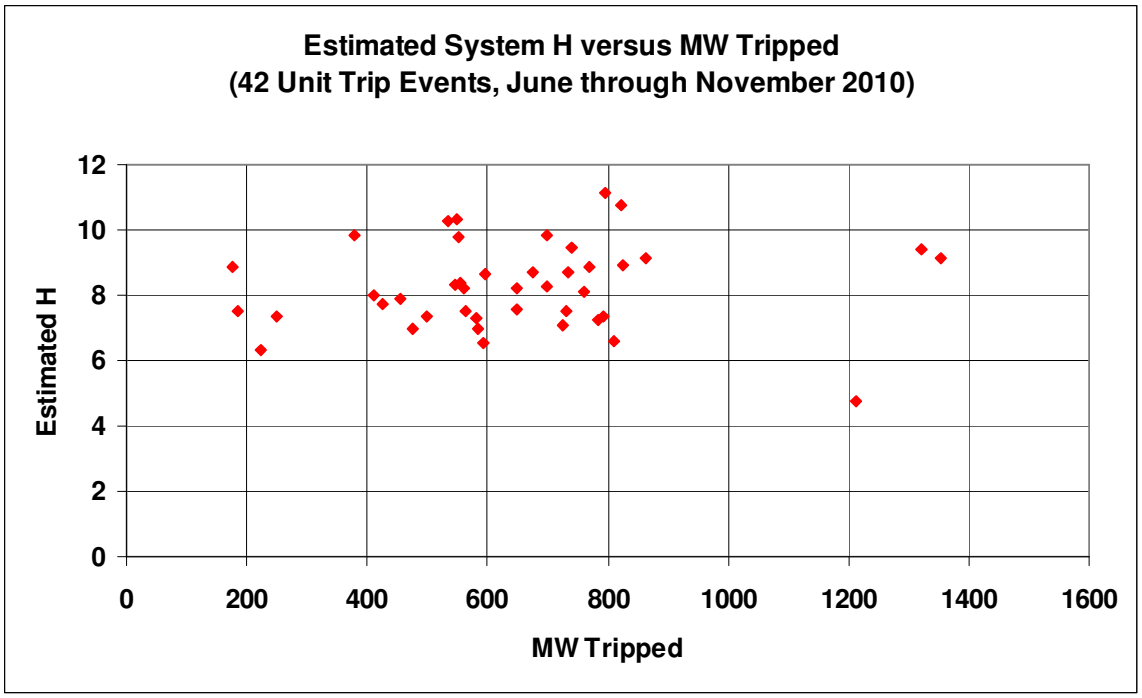

Figure 4.16: Scatter Plot of H Estimates versus MW Tripped

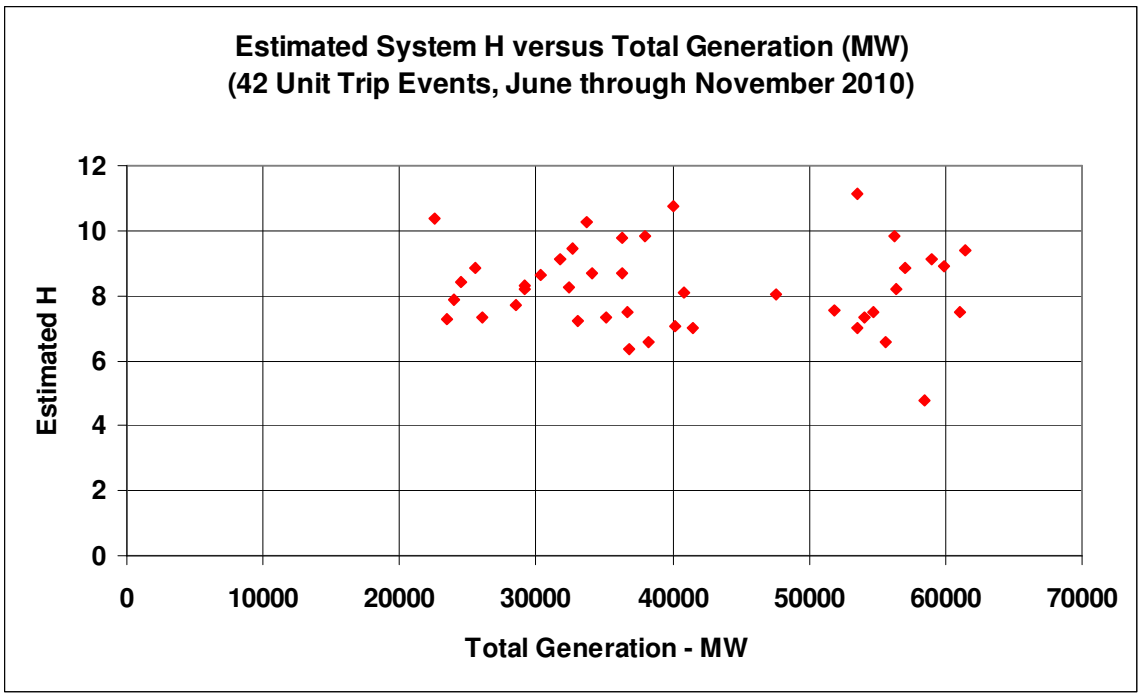

Figure 4.17: Scatter Plot of H Estimates versus Total Generation

H versus day of year is scatter plotted in Figure 4.18, where a slight correlation emerges. However, the main purpose of Figure 4.18 is to show that the unit trips span all six months.

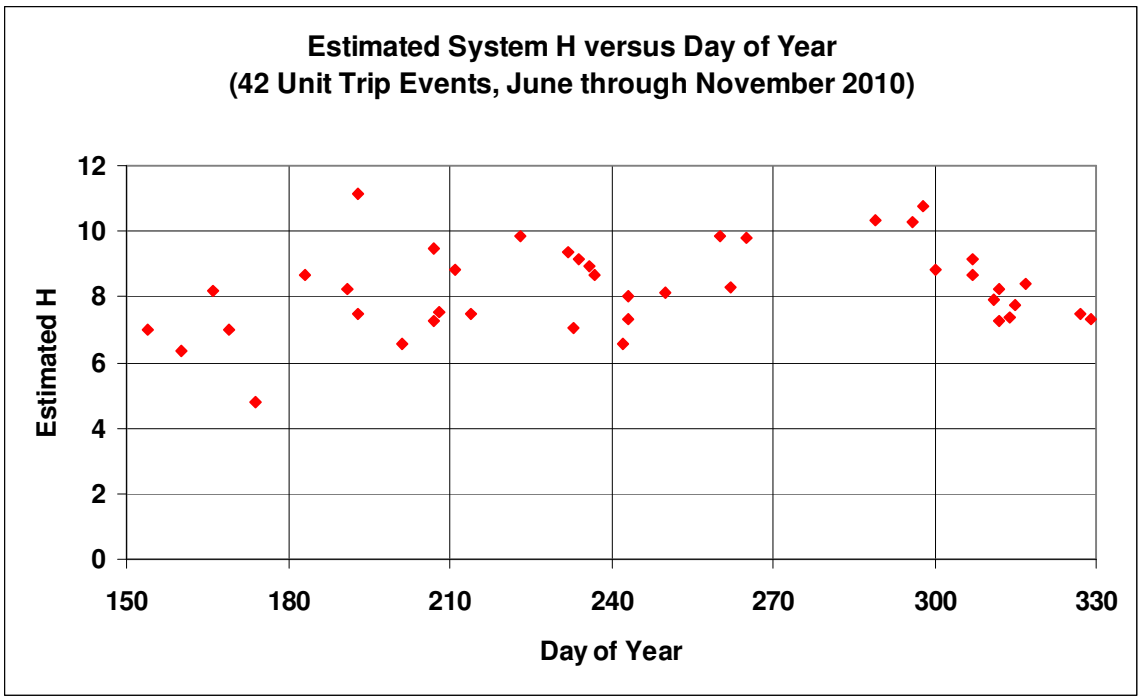

Figure 4.18: Scatter Plot of H Estimates versus Day of Year

It has long been recognized by ERCOT that wind generation does, in fact, affect grid frequency response to unit trips. However, as shown above, wind generation does not appear to lower the system inertia H observed in the initial frequency droop. Wind generators in ERCOT are typically operated at their maximum power points. Thus, even though they do contribute inertia during the initial frequency droop, they have little to no spinning reserve that can provide governor response to eventually arrest the drop in frequency.

By taking into account the maximum frequency drop known as the "nadir" of the curve, it is possible to decouple inertia and governor responses. A proposed new metric, Frequency Recovery Ratio (FRR) makes it possible to quantify the impact of wind generation (or other sources with no spinning reserve margin) on frequency response, while at the same time recognizing that wind does not lower system H.

Consider the maximum frequency drop ΔF_{nadir} and the time it takes to reach the nadir of the frequency drop curve, ΔT_{nadir}. The nadir slope line in Figure 4.19 has downward slope $\frac{\Delta F_{nadir}}{\Delta T_{nadir}}$ Hz per second. The proposed new metric is to compare how far down system frequency would have dropped at ΔT_{nadir} with inertia response alone (i.e., no governor action), to how far it actually dropped with governor action.

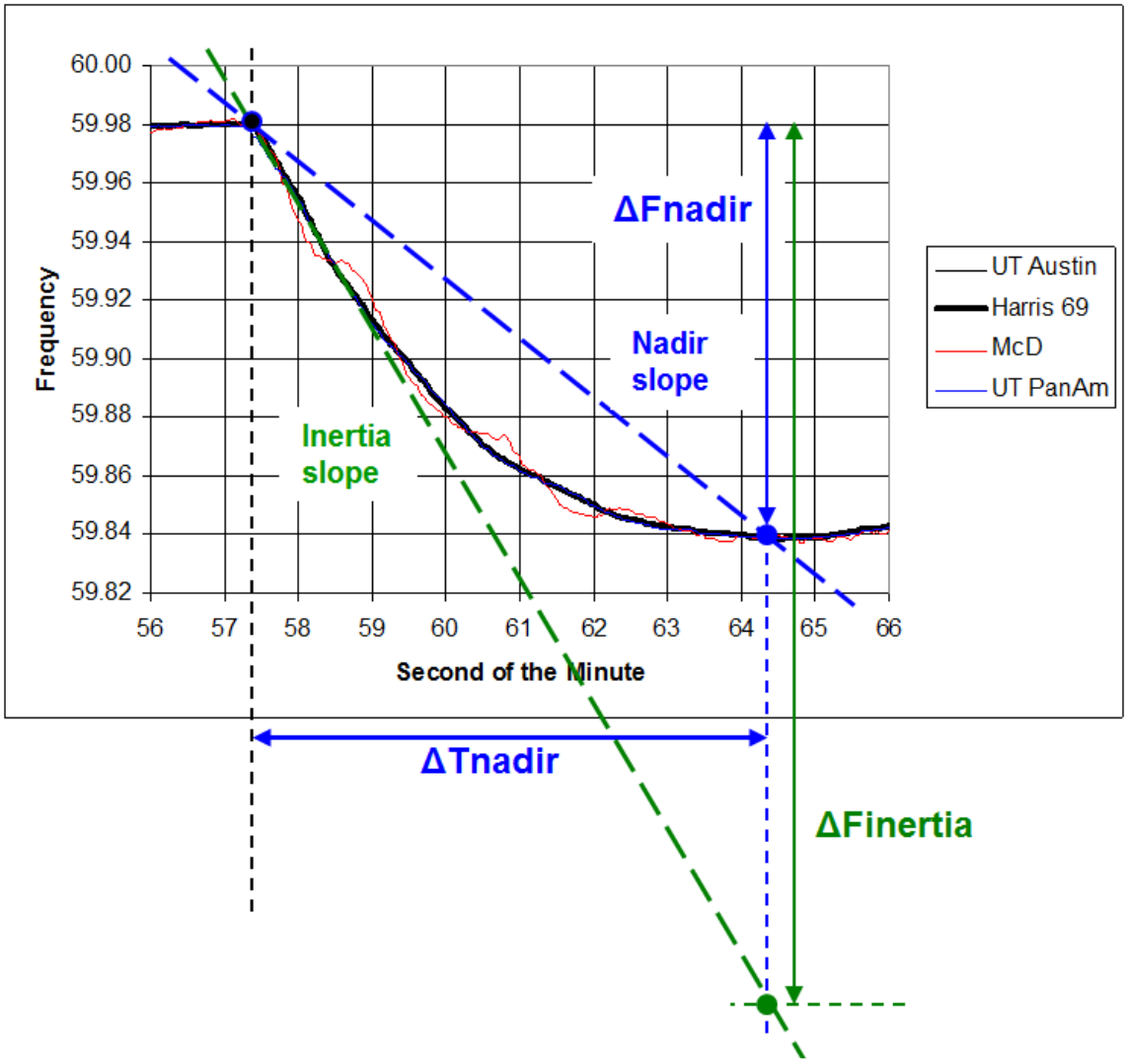

Figure 4.19: Frequency Plot showing Inertia Slope and Nadir Slope

This ratio is the proposed Frequency Recovery Ratio (FRR). Referring to Figure 4.19, it is defined as:

$$FRR \equiv \frac{\Delta F_{inertia}}{\Delta F_{nadir}} \tag{4-13}$$

Using the geometry in Figure 4.19,

$$FRR \equiv \frac{\Delta F_{inertia}}{\Delta F_{nadir}} = \frac{(Inertia\ Slope)\cdot\Delta T_{nadir}}{(Nadir\ Slope)\cdot\Delta T_{nadir}} = \frac{Inertia\ Slope}{Nadir\ Slope} \tag{4-14}$$

The FRR measures the strength of the governor response relative to the inertia response. Therefore a higher FRR indicates a stronger governor response. Before looking at the FRR, we show in Figure 4.20 that H appears to be independent of nadir frequency drop.

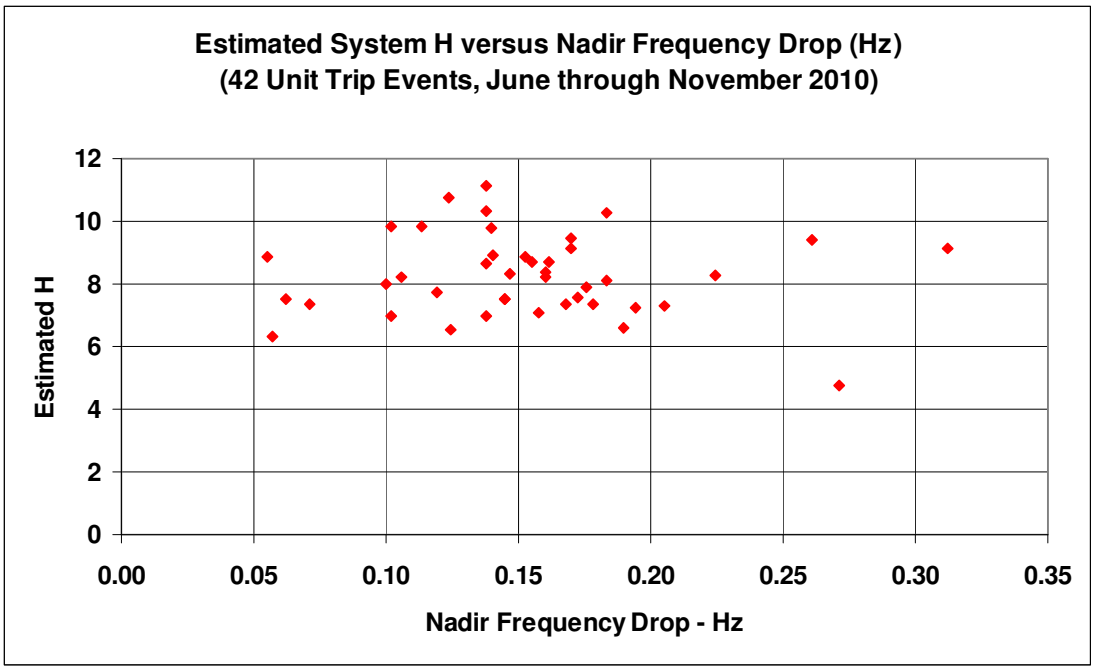

Figure 4.20: Scatter Plot of Estimated H versus Nadir Frequency Drop

Next, Figure 4.21 shows no clear correlation between FRR and nadir frequency drop.

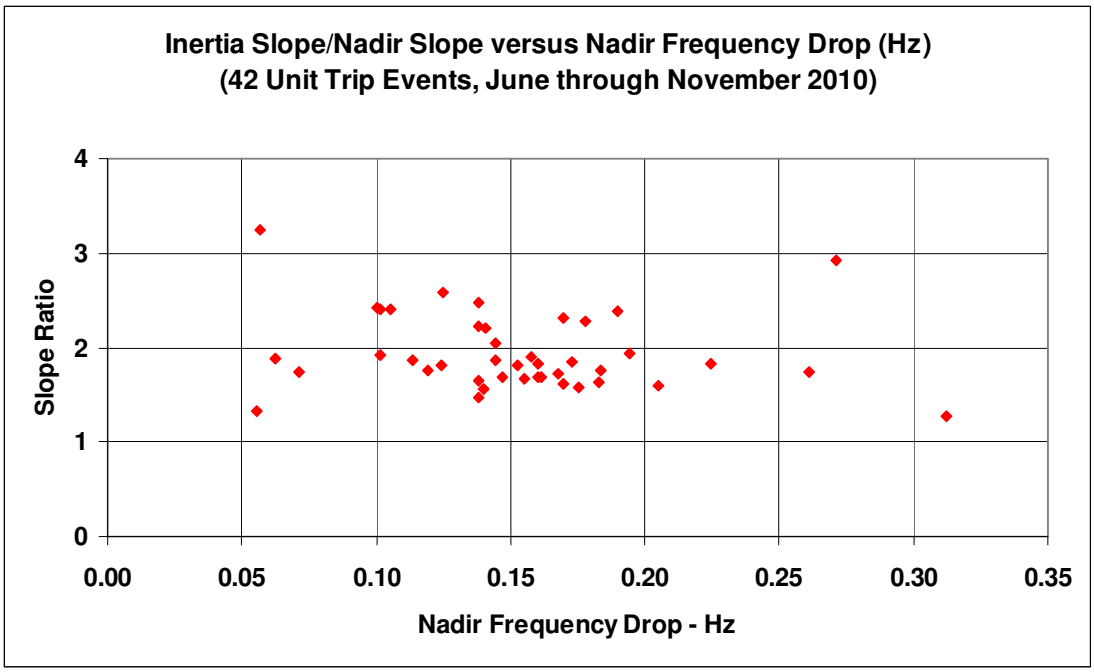

Figure 4.21: Scatter Plot of FRR versus Nadir Frequency Drop

A scatter plot of FRR versus wind generation, shown in Figure 4.22, does show a correlation. The slope of the straight-line fit shows that FRR drops 0.3 per 10% of wind generation, indicating even though H is not affected, the frequency recovery is less robust with high-penetration wind generation that is operating at or near the max power point.

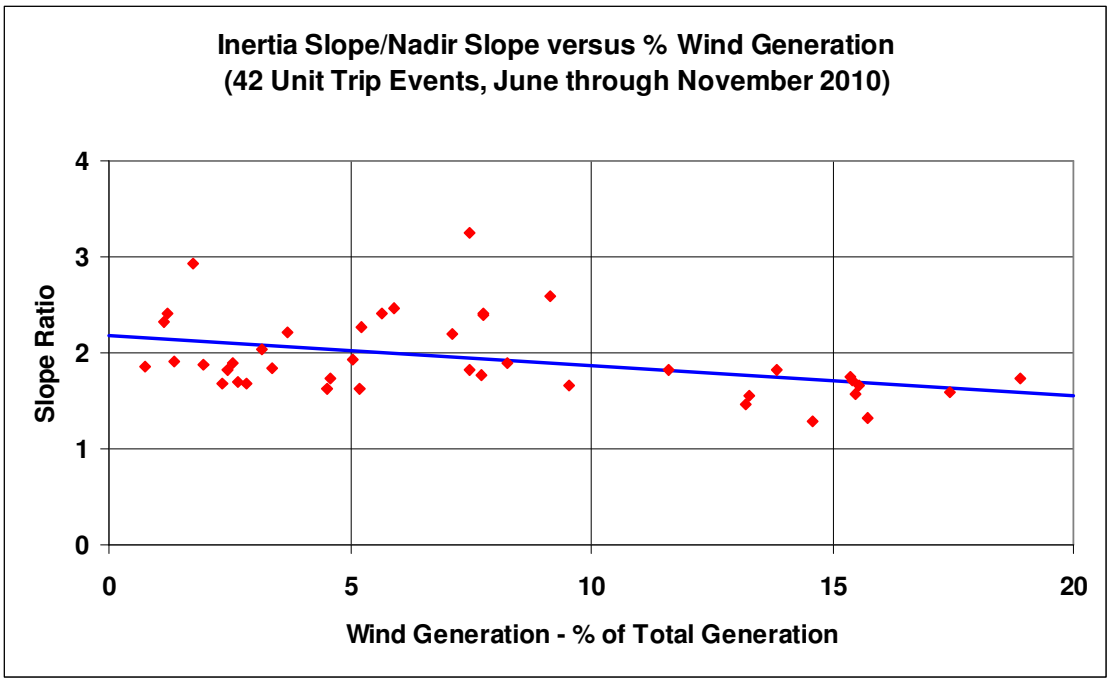

Figure 4.22: Scatter Plot of FRR versus Wind Generation (% of Total)

4.4: LESSON #4: WEST TEXAS THEVENIN EQUIVALENT IMPEDANCE

We are able to estimate X_{Th} with synchrophasor data. For example, April 24-25, 2010 were two days during which Wind Generation varied significantly. The correlation between the Wind Generation and West Texas phase angle with respect to Central Texas (U.T. Austin) also had strong positive correlation, except for a brief period shown by the arrows shown in Figure 4.23. We continue to assume a simple system to estimate the Thevenin equivalent grid impedance at West Texas shown in Figure 4.24.

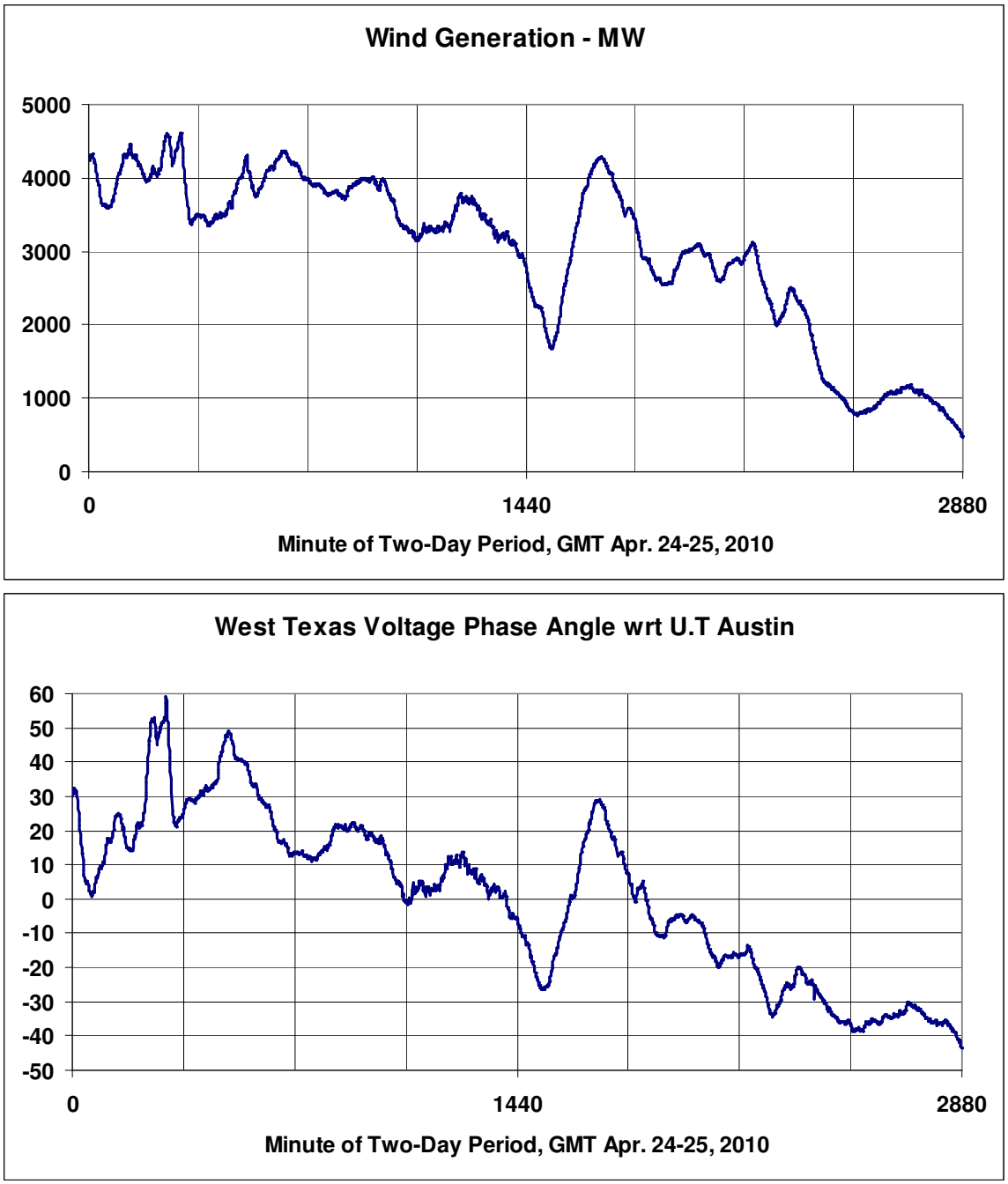

Figure 4.23: Wind generation and West Texas phase angle with respect to Central Texas (U.T. Austin) for April 24-25, 2010

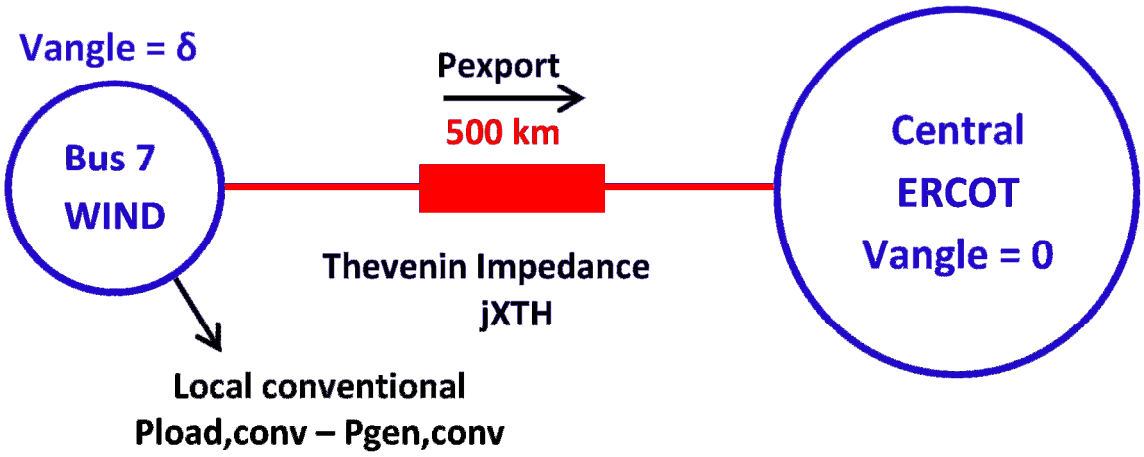

Figure 4.24: Proposed simplified system

Using the Wind generation and ERCOT total generation from the ERCOT website and the wind generation phase angle δ with respect to central Texas, we solve for the Thevenin impedance, jX_{th}, local conventional load minus generation in West Texas, and Pexport. Assuming a lossless environment, power balance states

$$P_{wind} - \left(P_{load,conv} - P_{gen,conv}\right) = \frac{V_{wind} \cdot V_{ERCOT}}{X_{TH}} \sin \delta \tag{4-15}$$

If we assume the local net convention varies linearly with ERCOT total generation:

$$P_{load,conv} - P_{gen,conv} = A \cdot P_{ERCOT\ Total\ Gen} + B \tag{4-16}$$

Since the system is assumed to be lossless, in per unit the right hand side is:

$$C = \frac{V_{wind} \cdot V_{ERCOT}}{X_{TH}} = \frac{1 \cdot 1}{X_{TH,pu}} \tag{4-17}$$

Using Excel to vary A,B, and C to minimize the sum of squared error:

$$\sum_{n=1}^{N} [P_{wind} - (A \cdot P_{ERCOT\ Total\ Gen} + B) - C \sin \delta]^2 \tag{4-18}$$

Figure 4.25 shows the result of the above method for a two-day period where there was an obvious change in the system that lowered the Thevenin impedance from j0.056pu to j0.033pu.

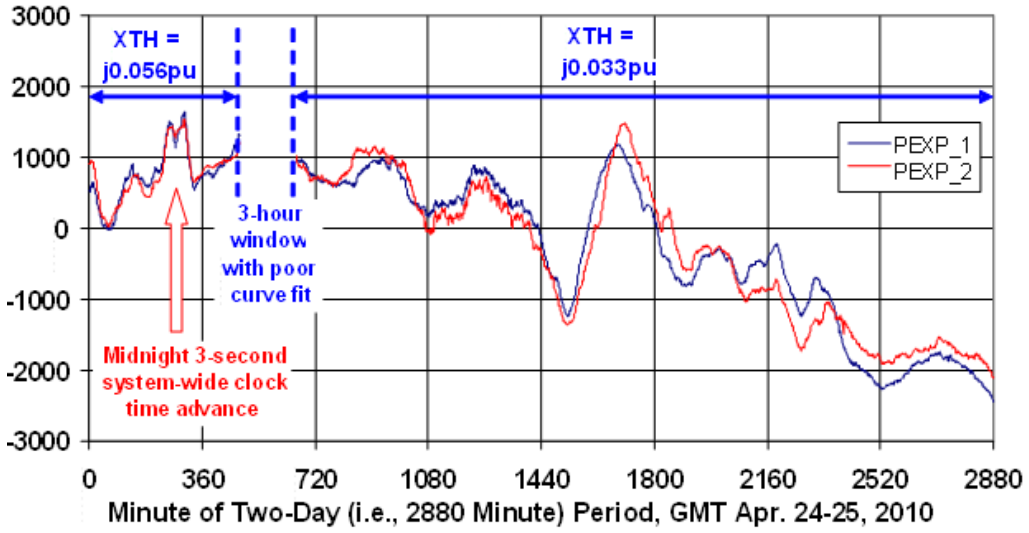

Figure 4.25: Estimated ERCOT thevenin impedance at West Texas

We next looked at the wind generation during Thanksgiving as it reached 25% of total generation (6881 MW which is very close to the all-time high), shown in Figure 4.26-27.

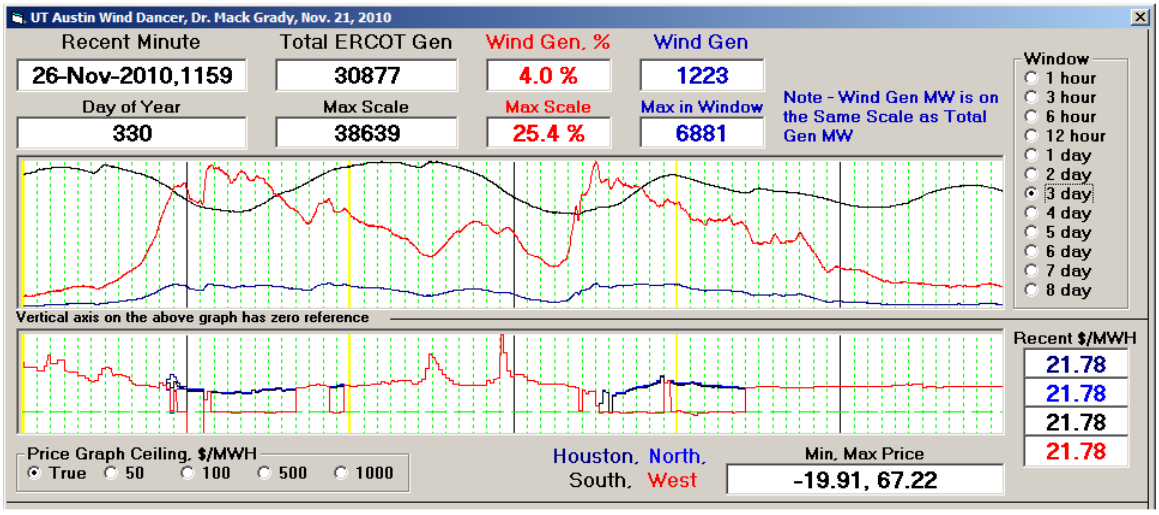

Figure 4.26: Wind generation plot on wind dancer, three day period starting Nov. 23, 2010

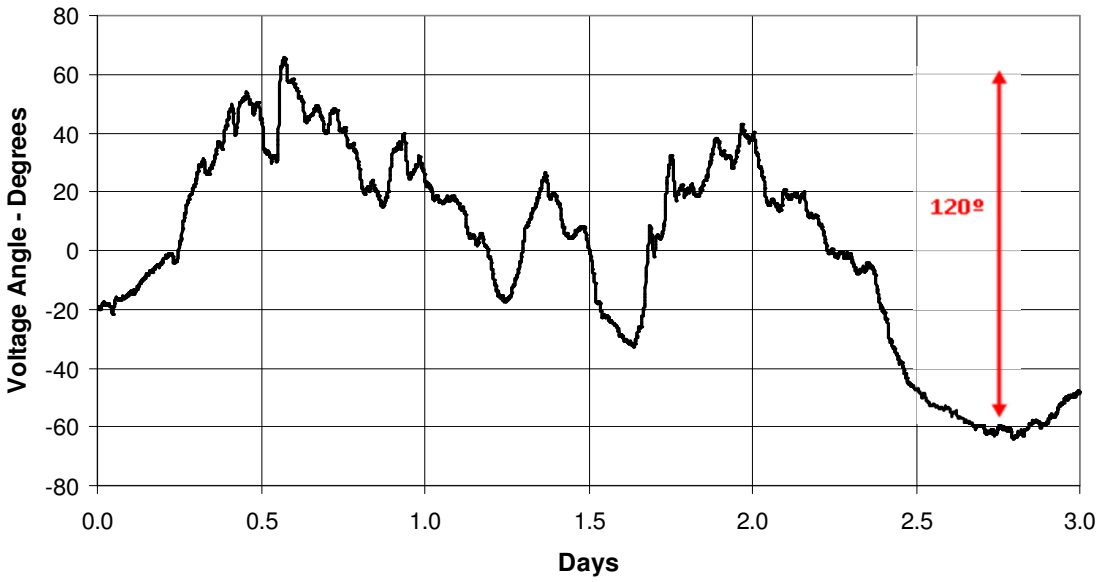

Figure 4.27: West Texas phase angle w.r.t. U.T. Austin, three day period starting Nov. 23, 2010

During these three day period of high and low wind generation, we can see strong correlation between the angle swing of West Texas with respect to Central Texas, one of the criteria that we are considering. When the Wind Generation is plotted with the sine of the voltage angle, we see periods of strong linear relationship but also a time of non-linear relationship, shown in Figure 4.28.

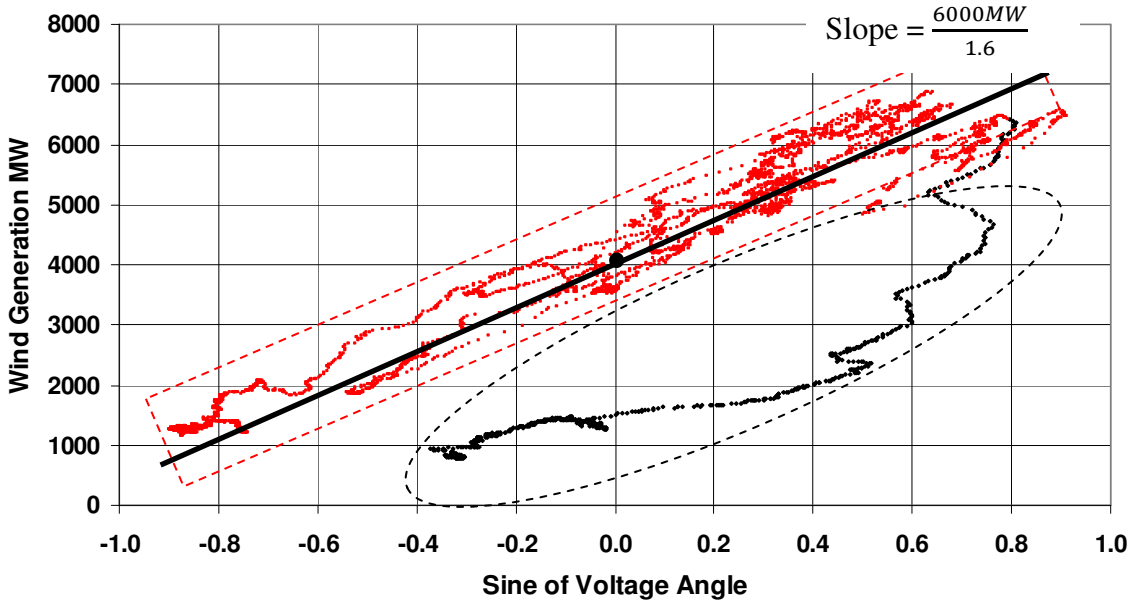

Figure 4.28: Wind generation (MW) versus sine of voltage angle, three day period starting Nov. 23, 2010

Using the points within the red rectangle for an estimate of the Thevenin equivalent impedance between West Texas and Central ERCOT, the approximate wind generation at zero phase angle is 4000 MW. The MW swing is ±3000 MW, and the sine swing is ±0.8. Using the slope of the red rectangle, it appears that the relationship between wind generation and voltage phase angle is approximately:

$$WindGen = 4000 + \frac{6000}{1.6}\sin(\delta) = 4000 + 3750\sin(\delta) MW. \quad (4\text{-}19)$$

On a 100 MW base, this becomes:

$$WindGen = 40 + 37.7\sin(\delta)\, pu \quad (4\text{-}20)$$

From the equation for an ideal reactive transmission line, $P_{pu} = \frac{V_{1pu}V_{2pu}}{X_{1-2,pu}}\sin(\delta_1 - \delta_2)$, we then estimate that for the period Wednesday, Thursday, Friday through noon $X_{Thev,pu} = \frac{1}{37.5} = 0.0267\ pu$ on a 100 MVA base.

Chapter 5: Other Observations

5.1: TURBINE VALVING

On Tuesday, March 31, 2009, the Texas Synchrophasor Network observed a strange 0.067 Hz oscillation that lasted around 15 minutes. Figure 5.1 shows the 20-minute frequency plot for Central Texas and West Texas. Figure 5.2 shows a 30-second zoom-in. This frequency variation had gone unnoticed at ERCOT due to its slow variation, but our weekly voltage phase angle plots made it very easy to spot. The issue was found to be the result of a throttle valving problem on a generator under test.

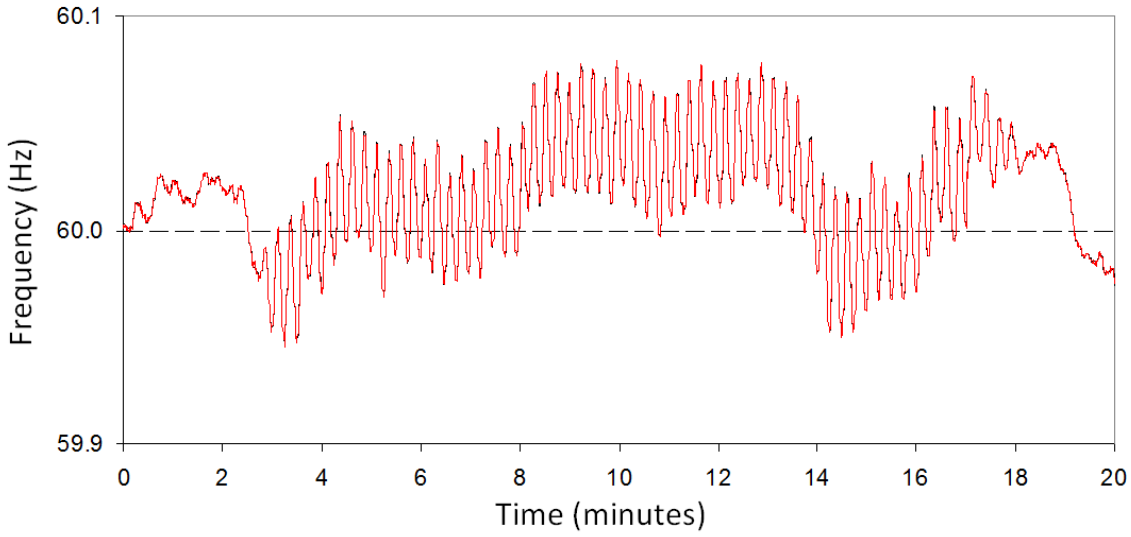

Figure 5.1 20-minute window of frequency oscillation observed on March 31, 2009.

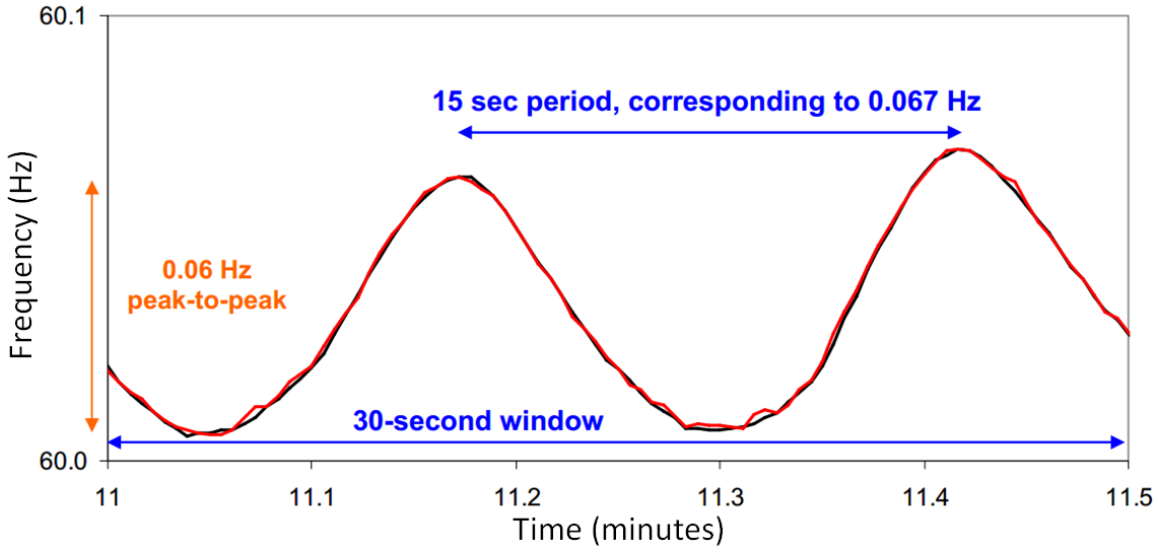

Figure 5.2: 30-second zoom-in of the 11th minute

5.2: DIRECTION FINDING

During a unit trip, the grid frequency drops and slowly recovers. Such a unit trip, shown in Fig. 5.3, occurred on April 3, 2012 at 07:08 GMT. Fig 5.4 shows the corresponding voltage angles for McDonald Observatory, Waco, and U.T. Pan Am with respect to U.T. Austin. Even though the frequency information allows you to know that a unit trip has occurred, it gives no information regarding the location of the unit. Using synchrophasor data, a general direction can be estimated by observing the change in steady state angle.

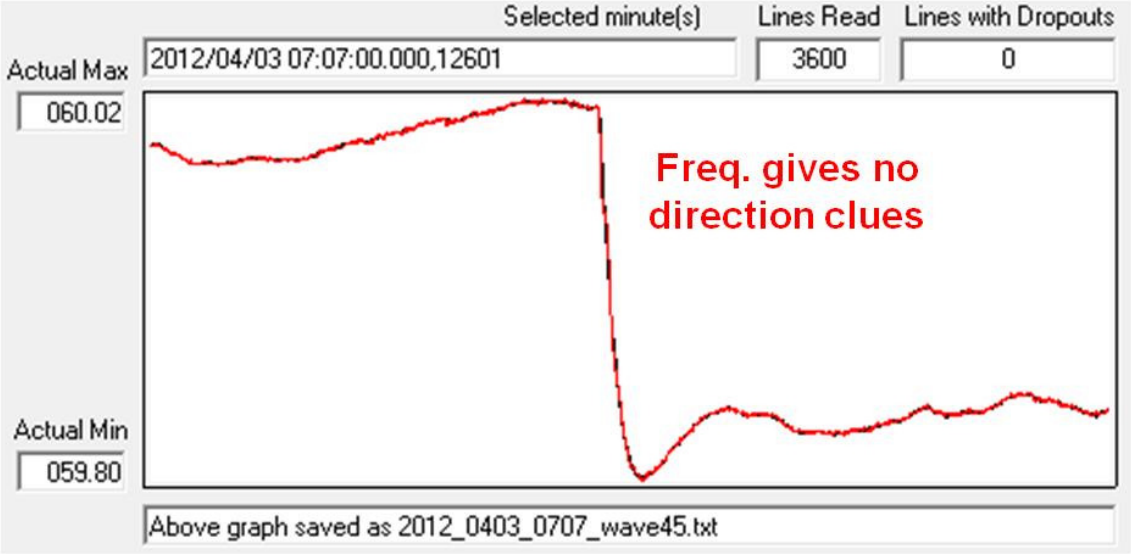

Figure 5.3: Frequency response for unit trip in ERCOT on April 3, 2012 at 07:08 GMT (2-minute window)

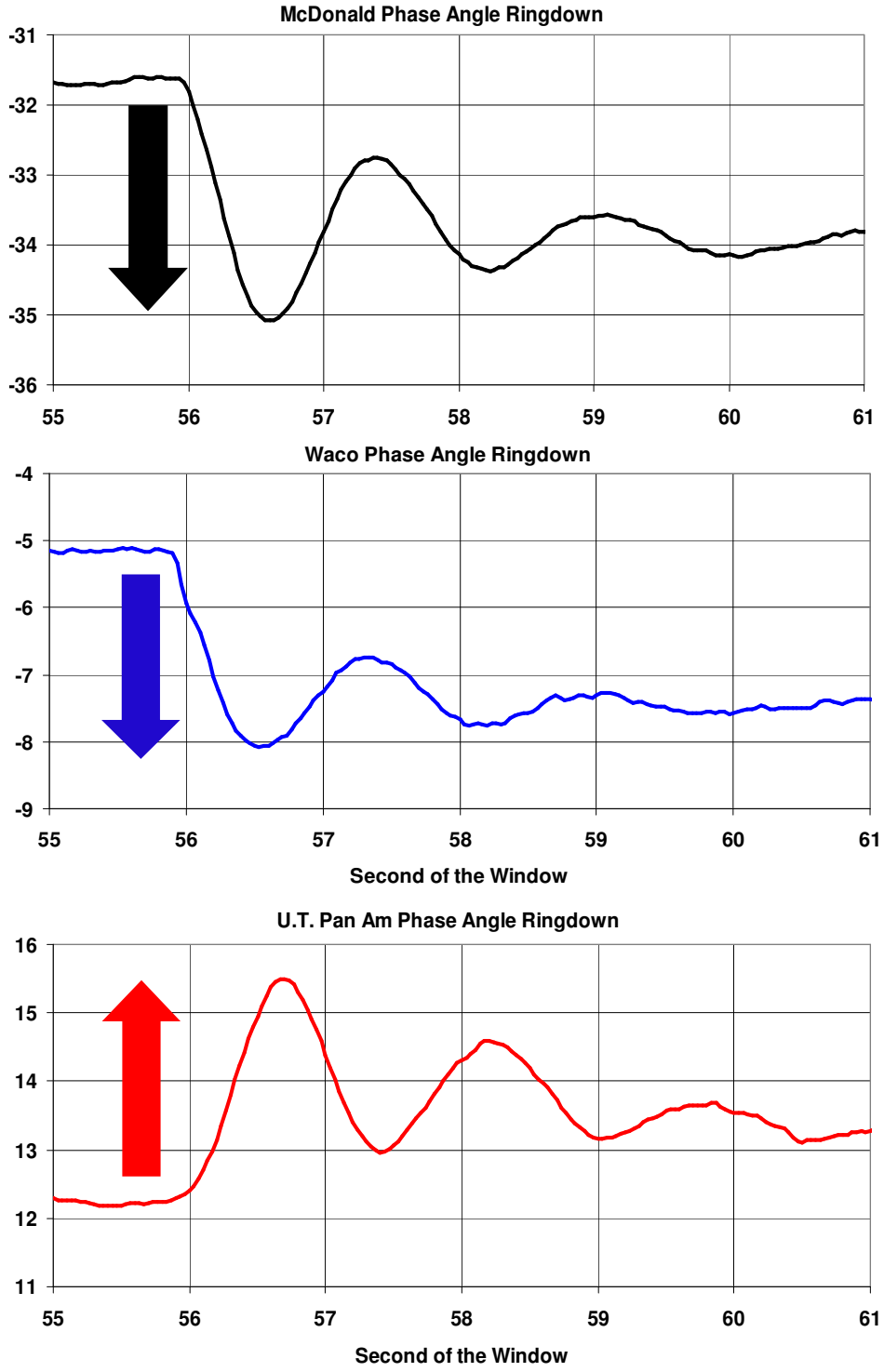

Figure 5.4: Voltage Phase Angle response for unit trip in ERCOT on April 3, 2012 at 07:08 GMT

The steady state voltage phase angle change shows that U.T. Pan Am is exporting more power after the event occurred. The phase angles in West Texas and Waco dropped, indicating that after the event more power is flowing north and possibly west. From this, we expect the unit trip to have occurred in North or West Texas. We also note that due to the second-order nature of the event, the direction of the initial swing also indicates the same direction. This is helpful when the steady state voltage phase angle changes very slightly. With good PMU placements such as described in [25]-[26], we will be able to determine the location of the unit trip more accurately.

5.3: RECLOSER EVENTS

There are many applications that can utilize PMU data. In this section, applications from using the voltage magnitude recorded by PMU's will be discussed. McDonald Observatory is served at the end of a long 12.5 kV distribution feeder that winds from the historic town of Fort Davis through a mountainous area to the 6500 ft. elevation observatory. On April 12, 2009 our 120V single-phase PMU at McDonald reported the rms voltage sag shown in Figure 5.5. The total time span of the window is 40 seconds.

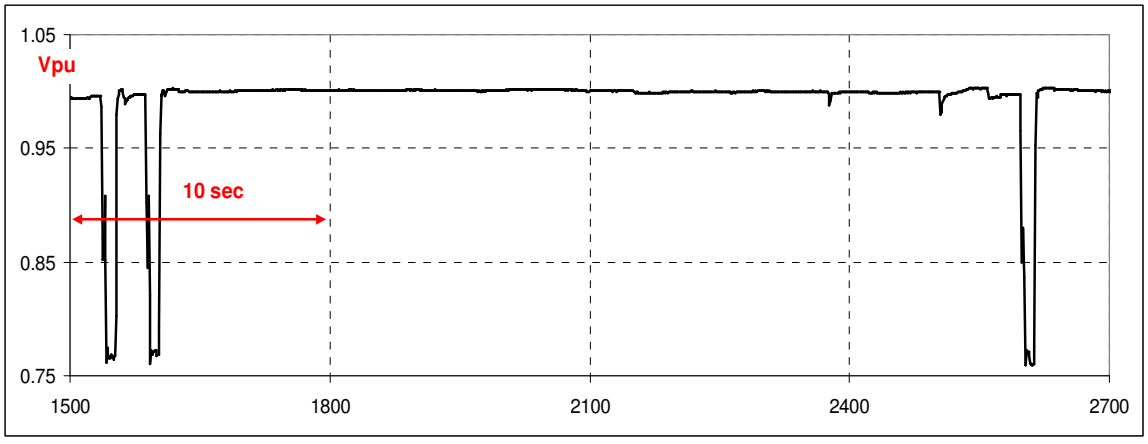

Figure 5.5: Voltage Sag event observed at McDonald Observatory

Figure 5.6 is a zoom-in of the first two voltage sags. The two sags are remarkably similar (and so is the third).

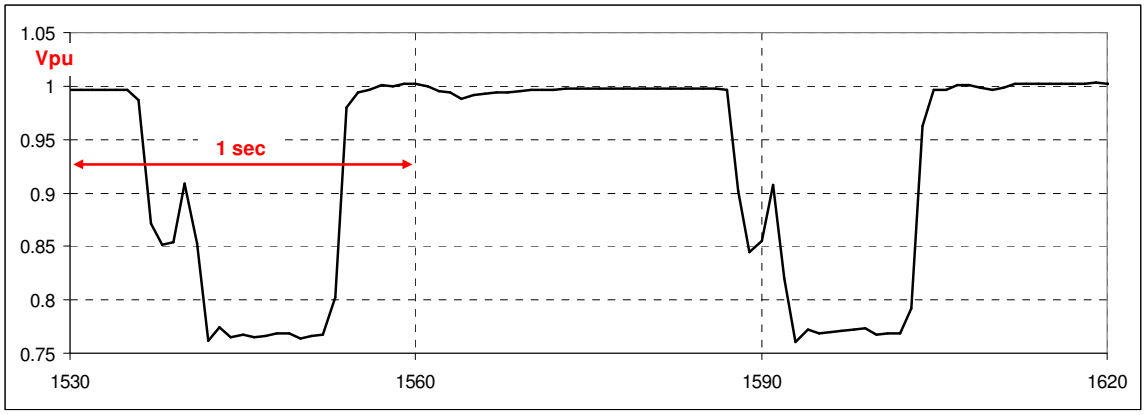

Figure 5.6: Zoom in of Voltage Sag event

This specific event was determined to be a fault and recloser operation on an adjacent distribution feeder. Applications that can stem from such observations include equipment operation schemes. With adequate PMU placements, the voltage sag can be traced to a particular region. Once this is done, the utility company can compare the reclosing times with the protection scheme they deployed at that region to determine whether the operation was correct. Such applications are already being used by the Oklahoma Gas and Electric Company (OG&E) [5]

Another important use for the voltage magnitude being recorded is a verification of the phase angle. When there is a sudden change in phase angle, a simple check of rms voltage can determine if the points involved should be treated as dropouts.

5.4: Observed Modes

5.4.1: West Texas Ambient Phase Angle Oscillations

We have seen in the past that many high-wind days have a well-developed 2 Hz mode, but that this mode is missing or not obvious on low wind days. Let us examine

two consecutive study days, Saturday and Sunday, Feb. 27th and 28th, 2010. In terms of load, they were very similar. In terms of wind generation, they were very different. Consider the three hour periods, 1-4pm. Figured 5.7 shows the wind generation for Saturday and Sunday. Figure 5.8 shows the corresponding ERCOT Total Generation. On Saturday, the wind generation was about 400 MW. On Sunday, it hit a record of above 6200 MW. This record wasn't broken until June 12, 2010 with 7001MW.

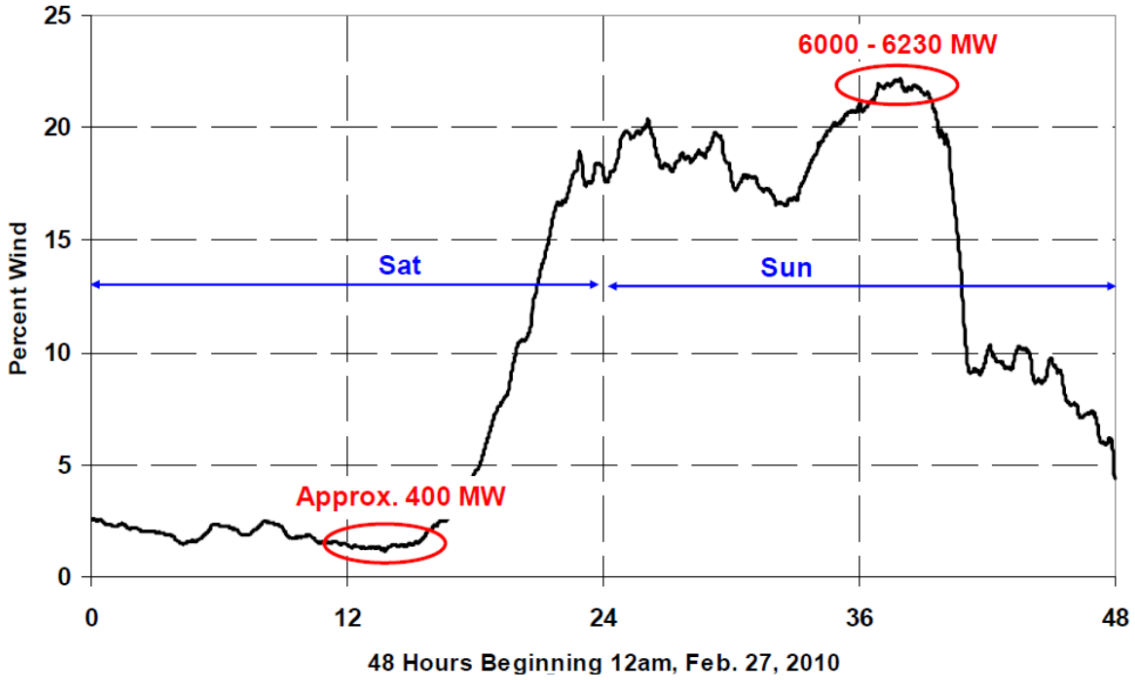

Figure 5.7: Wind Generation in ERCOT (Percent of Total Gen) for Feb. 27-28, 2010

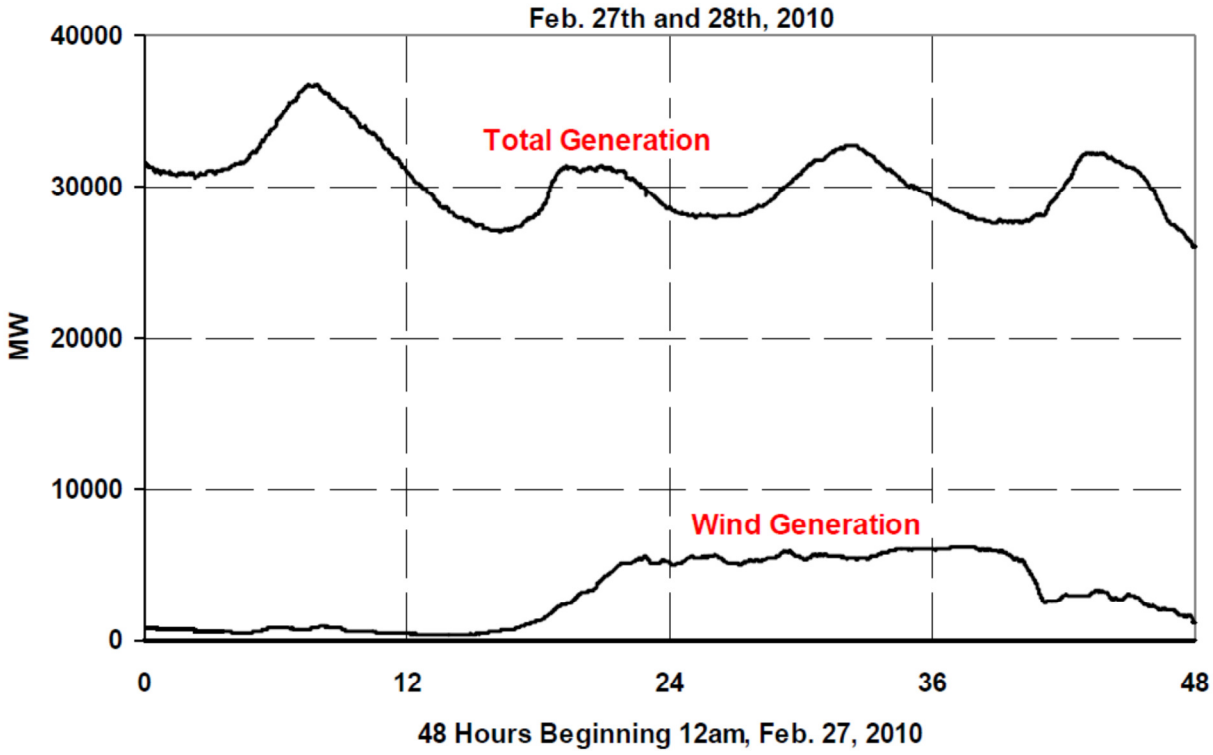

Figure 5.8: Total Generation and Wind Generation in ERCOT for Feb. 27-28, 2010

Even though there were no major ringing events during the two three-hour periods, modal analysis of the small ambient phase angle oscillations yield important information on system resonant modes and damping. The Schweitzer synchrophasor vector processor is programmed to produce modal results every 10 seconds. The scatter plots and summary tables are shown in Figures 5.9-10 and Tables 5.1-2.

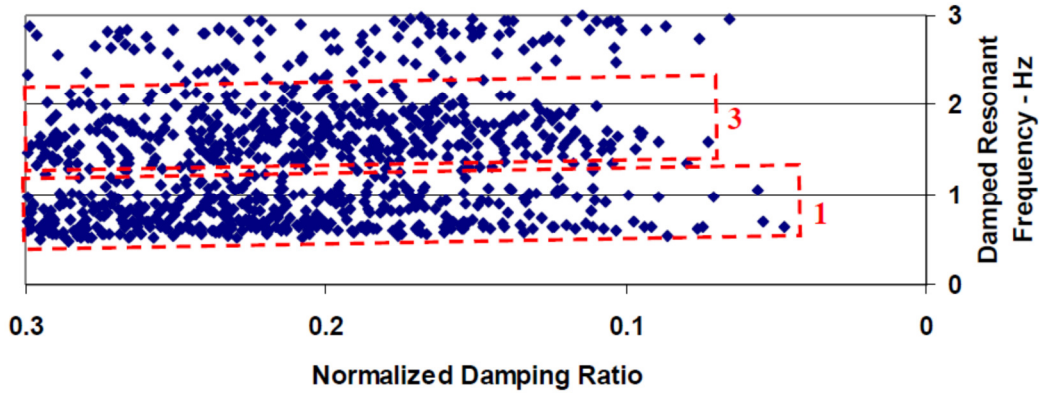

Figure 5.9: West Texas w.r.t. UT Austin Ambient Phase Angle Oscillations, Low Wind Generation Period, Feb. 27, 2010, 1-4pm

Table 5.1: Low Wind Day, Saturday, Feb. 27, 2010, 1-4 pm

Rectangle	Num. Points	Avg. Mag.	Avg. Freq.	Avg. Damp
2 Hz Mode	402	0.17 3	1.68	0.20 3
1 Hz Mode	428	0.20 1	0.80	0.22 2

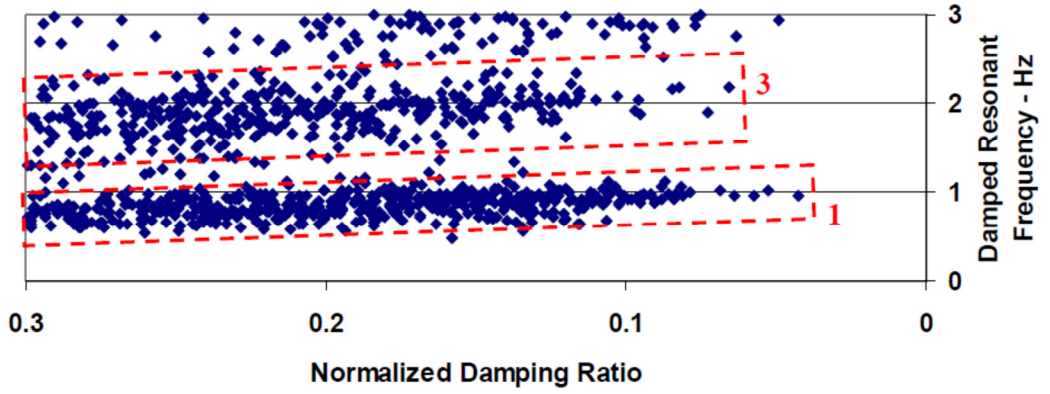

Figure 5.10: West Texas w.r.t. UT Austin Ambient Phase Angle Oscillations, High Wind Generation Period, Feb. 28, 2010, 1-4pm

Table 5.2: High Wind Day, Sunday, Feb. 28, 2010, 1-4 pm

Rectangle	Num. Points	Avg. Mag.	Avg. Freq.	Avg. Damp
2 Hz Mode	367	0.20 3	1.86	0.21 3
1 Hz Mode	533	0.20 1	0.86	0.19 2

Observations below are linked to Figure 5.9-10 according to their number:

1. It is clear that the normal 0.5 – 1.0 Hz mode is more tightly clustered on the high-wind day than on the low-wind day. The average magnitudes, however, are the same for high-wind or low-wind.

2. The 0.5 – 1.0 Hz normal mode has slightly less average damping on the high wind days (i.e. normalized damping ratio 0.19 for high wind compared to 0.22 for low wind).

3. On the high wind day, the 2.0 Hz mode is more tightly clustered, has slightly higher average magnitude, and approximately the same average damping as the low wind day.

1. & 3. All four of the average magnitudes are approximately the same.

In summary, it appears that the major difference between the high-wind day and the low-wind day are that the mode measurements are more tightly clustered even though the average magnitudes are approximately the same.

5.4.2: Modal Analysis Observations

Figure 5.11-13 shows the Main Mode plots for a 4-day period ending on June 8th, 2010. This initial observation showed a natural resonant frequency of approximately 0.8 Hz for McDonald Observatory and 0.7 Hz for UT Pan Am. The normalized damping ratio at UT Pan Am was also considerably less than McDonald Observatory and the magnitude for UT Pan Am was approximately one-half that of McDonald Observatory.

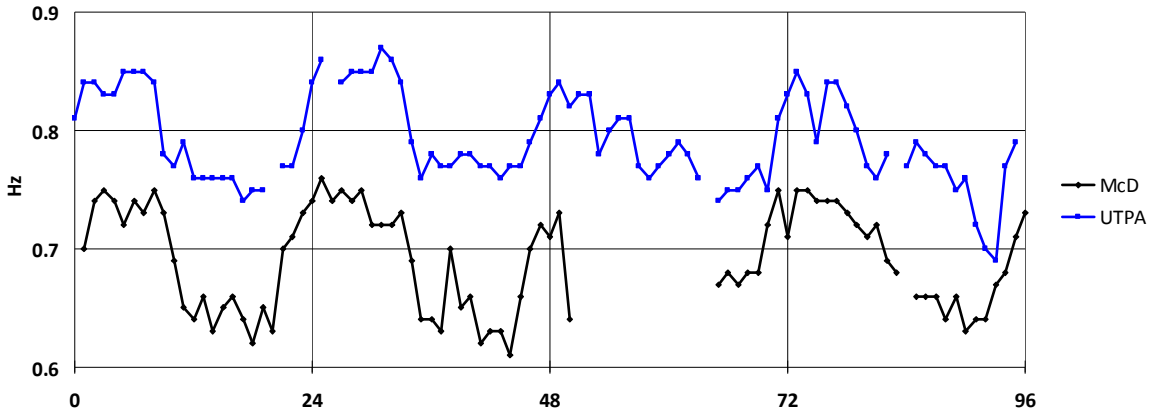

Figure 5.11: Frequency of Main Mode – Hz

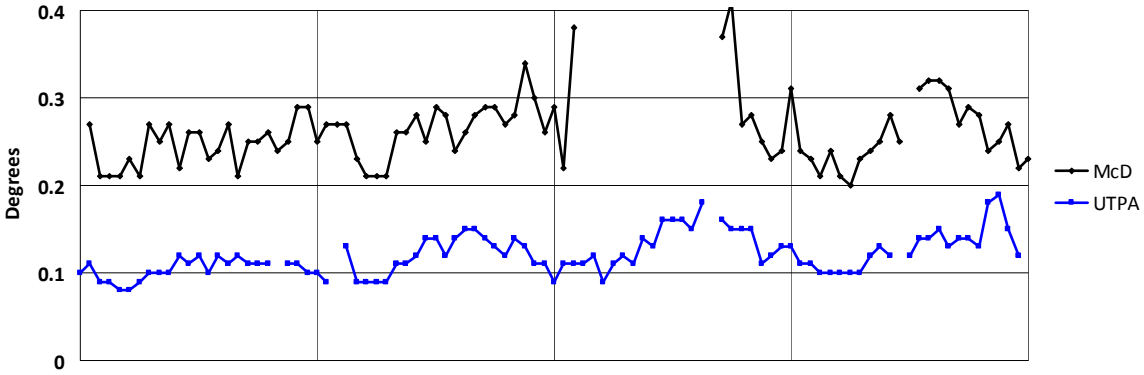

Figure 5.12: Magnitude of Main Mode – Degrees

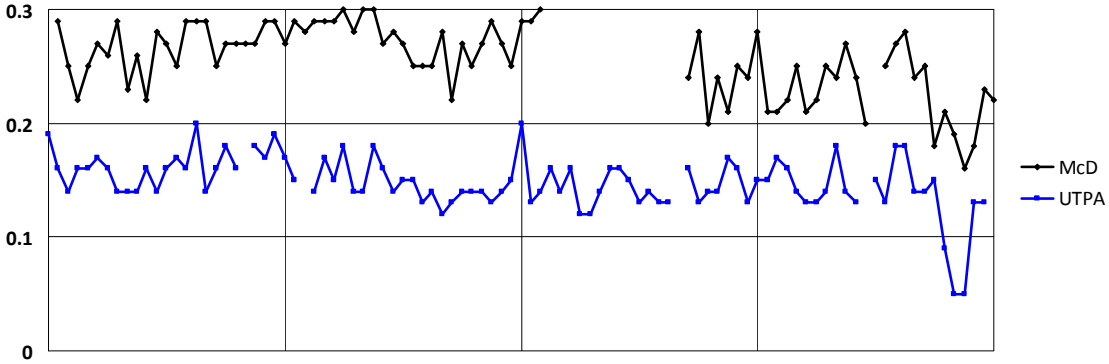

Figure 5.13: Normalized Damping Ratio of Main Mode

Figure 5.11 shows the resonant frequency at both locations varied approximately 0.1 Hz on a daily cycle. The conventional simplified power system stability model indicates that damped resonant frequency varies inversely with inertia H. We use the four-day period to see if this simplified relationship can be observed.

H can be estimated using the total generation on the grid. Figure 5.14 contains combinations of total generation (including wind), wind generation, and spinning reserve. Since the expected relationship is for frequency to vary inversely with H, we plot the inverse of the gigawatt (GW) generation in Figure 5.15. Figure 5.15 has a somewhat smoothed appearance because each hour is represented by an average of sixty minutes.

Now compare Figure 5.15 with Figure 5.16. Clearly there is a strong correlation between Figure 5.15 curves and both McDonald and UT Pan Am resonant frequencies. The actual linear correlations are shown in Table 5.3.

Table 5.3: Resonant Frequency Correlation with Generation

Inverse Variable	Linear Correlation with McDonald Resonant Frequency	Linear Correlation with UT Pan Am Resonant Frequency
Total Gen + Spinning Reserve	0.75	**0.82**
Total Gen + Spinning Reserve - Wind Gen	**0.82**	0.81
Total Gen	0.76	0.81
Total Gen- Wind Gen	0.78	0.79
Wind Gen	-0.33	0.04

The correlations are fairly strong, indicating that the simplified power system stability model is reasonable to a first approximation. The table indicates that wind generation has almost no impact on UT Pan Am's resonant frequency, but considerable

impact on McDonald. Almost all the wind generation is in West Texas where McDonald Observatory is also located.

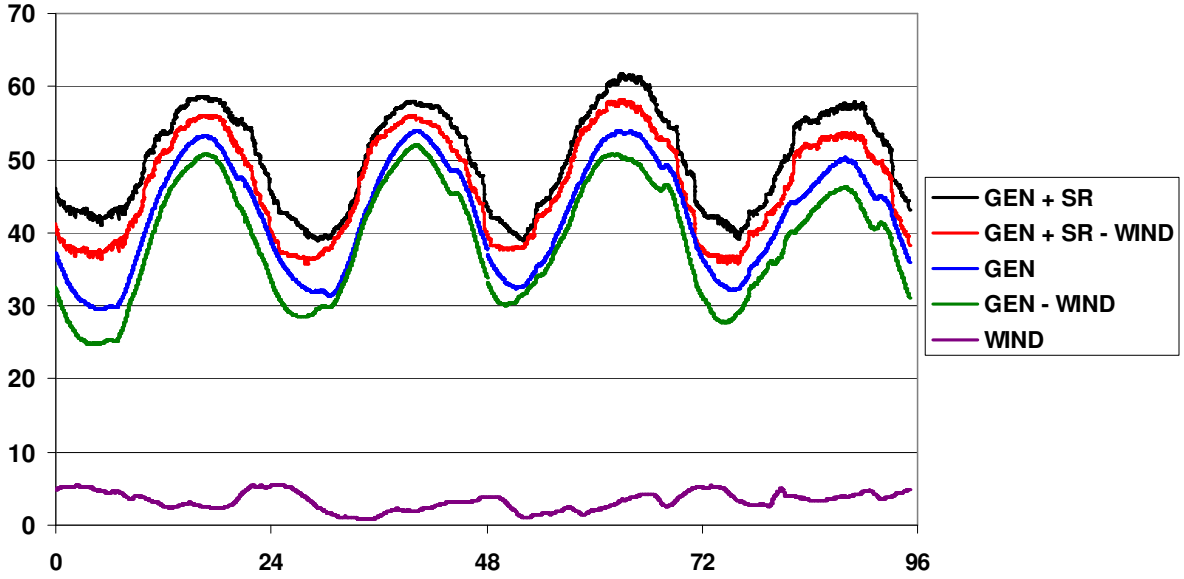

Figure 5.14: Generation (Total), Wind Generation, and Spinning Reserve – GW

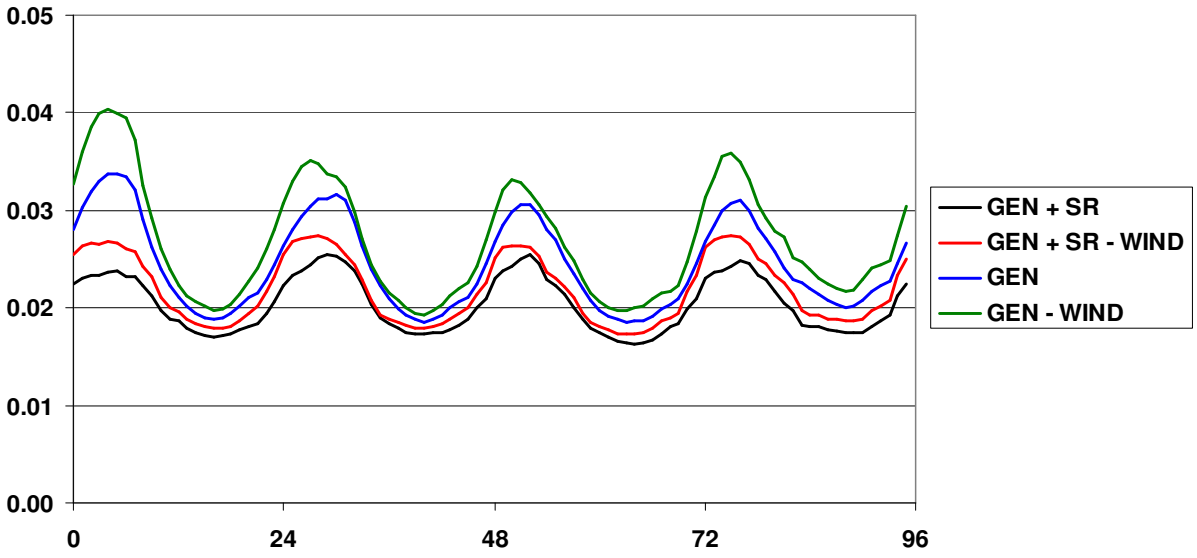

Figure 5.15: Inverse of Figure 2.2.4 - 1/ GW

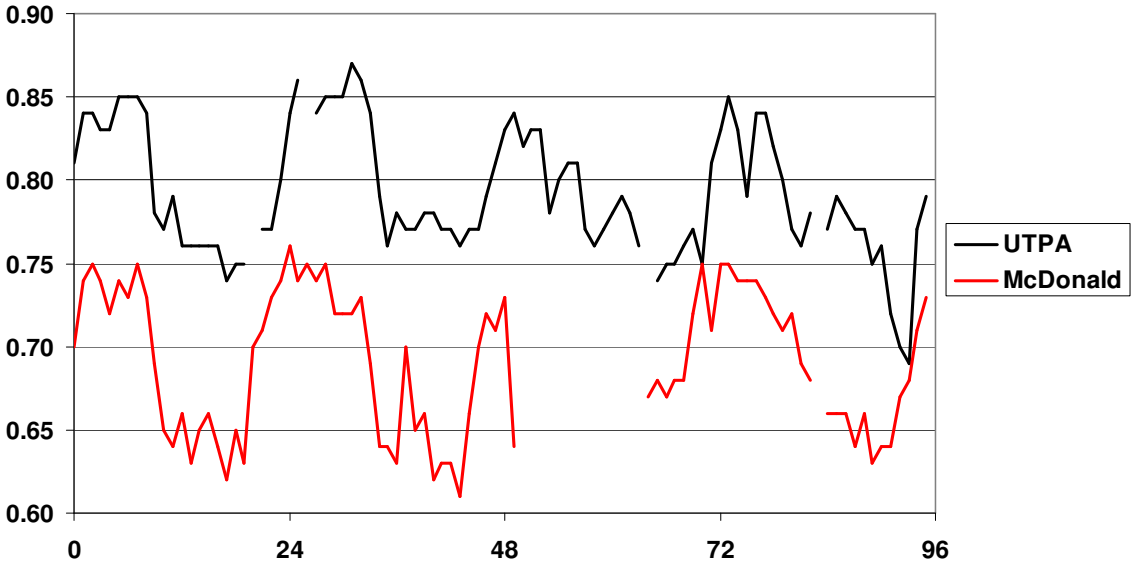

Figure 5.16: Dominant Natural Resonant Frequency – Hz

5.5: VOLTAGE ANGLE VARIATION ACROSS ERCOT

Power flow is directly tied to voltage phase angles. Therefore, it is important to know the typical angle variation that can be observed. It is also important to take into account the time frame of the variation. [27] has shown that minutes before the August 14, 2003 blackout, a 70 degrees voltage phase angle was observed. To put this variation into perspective of normal operation, the typical voltage phase angle swings across ERCOT north to south vary 40-50˚ over a period of 24 hours. Figure 5.17 shows the wind generation in ERCOT and the voltage phase angle of McDonald Observatory (West Texas) with respect to UT Austin (Central Texas). Angle swings of nearly 100 degrees in a 24 hour period are observed. This is attributed to the large wind generation capability located in West Texas. Figure 5.17 clearly shows that even during large wind ramping, large changes in voltage phase angle happens over a period of hours and not minutes.

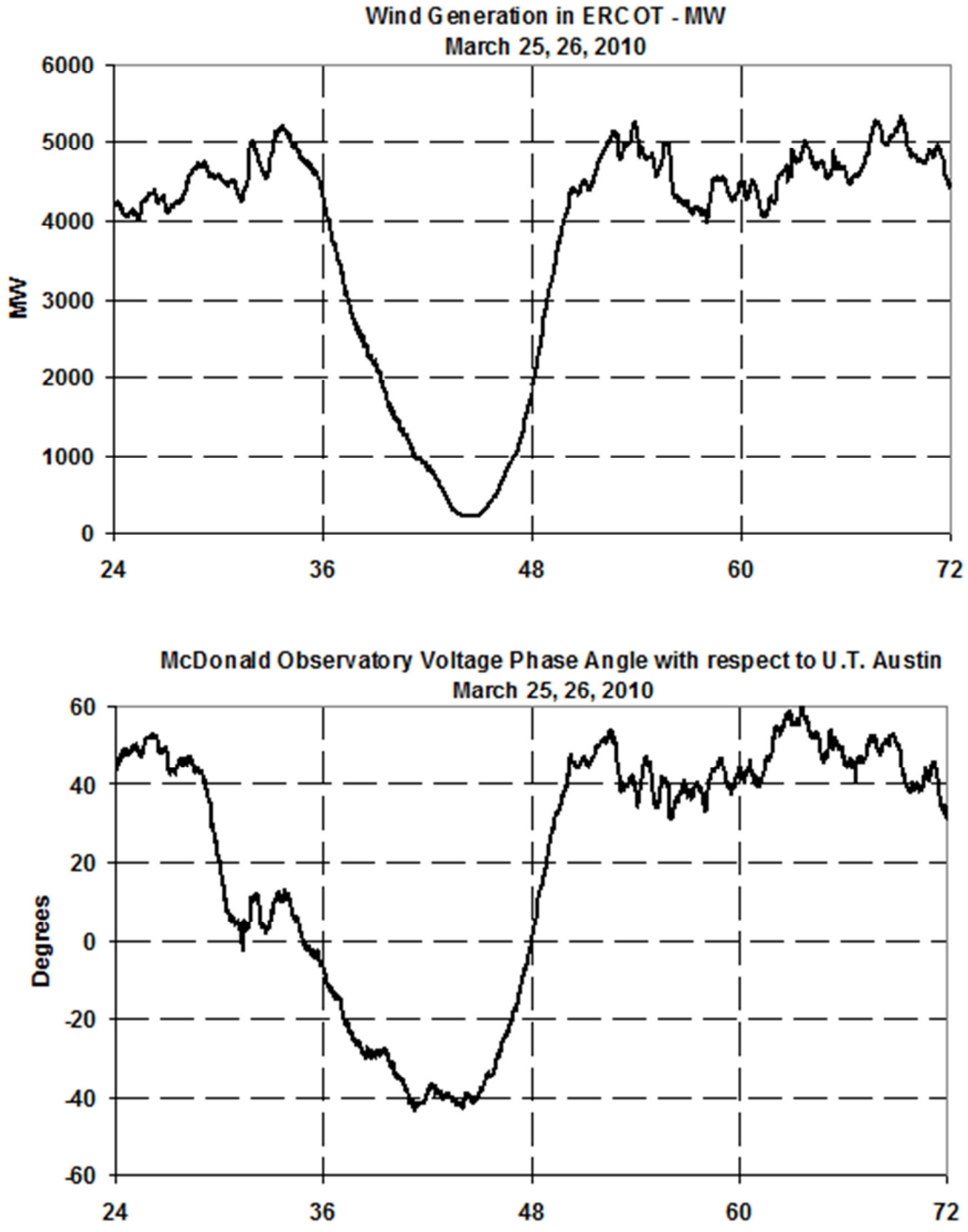

Figure 5.17: Wind generation in ERCOT and corresponding West Texas voltage phase angle

5.6: SYNCHROPHASORS PROVIDE HIGH RESOLUTION OVER 100'S OF MILES FOR TRANSMISSION SWITCHING EVENT

Synchrophasors also clearly show all major transmission switching events with high resolution across ERCOT. An example of this is shown in Figures 5.18-20. A transmission event occurred, causing very small frequency rings of 0.011 Hz peak-to-peak shown in Figure 5.18. The angle swing for this event is approximately 1 degree peak-to-peak, in Figure 5.19. This gave an increase of resolution from the 4th significant digit to the 2nd significant digit. This event happened to be a precursor to a minor frequency slump, shown in Figure 5.20.

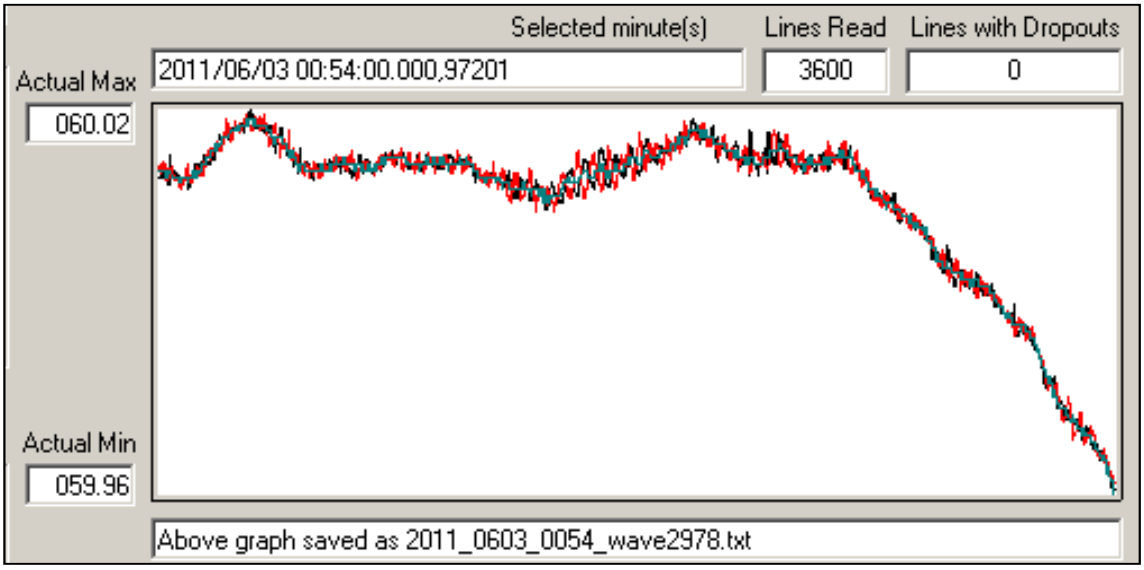

Figure 5.18: Frequency ring for transmission event (2-minute window)

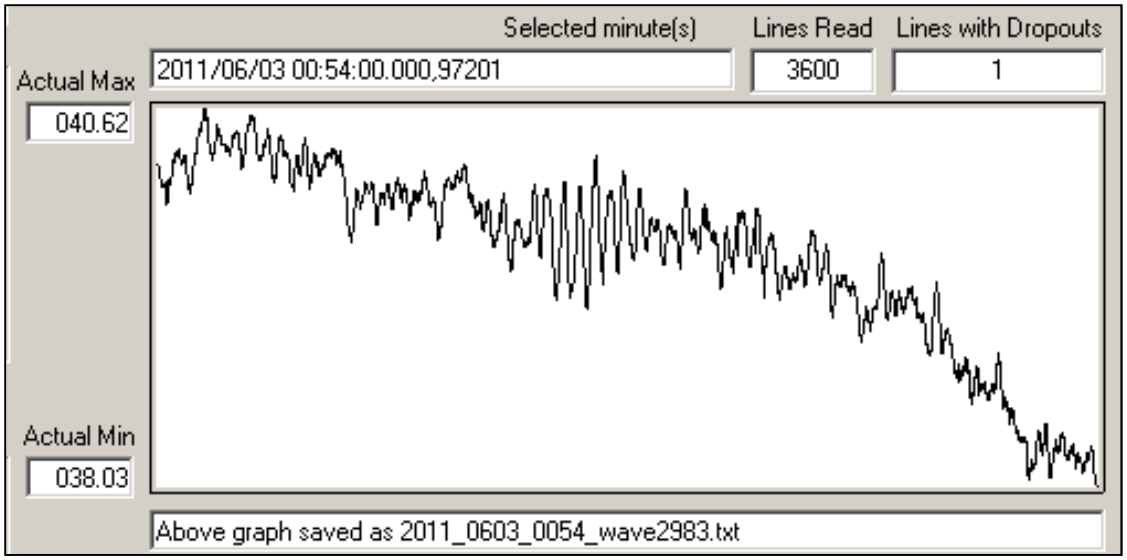

Figure 5.19: Voltage phase angle ring for transmission event (2-minute window)

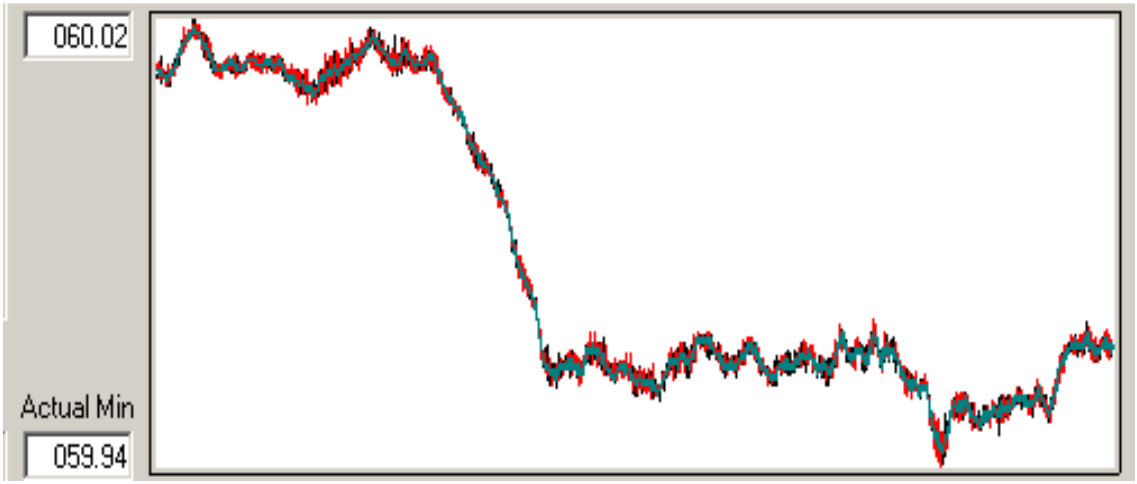

Figure 5.20: Frequency slump that occurred after the transmission event (5-minute window)

Chapter 6: Event Categories and Log

Reoccurring events can be identified and classified as unit trips, load shedding, protection events, switching events, or unique events. Unique events are simply events that seem to occur only once and do not fall under any of the other categories. All events are logged into a text file on a daily basis.

6.1: UNIT TRIPS

Events are categorized as a generator unit trip when the frequency decreases abruptly. Our ringdown screener allows us to detect both large and small unit trips. Large unit trips, defined by ERCOT as a loss of MW greater than 500 MW, are listed in ERCOT's operation messages [24]. The frequency of an example unit trip that occurred on April 4, 2012 at 12:17 GMT is shown in Figure 6.1. The corresponding voltage phase angle is shown in Figure 6.2.

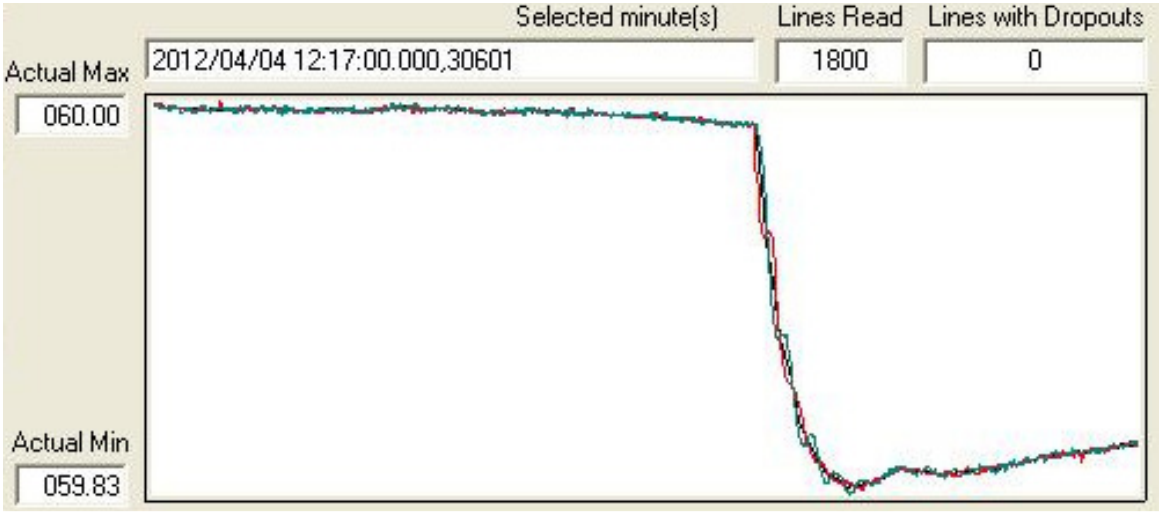

Figure 6.1: Frequency response of a unit trip on April 4, 2012 at 12:17 GMT

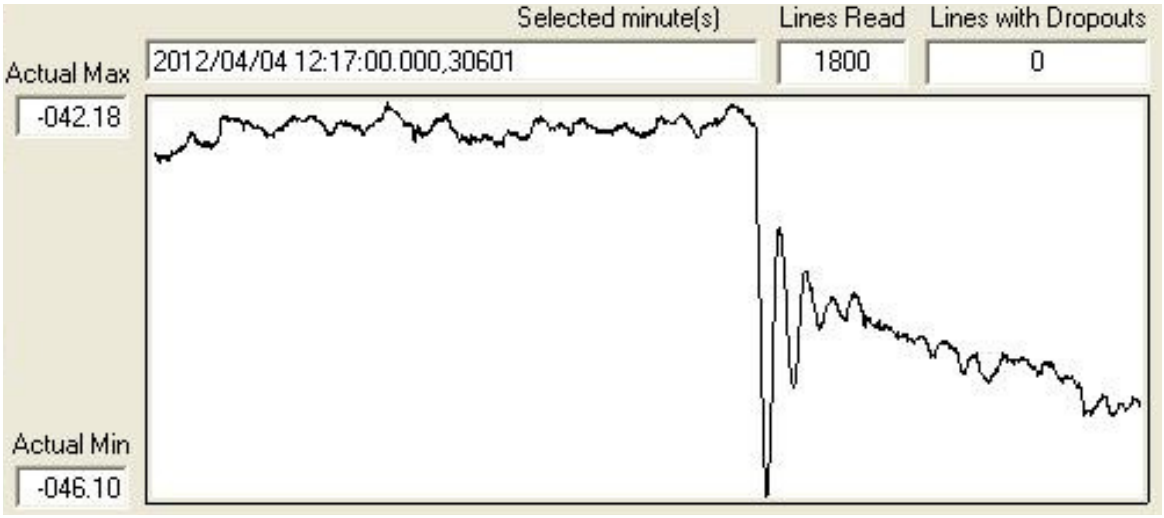

Figure 6.2: Corresponding McDonald Observatory voltage phase angle with respect to UT Austin for unit trip on April 4, 2012 at 12:17 GMT

6.2: LOAD SHEDDING

An event is classified as load shedding when the frequency response shows a large sudden increase. Figure 6.3 shows the load shedding event circled in red. The specific event occurred on November 29, 2011 and was the result of an initial combined generation loss of 1,356 MW, shown in blue. Similar to unit trips, direction finding can be used on the voltage phase angle to determine where most of the load shed happened.

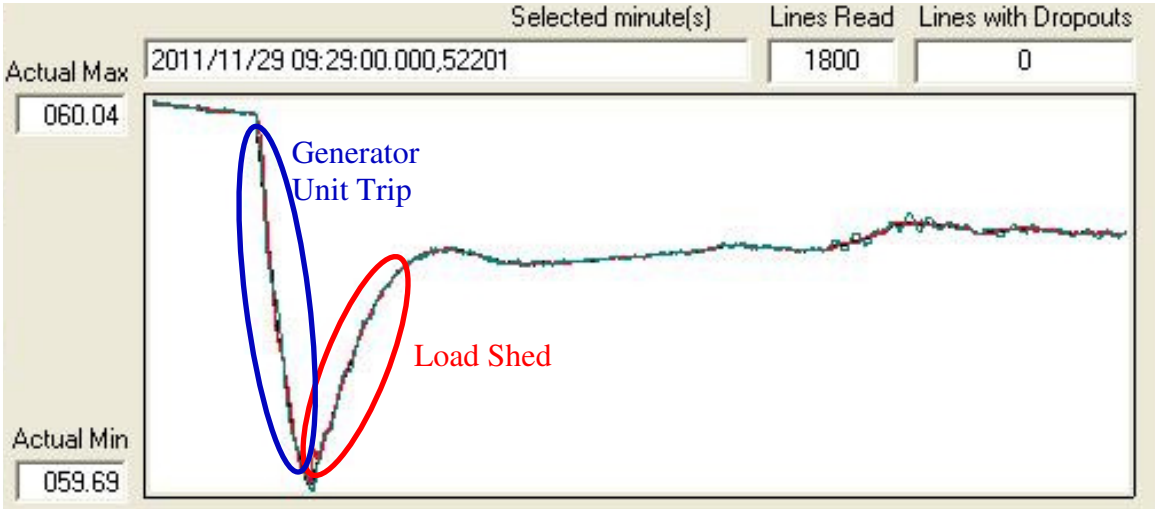

Figure 6.3: Frequency response of a load shed that occurred on November 29, at 09:29 GMT

6.3: SWITCHING EVENTS

Analysis of synchrophasor data has shown certain events to have pronounced ringing in phase angles and frequency and little to no steady-state angle changes and frequency. An example of such an event is shown in Figure 6.4 and 6.5. These events are classified as switching events of transformers, capacitors, or HVDC/transmission lines.

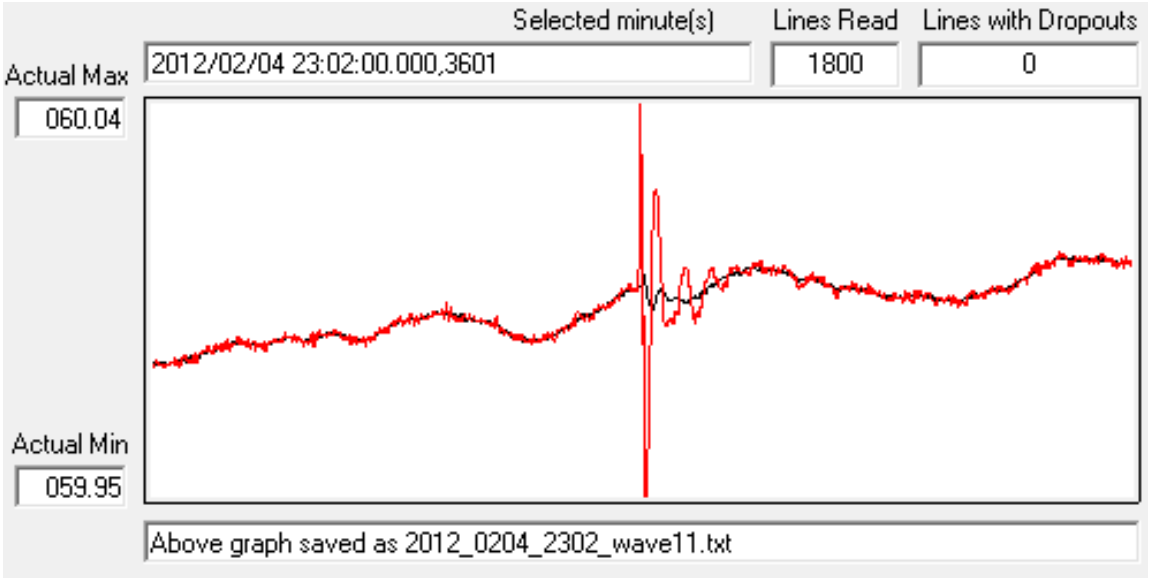

Figure 6.4: Frequency response of switching event that occurred on February 4, 2012 at 23:02 GMT

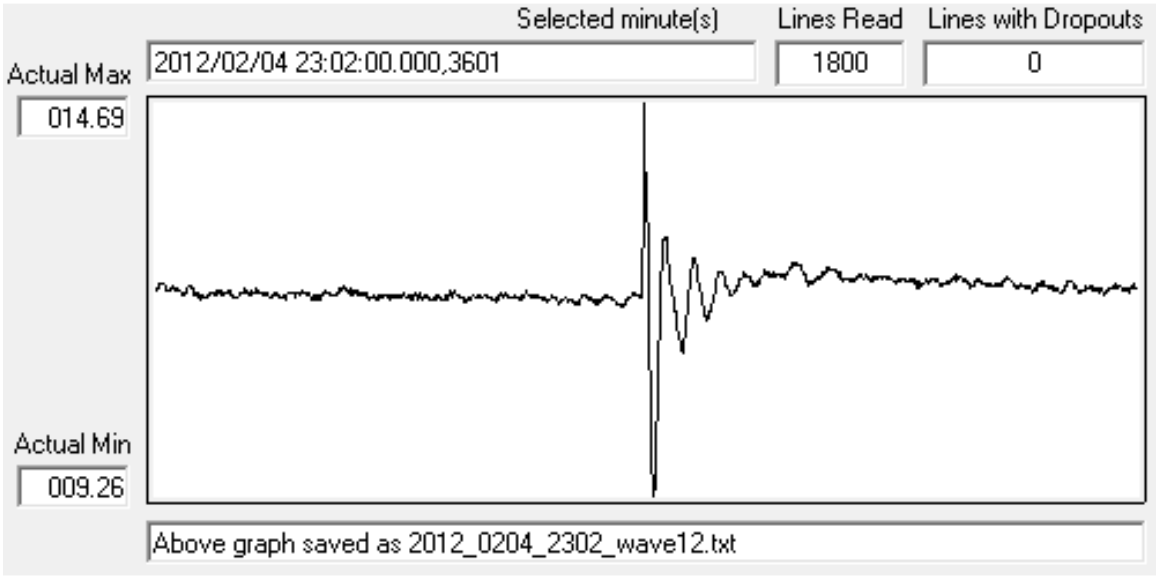

Figure 6.5: Corresponding McDonald Observatory voltage phase angle with respect to UT Austin for switching event that occurred on February 4, 2012 at 23:02 GMT

6.4: EVENT LOGGING

In order to keep up with the vast amount of data archived at the Texas Synchrophasor Network, daily screening of the data and a log of interesting events is made. The event log contains the date, time in GMT, and a description of the event. If the event is also logged on the ERCOT website, then it is copied into this event log. Appendix B contains the log for January through May 2012.

Chapter 7: Conclusion

This dissertation discussed the applications of synchrophasors as a grid health monitor. Even though synchrophasors have been available for some time, it was not widely used due to cost. However, synchrophasor capabilities have been added to commonly used relays. Because real time data is not easily accessible, the Texas Synchrophasor Network was established. Initially, the network only spanned the ERCOT grid, but has since expanded to both the Western and Eastern grids. The equipment and computer programs used in the network have been discussed.

The Texas Synchrophasor Network is an independent network; therefore access to high voltage is not readily available. As such, verification that 120V wall outlets are suitable for synchrophasors have been done. The verification was first done by comparing two 1-phase and one 3-phase connected PMUs. Then, a 69kV substation PMU was compared to a nearby 120V wall outlet connected PMUI. A statistical analysis to observe the impact of connecting synchrophasors in 1-phase or 3-phase has also shown 1-phase connection to be adequate.

Through second order analysis of ring downs, we have observed that wind generation does not have an impact on grid damping. It has also been shown through analysis of forty-two generator unit trips that wind generation does not have a correlation with grid inertia. However, it has also been shown that wind generation does impact the nadir point of a generator unit trip. A Frequency Recovery Ratio has been defined to better observe this phenomena.

Additional unique observations have been discussed, including a turbine valving problem that was only detected by our synchrophasor network due to its slow varying nature. A method to locate a generator unit trip through both the steady-state voltage

phase angle change and initial direction of its second order ring has been discussed. A recurring recloser event has also been shown with applications towards correctly identifying drop outs. In addition to the 2 Hz mode detected as a local generation event in the modal analysis, a 2Hz mode corresponding to wind generation has been shown. Finally, the categories of recurring events such as unit trips, load sheds, and switching events have been shown.

Appendices

Appendix A: Equipment Setup Instructions

INSTALLING THE PMU FIRMWARE

1. Power up the 421, connect an SEL C234A-8 null modem cable to the front RS232 port F.

2. Connect a Prolific PL-2303 USB-to-Serial cable. The driver is available at www.campbellsci.com, product #17394 support.

3. For Windows XP, call up Hyperterminal. For Windows 7, Hyperterminal doesn't exist. But, we found a workaround at www.helpdeskgeek.com. The workaround is to get two files from a computer that has Windows XP. These are C:\Program Files\Windows NT\hypertrm.exe and C:\Windows\System32\hypertrm.dll. Put both files in directory where you will also have your other SEL setup and instruction files.

4. Enter area code (is ignored), keep clicking OK, then on COM properties, use Bits per second = 9600, and Data bits = 8, Parity = None, Stop bits = 1, Flow control = None.

5. The Hyperterminal screen will appear. Press "Enter" and if a connection is made, you'll see an equal sign. Type in "acc" and press "Enter." You'll see "Password: ?". Then type in "OTTER" and press "Enter" to access Level 1

6. The "=>" indicates Level 1. Type in "2AC", press "Enter", then type 'TAIL" and press "Enter" to access Level 2. Level 2 is denoted by "=>>".

7. Disable the relay by typing "L_D" then press "Enter". Then, "Y" two times. You will see the message "Relay Disabled."

8. The prompt is now "!>" which indicates the firmware load mode.

9. Change the baudrate to the maximum by typing "BAU 115200" and press "Enter". Sometimes a character such as a dot is displayed after the above number.

10. Do not close the Hyperterminal program. However, disconnect from Hypterminal by pulling down the "Call" menu and selecting "Disconnect".

11. Now, reestablish communications at the new baud rate by selecting the "File" pulldown, then "Properties", then on the properties screen press "Configure", then on the port settings screen set the Bits per second to 115200. Close with "OKs".

12. Reconnect using the "Call" pulldown, then again "Call". Press "Enter" and you will see the prompt "!>".

13. At this point, you should have the PMU firmware file "r123421.s19" resident in your computer's folder that has SEL setup and instruction files.

14. Erase the old firmware by typing "REC" and pressing "Enter." You will see the "are you sure question." Type "Y" and press "Enter".

15. You will the words "Erasing" and "Erase successful" and ":Press any key … ". Next press any key.

16. Select the "Transfer" pulldown, and then select "Send File". Browse to find the r123421.s19 file, change Protocol to "1K Xmodem", then press "Send". Packets should start to flow, and the process takes about 15 minutes. Success is indicated by the message "Transfer completed successfully".

17. Type "exit" and press "Enter". Wait about 3 minutes until the 421 viewing screen returns to the rotating format.

18. Exit Hyperterminal using the "File" pulldown and then selecting "Exit" Answer "Yes" to the "Are you sure …" question, and then answer "No" to the "Do you want to save …" question.

INSTALLING SEL ACSELERATOR QUICKSET SOFTWARE

1. Go to the Schweitzer web site, www.selinc.com, then search for AcSELerator, then click on "Learn more about …" then click on "ACSELERATOR QuickSet Software", then "Login".

2. If you do not have a mySEL account, create one.

3. Login, and then click "Download" and run the setup. Keep answering "OK".

CHECKING AND UPDATING THE PART NUMBER OF THE SEL421

1. Open AcSELerator QuickSet

2. Pull down "Communications", then "Parameters", then view the "Communication Parameters" window.

3. Under "Active Connection Type", select "Serial", then under "Device", select the COM port, then click "OK". The "Working" window will appear. (Note – at this point,

we had to backup and use Hyperterminal to wake up the connection to the SEL421, after which AcSELerator worked fine). Blinking red and green light in the lower left screen and a "connected" message show that connection has been made

4. Pull down "Communications", then select "Terminal", then the "QuickSet Communication" window will appear with two equal signs, one under the other.

5. Type in "acc" and press "Enter." You'll see "Password: ?". Then type in "OTTER" and press "Enter" to access Level 1

6. The "=>" indicates Level 1. Type in "2AC", press "Enter", then type 'TAIL" and press "Enter" to access Level 2. Level 2 is denoted by "=>>".

7. Type in "CAL" and press "Enter", then enter password "Sel-1", then press "Enter".

8. You will see the 421's serial number, and the phrase "Level C".

9. Type in "ID" and press "Enter", then see the phrase "PARTNO". After the part number comes the characters "0421" followed by a "0","1","2", or "3". If "3", the part number is OK, and skip over Step 10.

10a. (For "0" or "1") To change the part number, you will need the "421_convertion_tool.htm" file. Double-click the file, and it opens in your default web browser. Past into the top box the old part number "0421 …….". Press "Convert" and a new part number will appear in the second box. If the new part number is"04212…" then change it to "04213…". Copy the second box, go back to AcSELerator QuickSet, type in "SET C PNUMBER", press "Enter", the old PNUMBER will be shown. Then, after the ?, past in the new PNUMBER and press "Enter". When "SNUMBER" appears, type "END" and press "Enter". You will see a long list of settings. Type "Y", and press "Enter".

10b (For "2"). Type in "SET C PNUMBER", press "Enter", and the old PNUMBER will be shown. Copy the old PNUMBER. Then, after the ?, past in the old PNUMBER, change the "04212 …" to a "04213 …" and press "Enter". When "SNUMBER" appears, type "END" and press "Enter". You will see a long list of settings. Type "Y", and press "Enter".

11. Verify the change by typing in "STA", and press "Enter". You should see a list of characters "FID=SEL-421-3 … ". If you do not have the "-3" then you made a mistake in the last step.

CHANGE A JUMPER SETTING TO ALLOW SERIAL PORT 3 TO OUTPUT +5VDC AND THUS PROVIDE POWER FOR THE ETHERNET TRANSCEIVER

1. Power down the SEL421. Remove the four screws from the front panel. Remove the front panel.

2. Remove the seven screws from the top of the SEL421. Remove the top cover.\

3. On the far left, at the back, there is a small black jumper labeled +5V, JMP1. Presently it is connected to only one of the two pins. Pull off the jumper, and place it back on so that it connects to both pins. The jumper shorts the pins together.

INSTALLING THE SYNCHROPHASOR SETTINGS

1. Open AcSELerator QuickSet, pull down "File", then "Active Database", find the *.rdb file that has the synchrophasor settings, and "Open". For example, "PMU_90_DC.rdb" is the Mike Bollen's station having the name "DC" and PMU ID = 90. AcSELerator QuickSet return to the main screen.

2. Pull down "Communications", then "Parameters", then choose "Serial", COM device, 9600 baudrate, and leave the defaults as they are. Click "OK".

3. Pull down "Communications", then "Terminal", press "Enter", and expect to see an "=" sign.

4. Pull down "File", then "Open", then click the example name shown (e.g., PMU_90_DC), and click "OK". On left side, expand "Global", then click "General Global Settings". This where the RID can be changed.

5. A few lines below, click "Synchronized Phasor Measurement". The PMSTN Station Name should match the RID (e.g., "DC"), and the unique PMID (e.g., "90") is set. PHDATAV is where one phase or all phases are selected. VCOMP phase angle offset can be entered.

6. A few lines below, expand "Front Panel", then "Display Points …", the top box should have the correct ID (e.g., "90"), the second box should have the correct RID (e.g., "DC")

7. Pull down "File", then click "Send". A "Settings Groups …" screen will appear. Click the box with the checkmark to select all. Then, uncheck "Port F", and click "OK".

8. A “Transfer Status …” window will appear. When finished, you will see the “=>>” response, and the SEL421 should be synchrophasor ready, with the appropriate rotating screen.

PROGRAMMING THE PROTOTYPE SEL-2891 ETHERNET TRANSCEIVER

The following steps apply to the prototype, unmarked, SEL-2891 ethernet transceiver. These are current used at UT Austin, UT Pan Am, McDonald Observatory, Harris Sub, Cloudcroft.

1. Open Hyperterminal, and enter a name such as SEL, then press “OK”. Select your COM port, and press “OK”.

2. Choose 9600 bits per second, and Flow control = “None”. Press “OK:

3. There are two types of cables that you can use now. The first option is SEL-C642, which has RS232 on both ends and a separate 5V wall wart. Connect either end to a USB-to-RS232 adaptor, and the USB to your PC. Plug in the 5V wall wart.

4. While holding down the “x” key on your keyboard, plug the RS323 end into the Ethernet transceiver. Wait until Hypterminal pops up with the MAC address and other info, and then release the “x” key. Quickly press “Enter”. You should see a list starting with “*** basic parameters” and you will now enter the “Change Setup” menu.

5. A list will scroll by, ending with “Your choice ?” Type in “0” and press “Enter”. Now, enter the IP address of the remote PMU, and press “Enter”.

6. Answer “Y” to “Set Gateway”, and enher the Gateway IP address for the remote PMU, and press “Enter”. Type in the Netmask Number of Bits (e.g., “8”), and press “Enter”. The “8” means “255.255.255.0”.

7. Enter “UT28” for the new password. (Note – on the new SEL-2890 ethernet transceivers, we use “UT2890” as the password.

8. For “Change Setup” choice, type in “1” and press “Enter”.

9. For :”Baudrate” enter “38400” and press “Enter”. For “I/F Mode” type in “4C” and press “Enter”. For “Flow” enter “02” and press “Enter”.

10. For “Port No” enter the unique port number for the remote station. For example, “2030” will Idaho National Lab. Press “Enter”.

11. For ConnectMode" type in "C0" and press "Enter". For "Send … " type in "N" and press "Enter". For "Auto increment …" type in "N".

12. Enter the IP address of the Synchrophasor Vector Processor (SVP), which is 128.83.52.136. Press "Enter".

13. For "Remote Port" and "DisConnMode" and "Flush… " and "DisConnTime" and "SendChar 1" and "SendChar 2", press "Enter" to keep faults.

14. For "Your choice ?" type in "9", and press "Enter" to save and exit. You will see the "Parameters stored" message.

Appendix B: 2012 Log of Events

2012/01/14 - none

2012/01/15 20:04:00.000,7201- unit trip

2012/01/16 16:48:00.000,86401 - unit trip - only seen at UTPA

2012/01/17 - none

2012/01/18 09:50:00.000,90001 - obvious oscillation, no stable angle change, odd freq

2012/01/18 19:15:00.000,27001 - switching event with stable angle change after event

2012/01/19 - none

2012/01/20 - none

2012/01/21 19:34:00.000,61201 - unit trip

2012/01/22 - none

2012/01/23 - none

2012/01/24 05:47:00.000,84601 - small unit trip, McD angle stays the same

2012/01/25 07:14:00.000,25201 - unit trip

2012/01/25 18:22:00.000,39601 - unit trip with load shed following

2012/01/25 20:29:00.000,52201 - unit trip with load shed following

2012/01/26 04:04:00.000,7201 - unit trip

2012/01/27 - none

2012/01/28 - none

2012/01/29 - none

2012/01/30 - none

2012/01/31 - none

2012/02/01 - none

2012/02/02 - none

2012/02/03 - none

2012/02/04 23:02:00.000,3601 - switching event

2012/02/05 13:59-14:00:00.000,1 - load shedding event

2012/02/06 - none

2012/02/07 - none

2012/02/08 11:16:00.000,28801 - odd oscillation but only lasted a few seconds.

2012/02/09 - none

2012/02/10 - none

2012/02/11 - none

2012/02/12 13:55:00.000,99001 - unit trip

2012/02/13 - none

2012/02/14 - none

2012/02/15 10:03:00.000,5401 - unit trip, voltage dip seen in all but McD

2012/02/16 - none

2012/02/17 - none

2012/02/18 08:48:00.000,86401 - insignificant unit trip

2012/02/19 01:00:00.000,1 - unit trip

2012/02/19 03:17:00.000,30601 - unit trip

2012/02/20 - none

2012/02/21 - none

2012/02/22 17:09:00.000,16201 - UTPA either load shed or switching event

2012/02/23 - none

2012/02/24 - none

2012/02/25 12:34:00.000,61201 - unit trip

2012/02/26 - none

2012/02/27 20:34:00.000,61201 - small load shed

2012/02/28 16:53:00.000,95401 - small unit trip

2012/02/29 15:50:00.000,90001 - small unit trip

2012/02/29 18:30:00.000,54001 - small switching event at UTPA

2012/03/01 19:59:00.000,106201 - switching event UTPA

2012/03/02 - nothing

2012/03/03 - nothing

2012/03/04 - nothing

2012/03/05 - nothing

2012/03/06 - nothing

2012/03/07 - nothing

2012/03/08 - nothing

2012/03/09 22:52:00.000,93601 - unit trip 59.7Hz

2012/03/10 - nothing

2012/03/11 - nothing

2012/03/12 - nothing

2012/03/13 - nothing

2012/03/14 - nothing

2012/03/15 02:52:00.000,93601 - 2 min window, unit trip 59.85 Hz

2012/03/15 06:03:00.000,5401 - double unit trip, both small (59.86 Hz low after both)

2012/03/16 - nothing

2012/03/17 05:28:00.000,50401 - possible McD voltage sag event

2012/03/18 11:21:00 000,37801 - possible voltage sag event on McD

2012/03/19 21:58:00.000,104401 - small unit trip with good rings 59.9 Hz low

2012/03/19 22:32:00.000,57601 - 59.87Hz low unit trip. UTPA angle does not change but shows rings.

2012/03/20 - nothing

2012/03/21 - nothing

2012/03/22 08:36:00.000,64801 - unit trip 59.73 Hz

2012/03/23 00:43:00.000,77401 - possible small unit trip at the end of the minute (freq was already low when this happened)

2012/03/23 19:39:00.000,70201 - 2 min window, 2 sequenctial small unit trips 59.93 Hz low

2012/03/23 19:47:00.000,84601 - unit trip 59.92 Hz low

2012/03/24 - nothing

2012/03/25 - nothing

2012/03/26 14:09:00.000,16201 - possible transmission line event, rings with small angle change.

2012/03/26 15:23:00.000,41401 - possible transmission line event

2012/03/27 20:09:00.000,16201 - McD trip, most likely small and local

2012/03/28 23:14:00.000,25201 - McD line distrubance, 1 cycle ring with large mag change

2012/03/29 15:39:00.000,70201 - McD local event, large angle change with good rings

2012/03/30 19:56:00.000,100801 - large unit trip, 59.77Hz low. Good rings.

On 3/30/12, a sudden loss of generation occurred at 14:56 totaling 855 MW. Frequency declined to 59.770 HZ, ERCOT load was 40, 354 MW.

2012/03/31 17:14:00.000,25201 - UTPA local event.

2012/03/31 22:10:00.000,18001 - McD local event.

2012/03/31 22:56:00.000,100801 - small unit trip (59.95 Hz low). large angle change in UTPA.

2012/04/01 17:28:00.000,50401 - odd drop in frequency then comes back up (change from to low of 59.88 and high of 60.02). Seen in angle of Waco and McD.

2012/04/02 22:54:00.000,97201 - large unit trip, 59.77 Hz low - good rings

On 4/02/12, a sudden loss of generation occurred at 17:54 totaling 850 MW. Frequency declined to 59.770 HZ, ERCOT load was 42, 573 MW.

2012/04/03 07:07:00.000,12601 - 2 min window, unit trip, 59.8 Hz low, typical ringdown

On 4/03/12, a sudden loss of generation occurred at 02:08 totaling 733 MW. Frequency declined to 59.803 HZ, ERCOT load was 28, 013 MW.

2012/04/04 12:17:00.000,30601 - gen unit trip 59.83 Hz low

On 4/04/12, a sudden loss of generation occurred at 07:14 totaling 594 MW. Frequency declined to 59.833 HZ, ERCOT load was 32, 800 MW.

2012/04/05 - none

2012/04/06 01:37:00.000,66601 - a few seconds of ringing - probably line transient of some sort

2012/04/07 - nothing

2012/04/08 02:20:00.000,36001 - trip at McD (VRMS went low), steady state angle changed at McD from 32 to 24.54

2012/04/08 21:27:00.000,48601 - small unit trip (59.98 Hz low), ringing is present but no steady-state angle change

2012/04/09 21:20:00.000,36001 - recloser event on McD vs 2012/04/09 15:00:00.000,1 is just a drop out on Austin.

2012/04/10 21:47:00.000,84601 - small continued oscillation for 2 mins

2012/04/11 17:03:00.000,5401 - switching event (increase then decrease in angle ring)

2012/04/12 17:15:00.000,27001 - prolonged oscillation (small mag), probably switching event

2012/04/12 19:59:00.000,106201 - prolonged oscillation (small mag), possible switching event for UTPA but McD rings do not grown then decline

2012/04/13 - nothing

2012/04/14 16:03:00.000,5401 - small unit trip (59.93 Hz low)

2012/04/15 04:33:00.000,59401 - small unit trip (59.95 Hz low)

2012/04/16 11:02:00.000,3601 - switching event. Good rings, but small mag.

2012/04/16 11:48:00.000,86401 - switching event or loss of load. very little to no steady state angle change, but obvious rings

2012/04/16 21:12:00.000,21601 - UTPA switching event

2012/04/17 - none

2012/04/18 13:16:00.000,28801 - Unit trip (59.89 Hz low)

2012/04/19 21:08:00.000,14401 - unit trip (59.89 Hz low)

2012/04/19 16:30:00.000,54001 - 2 min window, small unit trip (59.95 Hz low)

2012/04/20 - GMT 0300 to end of 1800 data is bad. After this time, SPP has been taken off.

2012/04/21 - none

2012/04/22 - none

2012/04/23 01:17:00.000,30601 - small unit trip (59.92 Hz low)

2012/04/24 - none

2012/04/25 - none

2012/04/26 - none

2012/04/27 - none

2012/04/28 - none

2012/04/29 00:56:00.000,100801 - unit trip. (59.86 hz low)

2012/04/30 - none

2012/05/01 - none

2012/05/02 - none

2012/05/03 - none

2012/05/04 - none

2012/05/05 02:05:00.000,9001 - very small unit trip (59.92 Hz low)

2012/05/05 15:17:00.000,30601 - possible line switching event

2012/05/06 - none

2012/05/07 22:49:00.000,88201 - unit trip (59.88 Hz low)

On 5/7/12, a sudden loss of generation occurred at 17:50 totaling 516 MW. Frequency declined to 59.882 HZ, ERCOT load was 51, 152 MW.

2012/05/08 - none

2012/05/09 15:07:00.000,12601 - unit trip, (59.82 Hz low)

On 5/9/12, a sudden loss of generation occurred at 10:07 totaling 759 MW. Frequency declined to 59.823 HZ, ERCOT load was 34, 732 MW.

2012/05/10 - none

2012/05/11 03:15:00.000,27001 - double switching transient

2012/05/11 03:23:00.000,41401 - small unit trip with rings (59.95 Hz low)

2012/05/11 03:32:00.000,57601 - small unit trip with good rings (59.97 Hz low)

2012/05/12 08:35:00.000,63001 - recloser operation on McD

2012/05/13 - none

2012/05/14 - none

2012/05/15 17:22:00.000,39601 - small unit trip (59.94 Hz low)

2012/05/16 - none

2012/05/17 - none

2012/05/18 - none

2012/05/19 - none

no observable angle change - frequency does see a drop to 59.9 Hz

On 5/19/12, a sudden loss of generation occurred at 02:11 totaling 511 MW. Frequency declined to 59.905 HZ, ERCOT load was 28, 714 MW.

2012/05/20 - none

2012/05/21 - none

2012/05/22 - none

2012/05/23 - none

2012/05/24 - none

2012/05/25 - none

2012/05/26 - none

2012/05/27 07:32:00.000,57601 - unit trip (59.87 Hz low)

On 05/27/12, a sudden loss of generation occurred at 02:32 totaling 510 MW. Frequency declined to 59.885 HZ, ERCOT load was 30, 750 MW.

2012/05/28 - none

2012/05/29 03:51:00.000,91801 - switching event, clear rings

2012/05/29 04:21:00.000,36001 - small load shed event

2012/05/30 17:17:00.000,30601 - line trip?

2012/05/31 - none

References

[1] A.G. Phadke, J.S. Thorp, Synchronized Phasor Measurements and Their Applications, Dordrecht: Springer, 2008

[2] E.O. Schweitzer, A. Guzman, G. Benmouyal, "Synchronized Phasor Measurement in Protective Relays for Protection, Control, and Analysis of Electric Power Systems," proceedings of the 29th Annual Western Protective Relay Conference, Spokane, WA, October 2002.

[3] Patel M, S Aivaliotis, E Ellen, et al. 2010. "NERC Real-Time Application of Synchrophasors for Improving Reliability". North American Electric Reliability Corporation [Online.] Available: https://www.naspi.org/site/StaticPDF/resource/rapir_final_20101017.pdf

[4] M.A. Kai, W.M. Grady, D. Costello, D. Brooks, J. Ramos, "Lessons Learned from the Texas Synchrophasor Network," IEEE Innovative Smart Grid Technologies (ISGT), Berlin October, 2012

[5] REN21, "Renewables 2011: global status report" Available: http://www.ren21.net/Portals/97/documents/GSR/REN21_GSR2011.pdf

[6] V. VanZandt, M. Bianco, "The Western Interconnection Syncrhophasor Program (WISP)", North American SynchroPhasor Initiative presentation, February 2010

[7] D. Zwergel, "Midwest ISO Smart Grid Investment Grant Overview", North American SynchroPhasor Initiative presentation, February 2010

[8] D. Ulmer, "PJM SynchroPhasor Technology Deployment Project", North American SynchroPhasor Initiative presentation, February 2010

[9] North American SynchroPhasor Initiative, NASPI Phasor Data NDAs [Online]. Available: http://www.naspi.org/nda/nda.stm September 2010

[10] "IEEE Standard for Synchrophasor Data Transfer for Power Systems," IEEE Std C37.118.2-2011 (Revision of IEEE Std C37.118-2005), December 2011

[11] North American SynchroPhasor Initiative, NASPI Basic Synchrophasor Technology Information, "Synchrophasor Fact Sheet"[Online]. Available: https://www.naspi.org/File.aspx?fileID=538

[12] Schweitzer Engineering Laboratories SEL-421 Protection, Automation, and Control System [Online]. Available: http://www.selinc.com/WorkArea/DownloadAsset.aspx?id=7195

[13] B. Bhargava, A. Salazar, “Synchronized measurement and analysis in real-time SMART® - system at Aousthern California Edison (SCE) Co,” 2008 IEEE/PES Transmission and Distribution Conference and Exposition: Latin America, August 2008

[14] Phasor Real Time Dynamics Monitoring System (RTDMS) [Online]. Available: http://www.phasor-rtdms.com/prtdms/rtdms_overview.html

[15] Network Management solutions, e-terravision [Online]. Available: http://www.alstom.com/Global/Grid/Resources/Documents/Automation/NMS/e-terravision.pdf

[16] PowerWorld Retriever [Online]. Available: http://www.powerworld.com/products/retriever/synchrophasor-visualization

[17] W.M. Grady, The Texas Synchrophasor Network [Online]. Available: http://users.ece.utexas.edu/~grady/Texas_Synchrophasor_Network.html

[18] W.M. Grady, D. Costello, "Implementation and application of an independent Texas synchrophasor network," 2010 63rd Annual Conference for Protective Relay Engineers, pp.1-12, March 29, 2010-April 1, 2010

[19] Y. Gong, A. Guzman, “Synchrophasor- Based Online Modal Analysis to Mitigate Power System Interarea Oscillation”, Schweitzer Engineering Laboratories, Inc.

[20] P. F. Ribeiro, “Time-Varying Waveform Distortions in Power Systems”,Wiley 2009, pp. 320

[21] J. F. Hauer, C. J. Demeure, and L. L. Scharf, “Initial Results in Prony Analysis of Power System Response Signals,” IEEE Trans. Power Systems, vol. 5, Feb. 1990

[22] D. J. Trudnowski, J. R. Smith, T. A. Short, and D. A. Pierre, “An application of Prony methods in PSS design for multi-machine systems,” IEEE Trans. Power Systems, vol. 6, Feb. 1991

[23] J. Kim and W.M. Grady, "Synchrophasor analysis of 221 generating unit trips in ERCOT," IEEE Power and Energy Society General Meeting, pp.1-4, July 2011

[24] Electric Reliability Council of Texas, Operations Messages [Online]. Available: http://www.ercot.com/services/comm/mkt_notices/opsmessages/

[25] R. Sodhi, S.C. Srivastava,S.N. Singh, "Optimal PMU placement to ensure system observability under contingencies," IEEE Power & Energy Society General Meeting, July 2009

[26] S. Kulkarni, A. Allen, S. Santoso, W.M. Grady, "Phasor measurement unit placement Algorithm," IEEE Power & Energy Society General Meeting, July 2009

[27] U.S.-Canada Power System Outage Task Force, Final Report on the August 14, 2003 Blackout in the United States and Canada: Causes and Recommendations, Apr. 2004 [Online]. Available: https://reports.energy.gov/BlackoutFinal-Web.pdf

Vita

Moses An Kai was born in Taipei, Taiwan, the son of Ying and Grace. After earning a diploma from International Christian School, Hong Kong, in 2003, he entered the University of Texas at Austin in the College of Electrical and Computer Engineering. In 2007, he graduated with a Bachelor of Science Degree in Electrical Engineering. Immediately after graduation, he enrolled in the graduate electrical engineering program at University of Texas at Austin where he earned his Masters of Science in Engineering degree in 2009. His primary focus has been on synchrophasors, renewable energy, and power system stability. He has helped establish the Texas Synchrophasor Network, develop a solar mount with unistrut, start a relay lab course, and improve the Power Electronics Lab course. While at school, he has served as a teaching assistant for the Power Electronics Lab course, which has an enrollment of more than 130 students per year. He has also participated in internships at Electric Reliability Council of Texas (ERCOT) and Austin Energy. He is student member of IEEE and a U.S. citizen.

e-mail address: moseskai@gmail.com

This dissertation was typed by Moses Kai.